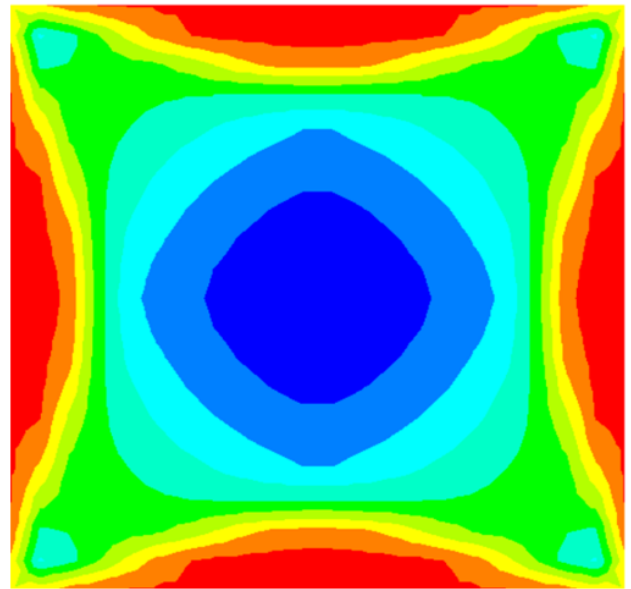
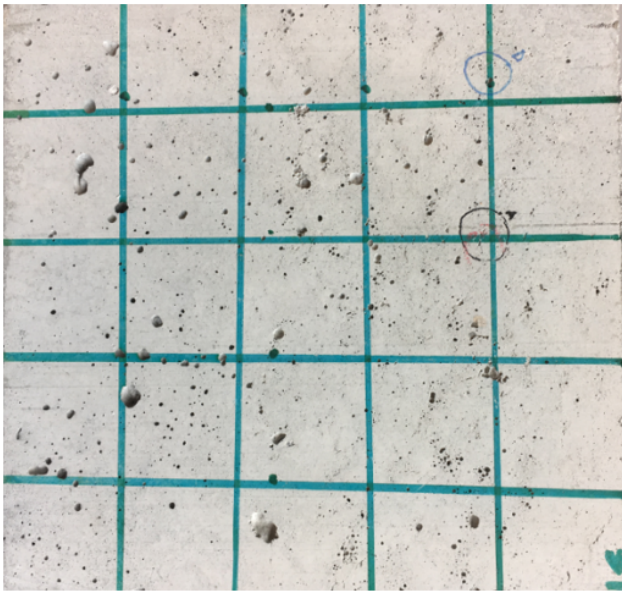


Development of Mechanical Properties of Concrete with Time

Experimental and Numerical Study

Nikhil Awasthy



Development of Mechanical Properties of Concrete with Time

Experimental and Numerical Study

by

Nikhil Awasthy

to obtain the degree of Master of Science
at the Delft University of Technology,
to be defended publicly on Friday October 25, 2019 at 3:00 PM.

Student number: 4717937
Project duration: February, 2019 – October, 2019
Thesis committee: Dr. ir. M. Lukovic, TU Delft, Chairman and Daily Supervisor
Dr. B. Savija, TU Delft
Prof. dr. ir. E. Schlangen, TU Delft

An electronic version of this thesis is available at <http://repository.tudelft.nl/>.

Acknowledgements

It is said that, "Difficult roads often leads to beautiful destinations". Two years back, I made the choice of taking a difficult road ahead and now it feels great to have reached the desired destination. Although, I must confess that this wouldn't have been possible without the help of many special people and I would like to take this opportunity to thank each one of them.

A master thesis study is an integral part of the Masters programme and I feel fortunate enough to have worked with a group of talented and kindest people. I would like to thank Mladena, the chair of my committee, and also my mentor. She has been a great support throughout the journey. Her presence and valuable suggestions in almost all the phases of the research ensured that I was always on the right track. Her out of the box thinking and critical approach towards tackling problems are few of the many skills which I really admire. Additionally, her knowledge of the subject matter, passion for learning every single day and commitment towards her work really inspired me (and still does). In short, in these last nine months, she has surely become my role model and I hope to have imbibed few of her qualities in myself.

I would like to thank Branko for his valuable suggestions especially at critical phases of the research. I really admire his spontaneous thinking skills which helped in shaping the project in the right direction. Moreover, his suggestion to use "FEMMASSE" worked well towards fulfilling the objectives of the research.

I owe my sincere thanks to Professor Erik too. Although, we had few interactions, but I feel each one of them was really productive. His critical feedback helped me understand when to dig deeper in the subject matter and when to come out of it. Moreover, he gave me the freedom to explore the software by myself, but he was always there to help me out whenever I got stuck.

I would also like to thank Ton, Maiko and Albert for making sure that the experimental work was done smoothly. Special thanks to Ton ! His sense of humour ensured that the lab sessions were never boring.

Being away from home was always tough. Moreover, the rigorous coursework at TU Delft did not help either. But, I was fortunate enough to be surrounded by a circle of wonderful friends. Thanks to each one of you. Special thanks to Vamshi (bhaiya). I think he was the perfect senior I could have ever asked for. All his valuable advices worked wonders for me.

In the end, thanks to the most special ones - Mom and Dad and my grandmother (Mummy, Papa and Dadi). Although they were miles away, but they ensured that I was motivated and mentally strong throughout the entire journey. Its their blessings which has worked wonders for me. Also, a final mention to my friends and family members back home in India. Thanks all for your everlasting support.

Nikhil Awasthy
Delft, October 2019

Abstract

The performance of concrete is usually governed by its "strength" and "stiffness" properties. As most of the concrete structures are usually designed to last in service for a period of about half a century, it is important to understand the development of these "strength" and "stiffness" properties over the course of time. Based on the standard codes and practices, these properties are assumed to continuously increase with age assuming standard conditions (moist curing environment and temperature of 20° C), or at least remain constant in case of other curing conditions. However, few studies [27] [13] have reported a reduction in the trend of the strength and stiffness properties with time for the ordinary concrete of different strength mixes, when exposed to drying at different relative humidities after an initial moist curing period. Moreover, such decrease in trend has also been reported for a Geopolymer concrete upon drying at controlled lab conditions (20° C and 50%RH) after an initial moist curing period of 28 days [35]. It is not clear if the reduction in the trend observed is only temporary as a result of the imposed shrinkage deformations and eigen stresses, or if it is a permanent reduction as a result of microcracking. In this regard, it is aimed to understand the uncertainty in the development of the strength and stiffness properties of particularly the ordinary concrete mixes, which have been used across the world for a long time.

Accordingly, it is hypothesized that a similar reduction upon drying in the trend of mechanical properties as reported by Prinsse [35] for a Geopolymer might also occurs for the ordinary concrete mixes of various grades, which are cured and tested in the same way as the aforementioned Geopolymer concrete. Based on that, parameters such as the curing conditions, specimen size and the grade of concrete mix are assumed to influence the trend and a comprehensive literature study is performed in order to understand the influence of these assumed parameters on the mechanical properties - namely the compressive strength, splitting strength and elastic modulus over time. From the literature study, it is understood that there is some uncertainty in understanding the trend which is aggravated by the complex interdependency between the assumed parameters. Accordingly, an experimental program is set up to firstly verify whether there is a similar reduction in trend like the Geopolymer concrete and secondly to give more clarity on the complex interdependency between the assumed parameters. Further, the development of eigen stresses is understood to play a huge role in the trend of the measured mechanical properties over time and their influence might vary for the different tests. However, due to its temporary occurrence and larger testing frequency days, they are difficult to capture in the experiments. Accordingly, a FEM tool known as "FEMMASSE" is used, which can simulate the concrete behaviour by incorporating the heat and moisture models. Apart from considering the material effects like hydration, FEMMASSE can also capture the eigen stresses developed as a result of the thermal and moisture gradients. The software mostly finds application in the design of bridges and tunnels. Although, in this research study, the main purpose of using FEMMASSE is to firstly capture the shrinkage induced eigen stresses by simulating the tests at smaller intervals and secondly single out the influence of the studied parameters in order to give more clarity on the obtained experimental results.

The obtained experimental results indicate no major reduction in the trend of the studied mechanical properties in time as compared to the Geopolymer concrete. With regard to the studied parameters, it is found that for the chosen curing regime (28DM regime), the trend of both compressive and splitting strength is seen to be affected by the development of the eigen stresses. Interestingly, for the trend of splitting strength, a general pattern of increasing and stabilizing behaviour is observed which seems to be dependent also on the specimen size. However, due to the lack of knowledge of the actual magnitude of the eigen stresses coupled with other phenomena like the size effect and current state of hydration, it becomes challenging to explain the trend merely on the basis of experimental results.

In this regard, the use of numerical tool FEMMASSE is shown to help understand the experimental results at greater depth. Owing to the limitations of the software, only the tensile tests are simulated. Initially, it is understood that the attainment of the hygral equilibrium is dependent on the specimen size and the type of concrete, with the smaller specimen sizes and lower strength mixes reaching the equilibrium relatively quickly. The model is then extended to simulate the tensile tests - splitting and flexural and direct tension tests. It is concluded that drying after a moist curing period of 28 days affects the these tensile tests differently. In case of

the splitting tests, drying results in the temporary increase of the strength owing to the apparent prestressing at the core of the specimen, with the gradual stabilization of the trend as the specimen attains moisture equilibrium. This trend of temporary increase and gradual stabilization is dependent on the specimen size with the smaller specimens stabilizing at a relatively quicker time due to the faster attainment of the moisture equilibrium. However, in case of the flexural and direct tensile test, drying results in the temporary reduction in the flexural strength due to the reduction in the tensile capacity at the surface, followed by an increasing trend as the specimen starts attaining hygral equilibrium. This indicates that the surface failure tests like the direct tension and flexural are negatively affected (temporarily) by drying as compared to the interior failure tests like splitting test which is positively affected (temporarily) by drying.

From the research study, it is evident that there are no major reduction in the trend of strength and stiffness properties over time obtained experimentally until the period of 155 days. However, the presence of the eigen stresses, which not captured in the experiments, does influence the trend of the measured material properties over time. As long as these eigen stresses are present, the material strength determined experimentally might be deceptive, as evident from the simulations of the tensile tests performed in the study. It is understood that unless there is hygral equilibrium (no eigen stresses) across the specimen, the measured material properties might underestimate the actual material strength in case of the flexural and direct tension tests and overestimate in case of the splitting tensile tests. In the engineering practice, especially in mass concrete structures, the eigen stresses could be present throughout the service life of the structure. Thus, the experimentally obtained material strength used for designing the structure might be deceptive due to the influence of the eigen stresses.

Contents

List of Figures	ix
List of Tables	xv
1 Introduction	1
1.1 Background and Motivation	1
1.2 Initial Hypothesis	5
1.3 Outline of the Thesis	6
2 Literature Review	7
2.1 General	7
2.2 Compressive Strength	8
2.2.1 Development with age	8
2.2.2 Influence of curing conditions	9
2.2.3 Influence of specimen size	14
2.3 Elastic Modulus	15
2.3.1 Development with age	16
2.3.2 Influence of curing conditions	17
2.3.3 Influence of specimen size	19
2.4 Splitting Tensile Strength	20
2.4.1 Development with age	21
2.4.2 Influence of curing conditions	22
2.4.3 Influence of specimen size	25
2.5 Drying Shrinkage	26
2.6 Conclusion	27
3 Methods	31
3.1 Introduction	31
3.2 Research Objectives	32
3.3 Research Questions	32
3.4 Research Strategy	33
3.5 Research Methodology - Experimental	35
3.5.1 Materials and Mix Design used	35
3.5.2 Casting, demoulding and curing procedures	37
3.5.3 Testing Procedures	40
3.6 Research Methodology - Numerical Modelling	45
3.6.1 "FEMMASSE" : An Introduction	45
3.6.2 General Description of the model used	45
3.6.3 Geometry of the model	46
3.6.4 Material properties	46
3.6.5 Hygral properties	47
3.6.6 Loading and Support conditions	48
3.6.7 Meshing and Analysis	49
3.6.8 Validation of FEMMASSE	49
3.6.9 Analytical approach of understanding drying profile	51
4 Results	53
4.1 Experimental Results	53
4.1.1 Compressive Strength	53
4.1.2 Splitting Tensile Strength	56
4.1.3 Elastic Modulus	59
4.1.4 Drying Shrinkage	60

4.2	Modelling Results	62
4.2.1	Validation for hygral behaviour	62
4.2.2	Stress profile and comparison with Analytical approach	66
4.2.3	Validation for Splitting tests	66
4.2.4	Simulation of Hygral Behaviour : Current Experiment	67
4.2.5	Simulation of Splitting Strength results : Current experiment	69
4.2.6	Simulation of the Direct Tensile Test	71
4.2.7	Simulation of the Flexural Strength test	72
5	Discussion	75
5.1	Comparison with Geopolymer concrete	75
5.2	Effect of the parameters on the trend of mechanical properties	77
5.3	Analysis of Modelling results	83
6	Conclusions and Recommendations	103
6.1	Conclusions.	103
6.2	Recommendations	105
	Appendices	107
A	Drying Shrinkage Models	109
B	Mesh Analysis	113
	Bibliography	115

List of Figures

1.1	Examples highlighting the properties of concrete	1
1.2	Development of compressive strength based on varied curing conditions [28]	2
1.3	Variation of the Compressive Strength (left) and E-modulus (right) of regular concrete (G1-G5) and mortar (M) under different drying and heating conditions [27]	2
1.4	Development of the splitting tensile strength with age for a High Strength concrete mixture (C55/67) [13]	3
1.5	Graph showing variation of Splitting Tensile Strength (STS) with age for NSC (C30) and HSC (C65) [12]	3
1.6	Development of properties relative to 28 day for (a) S50 (50%FA+50%BFS) mix and (b) S100 (100% BFS) mix [35]	4
1.7	(a) Development of properties with time for S50 (50% slag+50% Fly Ash) for Geopolymer concrete, (b) Variation of the Elastic Modulus of samples expressed as relative to the samples removed from curing room, (c) Relation between weight loss and Elastic modulus of S50 and S100 mixes [35]	5
2.1	Ratio of the development of Compressive Strength at any age / Compressive strength at 95 days with age. All specimens are cured at 100% RH until 2 hours before testing [9]	9
2.2	Development of compressive strength with age for untreated UHSC (The dotted line indicate the trend plotted using equation 2.3) [15]	9
2.3	Trend of compressive strength with age for UHSC with different types of curing regimes [32]	11
2.4	The effect of development of compressive strength with age based on different curing conditions [31]	11
2.5	(a) Trend of compressive strength with age based on different curing conditions for High Strength concrete (LH and UH: Lower bound mix of HSC and UHSC without silica fume , LU and UU : Upper bound mix of HSC and UHSC (with silica fume) [19] (b) Compressive Strength of 100x200 mm specimen at 28 days based on different curing regimes [24]	12
2.6	The influence of varying curing regime-s on the compressive strength [34]	13
2.7	The eigen stresses due to soaking (circumferential swelling) [6]	13
2.8	Variation of compressive strength with different cube sizes at 28 and 90 days [37]	14
2.9	Variation of compressive strength for 3 mixes with age for different sized specimens [3]	15
2.10	Relation between Modulus of Elasticity and Compressive Strength for different strength of concrete [28]	17
2.11	Development of Static (E_c) and Dynamic Modulus (E_{cu}) of Elasticity for air (S) and moist cured (N) specimens [21]	19
2.12	Correlation between static modulus of elasticity of 100mm and 150mm sized specimens [22]	19
2.13	Variation of modulus of elasticity of C45 and C60 specimens for different diameters [10]	20
2.14	Development of tensile strength/tensile strength at 28 days with age for different curing conditions [18]	22
2.15	Development of splitting tensile strength with age for Normal weight concrete and (b) Relative Humidity profile across the width of the specimen [17]	23
2.16	(a) Variation of splitting tensile strength with change in relative humidity for concrete and mortar .(b) Variation of Gap strain with change in relative humidity for two concrete mixes [23]	24
2.17	Variation of f_n/f_{n150} for different diameter sizes according to various authors [8]	25
2.18	Variation of Splitting tensile strength with length of the specimen [23]	25
2.19	Loss of water with varying relative humidity [28]	26
2.20	(a) Relation between shrinkage strain, water cement ratio, and cement content [38] (b) Comparison of Drying, Autogenous and Total Shrinkage of UHFRC with age	27
2.21	Shrinkage cracks on concrete surface	27

3.1	Figure depicting the region of influence of tensile eigen stresses	32
3.2	A schematic representation of the parameters investigated and mechanical properties tested	33
3.3	A schematic representation of number of prism specimens	34
3.4	A schematic representation of number of 50mm cubes	34
3.5	A schematic representation of the number of 150mm cubes	35
3.6	(a) Ingredients used for NSC and HSC mix (b) Ingredients used for UHSC mix	37
3.7	A 100L Concrete mixer for mixing the ingredients	37
3.8	(a) Adding of water mixed with superplasticizer (b) Adding of fibres in case of UHSC mix	38
3.9	Prepared mix for (a) NSC (b) UHSC	38
3.10	(a) Pouring of NSC mix in prismatic moulds NSC (b) Pouring of UHSC mix	39
3.11	Covering of moulds with plastic sheets	39
3.12	(a) Demoulding of UHSC prism (b) NSC specimens taken to the fog room	40
3.13	Preparation for E-modulus test (a) labelling of reference points with plastic mask (b) specimen after gluing of metallic devices	40
3.14	Specimen with LVDTs attached placed in the Toni Bank machine	41
3.15	Preparation for Compression Testing - (a) Marking of lines before wet sawing , (b) Wet sawing process	41
3.16	Testing of Compressive Strength of cube	42
3.17	Testing of Splitting tensile strength of cube specimen	43
3.18	(a) Test setup for measuring Drying Shrinkage. (b) Overview of the prisms used for drying shrinkage measurement	44
3.19	Inspection of surface cracking using portable microscope	44
3.20	General Model used for - (a) Splitting Tensile test (b) Flexural strength test (c) Direct tension test using a notch (d) Direct tension using an imperfection	46
3.21	Tensile softening curve defined for both NSC and HSC mixes	47
3.22	Diffusion curve as defined for (a) NSC mix and (b) HSC mix	48
3.23	Meshing layout for the splitting test for (a) 50mm (b)100mm (c) 150mm specimen and for the (d) flexural test of 100x100x400 prisms (e) direct tensile test with a notch (e) direct tensile test with an imperfection	50
3.24	Subdivision of shrinkage profile into its mean, gradient and eigen components	51
4.1	Trend of the Compressive Strength with time for different cement based concrete mixes. Note: CM - Continuously Moist cured until test age and 28DM - 28 day moist cured and then exposed to controlled lab conditions until test age	54
4.2	Trend of the Compressive Strength of different specimen sizes with time : Continuous moist cured regime. Note: CM - Continuously Moist cured until test age and 28DM - 28 day moist cured and then exposed to controlled lab conditions until test age	55
4.3	Trend of the Compressive Strength of different specimen sizes with time : 28 day moist cured regime. Note: CM - Continuously Moist cured until test age and 28DM - 28 day moist cured and then exposed to controlled lab conditions until test age	56
4.4	Trend of the Splitting Strength of different specimen sizes with time : 28 day moist cured regime. Note: CM - Continuously Moist cured until test age and 28DM - 28 day moist cured and then exposed to controlled lab conditions until test age	57
4.5	Comparison of the trend of the Splitting Strength of NSC and HSC specimens. Note: CM - Continuously Moist cured until test age and 28DM - 28 day moist cured and then exposed to controlled lab conditions until test age	57
4.6	Trend of the Splitting Strength of different specimen sizes with time : Continuous moist cured regime. Note: CM - Continuously Moist cured until test age and 28DM - 28 day moist cured and then exposed to controlled lab conditions until test age	58
4.7	Trend of the Splitting Strength of different specimen sizes with time : 28 day moist cured regime. Note: CM - Continuously Moist cured until test age and 28DM - 28 day moist cured and then exposed to controlled lab conditions until test age	59
4.8	Trend of the Elastic Modulus of different types of concrete with time. Note: CM - Continuously Moist cured until test age and 28DM - 28 day moist cured and then exposed to controlled lab conditions until test age	59
4.9	Drying Shrinkage strain with time for different concrete mixes	61

4.10	Variation of the Weight loss expressed as a % of initial value with age for the different cement based mixes	61
4.11	Hygral boundaries of the cubes and cylinder profile used for simulation	62
4.12	Cross section cut on cylinder and cube specimen	63
4.13	Humidity contour plots simulated by using FEMMASSE	63
4.14	Comparison of humidity profile of cubical and cylindrical specimens	64
4.15	Humidity profile across the concrete cross section based on the different values of film coefficient	65
4.16	Variation in the humidity profile based on different diffusion coefficients	65
4.17	Stress profile across the concrete section	66
4.18	Development of Splitting tensile strength (STS) with age : (a) Results of FEMMASSE (b) Experimental results by Hanson [17]	67
4.19	Contour plot of relative humidity of NSC mix for various specimen sizes	68
4.20	Major Stress contour plot for NSC mix of various specimen sizes	68
4.21	Relative Humidity and Major Stress contour plots for HSC mix	69
4.22	Relative humidity contour plot for 100mm cube at 3 years for (a) NSC mix (b) HSC mix	69
4.23	Simulation of the splitting tensile strength for the NSC specimens of different sizes	70
4.24	Simulation of the splitting tensile strength for the HSC specimen-100mm	70
4.25	Simulation of the splitting tensile strength for the HSC specimen-150mm	71
4.26	Simulation of the splitting tensile strength for the HSC specimen-50mm	71
4.27	Simulation of the direct tensile strength for the NSC specimen	72
4.28	Simulation of the direct tensile strength for the HSC specimen	72
4.29	Flexural strength development with time for NSC specimen -100x100x400mm	73
4.30	Flexural strength development with time for HSC specimen - 100x100x400mm	73
4.31	Flexural strength development with time for NSC specimen of size 50x50x400mm	74
5.1	Comparison of mechanical properties of cement based concrete mixes with the Geopolymer mix prepared by Prinsse [35] (a) Compressive Strength (b) Elastic Modulus (c) Splitting Tensile Strength	76
5.2	Comparison of the weight loss with increasing concrete ages of different concrete mixes	77
5.3	Comparison of mechanical properties of cement based concrete mixes with Geopolymer ones (a) Compressive Strength (b) Elastic Modulus (c) Splitting Tensile Strength	79
5.4	Comparison of the splitting tensile strength of 28DM regime to the CM regime for NSC mix with the data from Hanson [17]	80
5.5	Comparison of the elastic modulus of various regimes as reported in Asselanis et al. [5]	81
5.6	Comparison of the compressive strength of various regimes based on different specimen sizes with the results of Soroka and Baum [37]	82
5.7	Development of Splitting tensile strength (STS) with time for Normal Strength concrete (NSC) of different sizes	83
5.8	Mechanical scheme of the splitting test on a cube	84
5.9	Cross section cut as indicated by the dotted black line for the NSC specimens	84
5.10	Development of Splitting tensile strength (STS) with time for Normal Strength concrete(NSC) specimens. In the figure A,B,C,D corresponds to concrete age of 56 days,155 days, 2 years and 5 years respectively and 1,2,3 indicate the specimen size of 50mm,100, and 150mm respectively	85
5.11	Major stress contours for (a) Point A1 - 50mm specimen (b) Point A2- 100mm specimen and (c) Point A3 - 150mm specimen (d)Combined Stress Profile at location A across the cross section as indicated in 5.9	85
5.12	Major stress contours for (a) Point B1 - 50mm specimen (b) Point B2- 100mm specimen and (c) Point B3 - 150mm specimen (d)Combined Stress Profile at location B across the cross section as indicated in 5.9	86
5.13	Major stress contours for (a) Point C1 - 50mm specimen (b) Point C2- 100mm specimen and (c) Point C3 - 150mm specimen (d)Combined Stress Profile at location C across the cross section as indicated in 5.9	86
5.14	Major stress contours for (a) Point D1 - 50mm specimen (b) Point D2- 100mm specimen and (c) Point D3 - 150mm specimen (d)Combined Stress Profile at location D across the cross section as indicated in 5.9	87

5.15 Development of Splitting tensile strength (STS) for high strength concrete (HSC) specimen - 100mm cube	88
5.16 Development of the splitting tensile strength with age for a High Strength concrete mixture (C55/67) [13]	88
5.17 Development of Splitting tensile strength (STS) with time for High Strength concrete(HSC) specimens. In the figure A,B,C,D correspond to the concrete age of 35 days, 49 days, 91 days and 2 years respectively. Index 1,2,3 indicate the point corresponding to the 50mm, 100mm and 150mm specimens respectively	89
5.18 Major stress contours at location A - 35 days (a) A1-50mm specimen (b) A2-100mm specimen and (c) A3- 150mm specimen ; (d)Combined Stress Profile at location A - 35 days across the cross section as indicated in 5.9	90
5.19 Major stress contours at Location B - 49 days (a) B1- 50mm specimen (b) B2- 100mm specimen and (c) B3-150mm specimen ; (d)Combined Stress Profile at point B -49 days across the cross section as indicated in 5.9	90
5.20 Major stress contours at Location C - 91 days (a) C1- 50mm specimen (b) C2- 100mm specimen and (c) C3-150mm specimen. (d)Combined Stress Profile at point C -91 days across the cross section as indicated in 5.9	91
5.21 Major stress contours at Location D - 2 years (a) 50mm specimen (b) 100mm specimen and (c) 150mm specimen ; (d) Combined Stress Profile at point D -2 years across the cross section as indicated in 5.9	91
5.22 Development of direct tensile strength with age for (a) NSC specimens (b) HSC specimens	92
5.23 Mechanical scheme of the direct tensile model used in FEMMASSE	93
5.24 Major stress profile across the cross section for the various locations as indicated in 5.22 for (a) NSC specimens (b) HSC specimens	93
5.25 Major stress contours for NSC specimens at (a) Point A - 38 days (b)Point B- 56 days (c) Point C - 2 years and (d) Point D- 20 years	94
5.26 Major stress contours for HSC specimens at (a) Point A - 38 days (b)Point B- 56 days (c) Point C - 2 years and (d) Point D- 20 years	94
5.27 Development of the direct tensile strength for the model with a notch and an imperfection. Note : A1 and A2 indicates the value of the imperfection and notch model respectively at 38 days. B1 and B2 indicates the value of the imperfection and notch model respectively at 91 days	95
5.28 Major stress contour plots at the location (a) A1 - 38 days (b) B1- 38 days (c) A2 - 91 days (d) B2 - 91 days	96
5.29 Crack width contours at the location (a) A1 - 38 days (b) B1- 38 days (c) A2 - 91 days (d) B2 - 91 days	96
5.30 Comparison of the direct tensile trend of (left) current simulation using FEMMASSE and (right) trend from the study of Bonzel	97
5.31 (a) Cross section cut as indicated by dotted black line for the flexural test specimen (b) General deformed shape of the specimen loaded under flexural test set up	97
5.32 Development of flexural strength with age for (a) NSC specimens (b) HSC specimens	98
5.33 Horizontal stress contours for NSC specimens at (a) Point A - 38 days (b)Point B- 91 days (c) Point C - 2 years and (d) Point D- 20 years	98
5.34 Horizontal stress contours for HSC specimens at (a) Point A - 38 days (b)Point B- 91 days (c) Point C - 2 years and (d) Point D- 20 years	99
5.35 Horizontal stress (Sxx) profile across the cross section for the various locations as indicated in 5.32 for (a) NSC specimens (b) HSC specimens	99
5.36 Development of Flexural strength with age for 100x100 and 50x50mm specimens	100
5.37 (a) Combined Horizontal stress profile across the width at 38 days (b) Horizontal stress contour plot for 100x100 specimens at 38 days and (c) Horizontal stress contour plot for 50x50 specimen at 38 days	101
5.38 (a) Combined Horizontal stress profile across the width at 2 years (b) Horizontal stress contour plot for 100x100 specimens at 2 years and (c) Horizontal stress contour plot for 50x50 specimen at 2 years	101
5.39 Comparison of the trend of (left) direct tensile strength using both notch and imperfection model and (right) flexural strength model	102

B.1	NSC concrete specimen of mesh element size (a) 2.5mm (b) 5mm (c) 10mm	113
B.2	(a) Variation of relative humidity profile across the width of the specimen - 28 days (b) Variation of major stress across the width at 28 days	114

List of Tables

1.1	Splitting tensile Strength (STS) values at different age of concrete for both NSC(C30) and HSC (C65) [12]	4
2.1	Concrete strength classification according to fib 2010 [14]	7
2.2	The strength attained after drying as a fraction of the strength attained on moist curing until test age (indicated by R) for normal and high strength concrete mixes [9]	10
2.3	Ratio of compressive strength after one year in case of the moist cured (fcW'), air cured (fcA') and sealed (fcS') specimens [3]	10
2.4	Compressive strength of concrete based on various curing conditions at various ages [34]	13
2.5	Values of compressive strength for various mixes exposed to different curing regimes at 7,28 and 90 days [16]	15
2.6	Predictive empirical equations collected from literature relating Elastic Modulus with the compressive strength of concrete	16
2.7	Comparison of Elastic Modulus for different curing conditions [5]	18
2.8	Relation between Compressive and Direct Tensile strength of concrete [28]	20
2.9	Predictive equations of Splitting tensile strength from Compressive strength	21
2.10	Splitting tensile strength for water and air cured specimens at 84 and 365 day [11]	24
3.1	Mix Design for NSC	36
3.2	Mix Design for HSC	36
3.3	Mix Design for UHSC	36
4.1	Compressive Strength values for the three types of concrete mixes. Note: CM - Continuously Moist cured until test age and 28DM - 28 day moist cured and then exposed to controlled lab conditions until test age	54
4.2	Compressive strength values for NSC of different specimen sizes. Note: CM - Continuously Moist cured until test age and 28DM - 28 day moist cured and then exposed to controlled lab conditions until test age	55
4.3	Splitting tensile strength values for the three types of concrete mixes. Note: CM - Continuously Moist cured until test age and 28DM - 28 day moist cured and then exposed to controlled lab conditions until test age	56
4.4	Splitting tensile strength values for NSC mix of different sizes. Note: CM - Continuously Moist cured until test age and 28DM - 28 day moist cured and then exposed to controlled lab conditions until test age	58
4.5	Elastic modulus values for the three types of concrete mixes. Note: CM - Continuously Moist cured until test age and 28DM - 28 day moist cured and then exposed to controlled lab conditions until test age	60
5.1	Mechanical properties for the three types of concrete mixes relative to 28 days	78
5.2	Comparison of the compressive strength of 28DM regime to the CM regime from various literature	80
5.3	Comparison of CM/28DM regime for Elastic Modulus of different mixes at 91 days	81

1

Introduction

1.1. Background and Motivation

Apart from water, concrete is the most consumed material on the planet. An ordinary concrete is composed of cement, aggregates and water. The excellent water resistant capacity of concrete, as shown in figure 1.1a, the ability of concrete to be molded into different forms, as shown in figure 1.1b, combined with its cheap value in the market, makes it an ideal material in the construction sector as compared to steel [28]. While using concrete as a building material, the two important characteristics which influences the performance is its "strength" and "stiffness". The strength of the concrete is dependent on factors like the water cement ratio, aggregate characteristics, admixtures type, curing conditions, etc. On the other hand, the stiffness or the Elastic Modulus of concrete depends on aggregate type, influence of the cement paste matrix and testing parameters like mix proportions and curing conditions.



(a) Eastern Scheldt Storm Surge Barrier, The Netherlands

(b) Santa Cruz de Tenerife, Spain

Figure 1.1: Examples highlighting the properties of concrete

As most of the concrete structures are designed for a service period of 50 to 60 years, it becomes necessary to understand the development of "strength" and "stiffness" properties of concrete with time. According to the various concrete codes and widely known textbooks, the strength of concrete is usually believed to increase continuously with age, assuming standard conditions (moist curing environment and normal temperature of 20° C). As an example, it is reported in [28] that under moist curing conditions, the compressive strength continuously increases with age. As a matter of fact, even for other curing conditions, the compressive strength is seen to increase at a relatively lesser rate or at least remain constant after a certain age (see figure 1.2). Moreover, the elastic modulus is usually empirically related to the compressive strength implying that it follows a similar trend too. However, a question which strikes at this point is, "Is this always true ?"

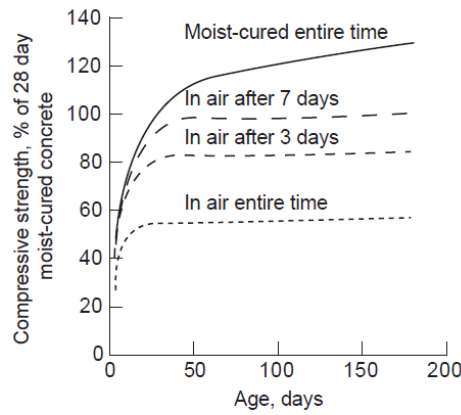


Figure 1.2: Development of compressive strength based on varied curing conditions [28]

Interestingly, there have been researches recently, which haven't shown a steady increase of strength or stiffness with time for an ordinary concrete, as believed in the concrete codes and text books. To make matter worse, there have been occasions where the strength and stiffness have decreased with time. A study by Maruyama et al. [27] report that drying at varying degree of relative humidity can lead to fluctuations in the compressive strength and elastic modulus of ordinary concrete mixes. All the concrete specimens are sealed cured for the duration of two months at 20° C and then some of the specimens are placed in RH controlled chambers and others in temperature controlled chambers for a duration of 5 months. Interestingly, at a relative humidity between 40 to 60 %, there is a reduction of both compressive strength and elastic modulus (as indicated by red dotted line in the figure 1.3). This reduction is explained by the development of cracks as a result of the differential shrinkage between the aggregate and mortar. It is important to note that the extent of decrease varies for the different types of aggregate and the concrete mixtures used.

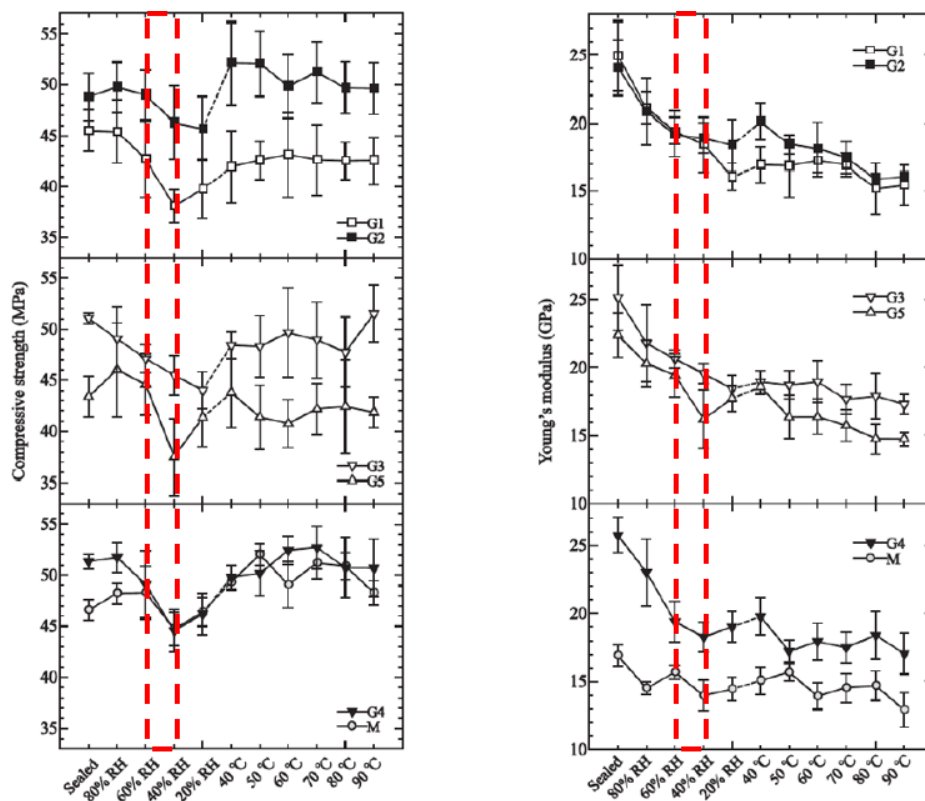


Figure 1.3: Variation of the Compressive Strength (left) and E-modulus (right) of regular concrete (G1-G5) and mortar (M) under different drying and heating conditions [27]

As a part of a larger study, Eva O. L. Lantsoght [13] studied the development of mechanical properties of a high strength concrete mix (C55/67) for a period of 20 years. The specimens are casted along with the bridge segments and stored in the box girder bridge all the while before testing. It is observed (see figure 1.4) that in case of the splitting tensile strength, there is an initial increase followed by a reduction at a period of 2 years and finally a constant value from 5 years onward until 20 years. Although, the reduction in strength (as indicated by the red dotted line) is only temporary, it becomes important to understand the reason behind it.

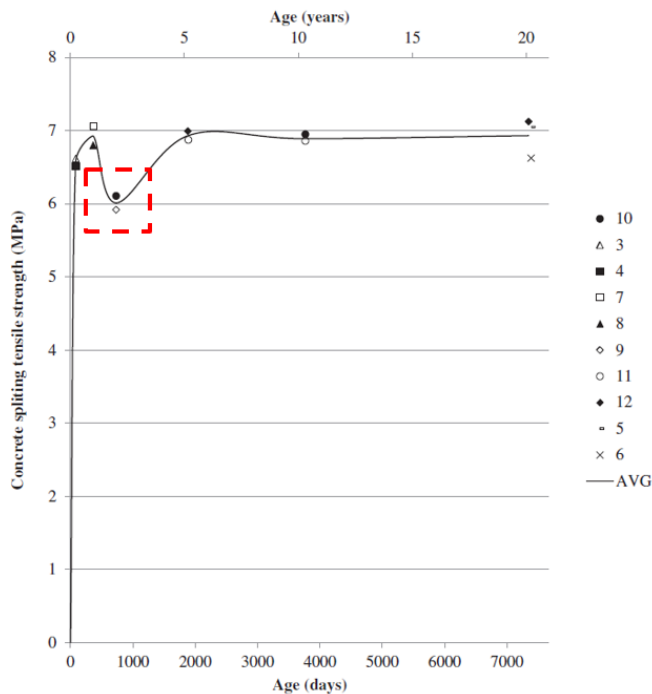


Figure 1.4: Development of the splitting tensile strength with age for a High Strength concrete mixture (C55/67) [13]

Moreover, at Stevin II Lab, Dr. ir. Y. Yang [12] observed that even after applying moist conditions throughout until testing, the trend of the splitting tensile strength (STS) with age for Normal Strength Concrete (NSC) increases gradually for 28 days and becomes almost constant at 56 days. However, for High Strength Concrete (HSC), it increases sharply attaining maximum at 56 days and strangely drops at 196 days. However, on looking at the standard deviation from table 1.1 and figure 1.5 , it seems that the decrease is just due to scatter.

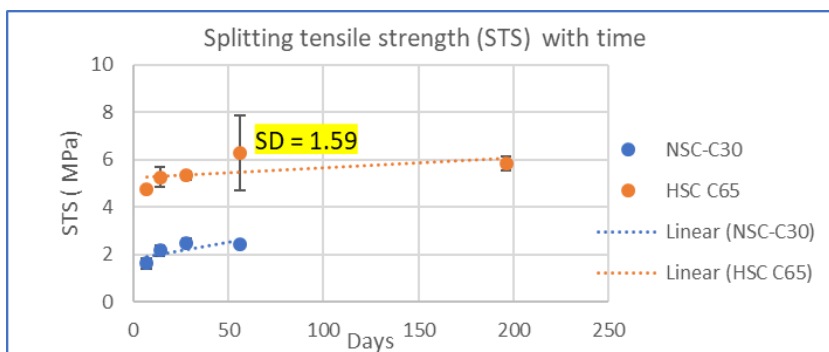


Figure 1.5: Graph showing variation of Splitting Tensile Strength (STS) with age for NSC (C30) and HSC (C65) [12]

Table 1.1: Splitting tensile Strength (STS) values at different age of concrete for both NSC(C30) and HSC (C65) [12]

DAYS	STS(NSC : C30)			STS (HSC: C65)		
	Value	Mean	SD	Value	Mean	SD
7	1.46	1.497	0.025	4.64	4.74	0.063
	1.49					
	1.52					
	1.52					
14	1.88	1.953	0.077	5.34	5.27	0.3
	1.95					
	2.08					
	1.9					
28	2.27	2.435	0.102	5.53	5.34	0.122
	2.44					
	2.49					
	2.54					
56	2.27	2.4725	0.165	8.12	6.29	1.123
	2.73					
	2.46					
	2.43					
196	no value	no value	no value	5.81	5.86	0.303

Apart from the regular concrete, there have also been signs of reduction in the mechanical properties in time for a Geopolymer concrete, as reported in the master thesis study of Prinsse [35]. In a Geopolymer, unlike the regular concrete, portland cement is completely replaced by an alternative binder initiated using alkaline activators. In the study of Prinsse [35], two types of mixes are prepared : S50 mix (50% Fly Ash (FA) and 50% Blast Furnace Slag (BFS)) and S100 mix (100% BFS). The samples from both the mixes are kept under moist curing conditions for 28 days (fog room at 20° C and 99% RH), then exposed to the controlled lab conditions (20° C and 55% RH) and finally tested at 28, 56 and 91 days. It is initially hypothesized that the mix with the higher percentage of BFS will result in the reduction of the various mechanical properties over time. However, the results show that there is a higher reduction for the strength and stiffness properties of S50 type mix as compared to S100 mix, implying that the hypothesis is not true (as shown in figure 1.6).

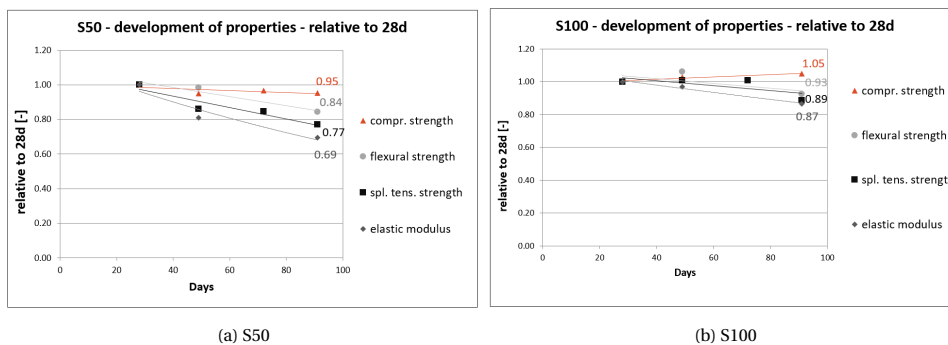


Figure 1.6: Development of properties relative to 28 day for (a) S50 (50%FA+50%BFS) mix and (b) S100 (100% BFS) mix [35]

Subsequently, in the later study, it is expected that the reduction in the strength and stiffness properties is due to the influence of drying. This further study is focused on the elastic modulus as it shows the largest reduction among all the properties (31 % for S50 and 13% for S100). During the course of the study, some samples are kept in the moist room for a period of 92 days and then tested for elastic modulus. In this case, an

increase in the properties is found as compared to 28 days value, as shown in figure 1.7a. However, when these 92 day cured samples are placed under controlled lab conditions (20° C and 55% RH) again, the development of elastic modulus over time follows a similar decreasing trend (shown in figure 1.7b) as observed before for the samples exposed to the lab conditions after moist curing for 28 days. With this, it was indicated that the decrease is due to the influence of drying. This was supported by the linear relation between the moisture loss and reduction in the elastic modulus, as shown in figure 1.7c.

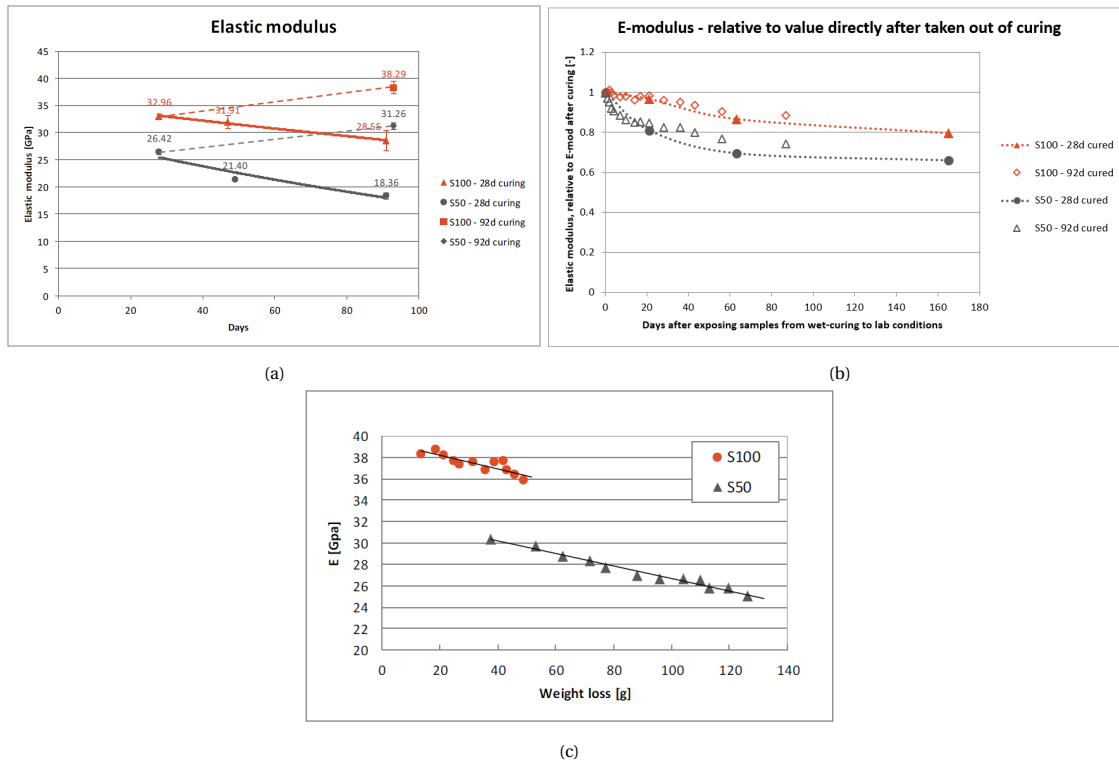


Figure 1.7: (a) Development of properties with time for S50 (50% slag+50% Fly Ash) for Geopolymer concrete, (b) Variation of the Elastic Modulus of samples expressed as relative to the samples removed from curing room, (c) Relation between weight loss and Elastic modulus of S50 and S100 mixes [35]

It is pointed out by Prinsse [35] that Geopolymer concrete is relatively new in the concrete industry and plenty of research is still going on with regard to its mechanical properties and structural applicability. However, the regular concrete mixes have been used for a long time across the world and a much comprehensive understanding of the development of the mechanical properties with time becomes even more vital. Until now, there is some uncertainty seen in the development of these properties over time. On one hand, the results of the study by Dr. ir. Y. Yang [12] indicate that the reduction in the properties could be just due to scatter. On the other hand, the study by Maruyama et al. [27] show that drying can have a negative influence on the mechanical properties of ordinary concrete too, similar to the Geopolymer concrete reported by Prinsse [35]. Thus, there is a need of a detailed investigation to get more insight on the development of mechanical properties of ordinary concrete with time.

1.2. Initial Hypothesis

A similar reduction in the trend of the strength and stiffness properties over time for a Geopolymer mix designed by Prinsse [35] is assumed to occur for the ordinary concrete mixes. If drying does affect the development of strength and stiffness properties with time, it is expected that the specimen size could play a role. Moreover, based on the results of Eva O. L. Lantsoght [13], it is also expected that the effect of drying on the mechanical properties could depend on the strength of the ordinary concrete mix designed. In this regard, as an initial step, it becomes important to dig deeper in the literature to understand the development of various mechanical properties in time for the ordinary concrete mixes based on the possible parameters stated

previously like the varying curing conditions, specimen size and strength grade.

1.3. Outline of the Thesis

Chapter 1 covers the general background and the motivation behind carrying out the research study. An initial hypothesis is also postulated in this chapter.

Chapter 2 covers the literature study where the current research outlook of the mechanical properties of different types of cement based concrete based on the assumed parameters - development with age, influence of curing condition and varying specimen size, is understood.

Chapter 3 covers the methods used in the research study. The research objectives and questions are stated along with the research strategy used. Accordingly, the two major research methodology used in this research - experimental and modelling approach are discussed in detail.

Chapter 4 covers the experimental and modelling results found out in the study.

Chapter 5 covers the discussion of the obtained modelling and experimental results with respect to the research objectives and questions.

Chapter 6 covers the major conclusions of the study along with few recommendations for future works.

2

Literature Review

2.1. General

The understanding of the mechanical properties of concrete is very important for its structural application. The properties like the compressive strength and the elastic modulus usually governs the construction process of the concrete structures. As an example, the ideal time of formwork removal and application of prestressing is highly influenced by the above two properties [43]. As concrete is weaker in tension, the tensile strength of concrete is equally important, especially when it comes to resisting cracking for serviceability limit state (SLS). The improper understanding of these properties could lead to catastrophic failure of the structure.

Even more important is the understanding of the development of these properties with time, as concrete structures are built to last for approximately 50-60 years. As mentioned in the previous chapter, an initial hypothesis is postulated wherein a similar reduction in the trend of the strength and stiffness over time for a Geopolymer mix designed by Prinsse [35] is assumed to occur for the ordinary concrete mixes. Accordingly, it is stated that parameters like the curing conditions, specimen size and type of concrete could play a role. Thus, it becomes important to initially understand the influence of each of these parameters on the mechanical properties of concrete.

The mechanical properties of concrete considered in this study are the same as considered by Prinsse [35] namely the compressive strength, splitting tensile strength and the elastic modulus. For each of these properties, the initial focus is to understand the development with age, the influence of curing conditions, the influence of varying specimen sizes for the different grades of regular concrete. Additionally, the drying shrinkage behavior of the various types of concrete is also measured. For classifying the types of concrete based on strength, the following strength classification by fib [14] as shown in figure 2.1 is used.

Table 2.1: Concrete strength classification according to fib 2010 [14]

concrete type	strength class $f_{ck}/f_{ck,cube}$						
low strength concrete	C8/10	C12/15	C16/20				
normal strength concrete	C20/25	C25/30	C30/37	C35/45	C40/50	C45/55	C50/60
high strength concrete	C55/67	C60/75	C70/85	C80/95	C90/105	C100/115	
ultra-high strength concrete ¹⁾	C110/130, C120/140						

2.2. Compressive Strength

It is widely known that concrete is much stronger in compression as compared to tension. This itself highlights the importance of the compressive strength of concrete. Moreover, most of the codes and practices adopt compressive strength as the benchmark and the other properties like the modulus of elasticity and the tensile strength are empirically related to it. The designers and contractors are often concerned about the 28th day compressive strength, as it is believed that concrete gains sufficient strength by that time. It is observed from figure 1.2 that the strength is believed to continuously increase with time under moist curing conditions or at least stay constant under various curing conditions. However, it is seen from few studies [27] [12], that there could be certain discrepancies.

The trend of compressive strength with increasing age can vary for the different types of concrete mixes considered. Moreover the influence of varying curing conditions and specimen sizes can also have a different effect on the development of compressive strength for different types of concrete considered.

2.2.1. Development with age

The trend of the compressive strength with age is different for the various types of concrete considered. It is often difficult to make a comparison due to the wide range of variable parameters used in order to generate a concrete mix. Nevertheless, the idea is to understand the basic trend of compressive strength with time for the different concrete types.

According to Eurocode 2 [2], the compressive strength of concrete increases with increasing age and at any age "t", it is given by equation 2.1.

$$f_{cm}(t) = \beta_{cc}(t) f_{cm} \quad (2.1)$$

where,

$$\beta_{cc}(t) = \exp \left\{ s \left[1 - \left(\frac{28}{t} \right)^{0.5} \right] \right\}$$

s is the coefficient depending on type of cement

f_{cm} is the mean compressive strength in MPa

It is important to note that equation 2.1 is formulated assuming a mean temperature of 20° C and moist curing until test age. Moreover, it is only valid for a strength class lower than C90/105.

According to ACI [1], the compressive strength of concrete at any time "t" beyond 28 days is given by,

$$f_{c,t} = f_{c,28} \left\{ \frac{t}{\alpha + (\beta \cdot t)} \right\} \quad (2.2)$$

where, α and β are parameters depending on cement type and curing methods respectively.

According to Carrasquillo et al. [9], there is a higher rate of increase of compressive strength of High Strength concrete, HSC (at least 62 MPa) at earlier stages as compared to Medium Strength concrete, MSC (41 to 62 MPa) and Normal Strength concrete, NSC (21 to 41 MPa). However, at later stages, there are almost no differences (see figure 2.1). It is reported that the increase in the strength of HSC at earlier stages is due to the high heat of hydration as a result of the high cement content. The ratios of the 7 day to 95 day strength is 0.6 for NSC, 0.65 for MSC and 0.73 for HSC.

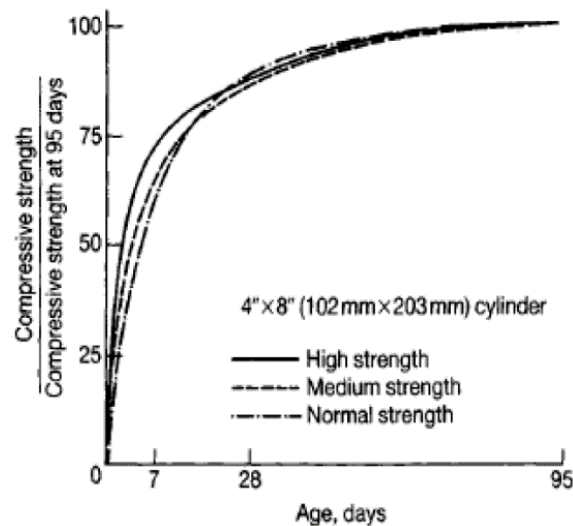


Figure 2.1: Ratio of the development of Compressive Strength at any age / Compressive strength at 95 days with age. All specimens are cured at 100% RH until 2 hours before testing [9]

Graybeal [15] reported that the compressive strength of the untreated UHSC (126 MPa to 193 MPa) increases with age and the trend (for $f_c = 126$ MPa) is found to be in line with the Weibull Cumulative function given by the equation 2.3

$$f_{c,t} = f_c \left\{ 1 - \exp \left\{ - \left\{ \left(\frac{t - 0.9}{3} \right)^{0.6} \right\} \right\} \right\} \quad (2.3)$$

where, f_c is the 28 day compressive strength in MPa

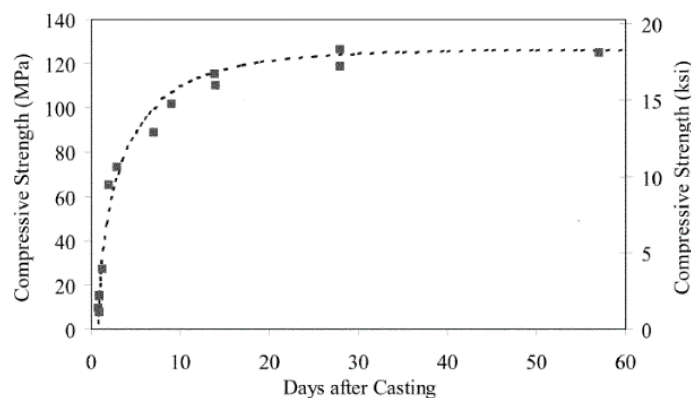


Figure 2.2: Development of compressive strength with age for untreated UHSC (The dotted line indicate the trend plotted using equation 2.3) [15]

2.2.2. Influence of curing conditions

The curing of concrete is vital for the attainment of its target compressive strength. The curing conditions can be varied in terms of temperature, relative humidity, moisture condition, duration, etc. In the past, various researchers have reported that different curing conditions could cause such varying strength behaviour over time for the ordinary concretes of different grades.

Way back in the 1980s, Carrasquillo et al. [9] did a study on the effect of curing on the compressive strength for both Normal Strength Concrete (NSC) and High Strength Concrete (HSC) mixes. It is reported that drying at 50 % RH after an initial 7 and 28 day moist curing period results in reduction of the compressive strength at

28 days and 95 days respectively relative to the specimens which are continuously moist cured (refer table 2.2 for exact figures). Moreover, the HSC specimens shows higher reduction as compared to the NSC ones. This is in consistent to what is reported by Hameed [16] later on. The greater reduction for HSC mixes is mentioned by Klieger [20] to be as a result of the insufficient hydration due to its low w/c ratio.

Table 2.2: The strength attained after drying as a fraction of the strength attained on moist curing until test age (indicated by R) for normal and high strength concrete mixes [9]

Moist cured, days	Drying period, days	Test age, days	R = $\frac{\text{Strength attained after drying}^*}{\text{Strength attained when moist cured until test age}}$			
			Compressive strength, f'_c		Modulus of rupture, f'_r	
			Normal strength	High strength	Normal strength	High strength
0-7	8-28	28	0.98	0.91	0.83	0.74
0-7	8-28	28	0.94	0.89	0.86	0.74
0-7	8-28	28	0.95	0.88	0.88	0.74
0-28	29-95	95	0.99	0.95	0.97	0.91
0-28	29-95	95	1.01	0.96	0.96	0.93
0-28	29-95	95	0.99	0.96	0.99	0.91

The study by Aitcin et al. [3] highlights the importance of moist curing conditions. In their study, the influence of three curing conditions i.e. air dried, sealed and moist cured on the development of compressive strength of various grades of concrete (35 MPa, 90 MPa and 120 MPa) with time is studied. The respective curing conditions are employed starting from the day after demoulding until test age. It is reported that the moist cured samples have the largest strength, followed by the sealed samples and finally the air dried ones, which have the lowest strength.

Table 2.3: Ratio of compressive strength after one year in case of the moist cured (f_{cW}), air cured (f_{cA}) and sealed (f_{cS}) specimens [3]

Concrete	$\frac{f_{cA}}{f_{cW}}$	$\frac{f_{cA}}{f_{cS}}$	$\frac{f_{cW}}{f_{cS}}$
35 MPa	0.83	0.85	1.03
90 MPa	0.79	0.81	1.03
120 MPa	0.78	0.87	1.13

As shown in table 2.3, it can be observed that the largest difference is between the air cured and moist cured samples, where the former has 17-22% lesser strength than the latter. Also, an interesting thing to note is the ratio of water cured to sealed cured samples where the increase is just 3% for the 35 and 90 MPa samples, but is 13% for 120 MPa samples. This is attributed to the low water cement ratio of the 120 MPa samples due to which probably complete hydration did not take place under sealed conditions.

For Ultra High Strength concrete, it is observed in literature that mostly steam curing method is employed in order to achieve such high strength at earlier ages. Although, the final strength obtained using steam curing could be lower. However, there have been studies in the past to check if the specified strength can be achieved even with normal moist curing treatments. As reported in Park et al. [32], it is possible to achieve the specified compressive strength at 91 days even under moist cured conditions at standard temperature of 20° C (see figure 2.3). However, under air dry condition, only 80% of the specified strength is achieved. This shows the importance of moist curing conditions for UHSC. Moreover, Yunsheng et al. [42] reported that if the curing age is increased from 28 to 90 days, the specified strength can be reached with standard curing conditions (defined as with 20° C and 100% RH), as compared to steam and autoclave curing, where the specified strength is achieved earlier.

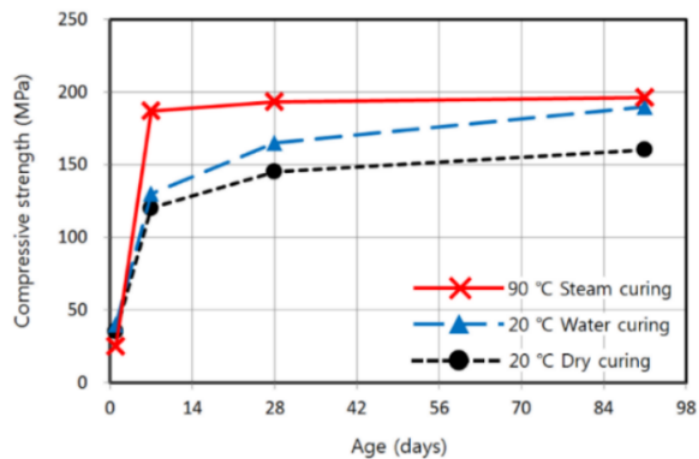


Figure 2.3: Trend of compressive strength with age for UHSC with different types of curing regimes [32]

Moreover, Ozer and Ozkul [31], in their study, report that the compressive strength of the NSC specimens (specified cube strength of 25 MPa) under intermittent curing conditions (defined as moist curing till 28 days and then exposed to lab conditions until testing) shows higher strength at 90 days compared to continuous moist cured specimens, as shown in the figure 2.4. This is explained by the combined effect of the increased Van der Waal forces between the surfaces of cement paste and reduced disjoining pressure due to drying. However, at a slightly longer period of 180 days, the strength of the continuous moist cured specimens is higher. This is explained by the lack of sufficient water for hydration and increase in the microscopic defects due to drying shrinkage.

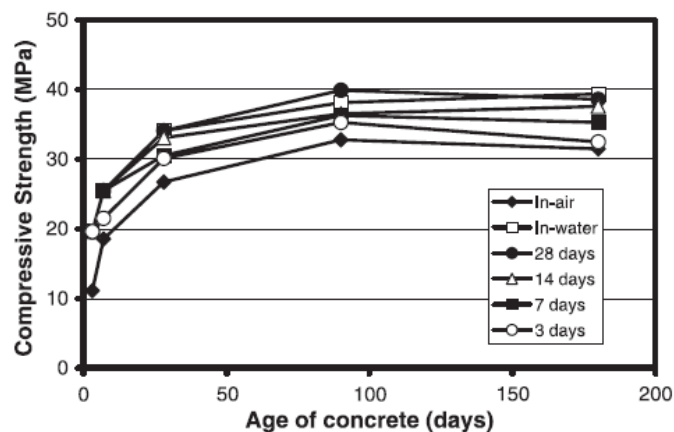


Figure 2.4: The effect of development of compressive strength with age based on different curing conditions [31]

However, Iravani [19] found that for a High Strength concrete (HSC) mix (65-120 MPa), drying has a positive influence on the compressive strength, as shown in figure 2.5a. It is reported that the continuously moist cured specimens were dried for 2 hours before testing, whereas the 3 or 7 weeks moist specimens were tested in the moisture conditions that they had reached at testing time. No explanation of the behaviour is given. Similarly, Logan et al. [24] also found that for a HSC mix tested at 28 days, there is an increase in the compressive strength for the ones exposed to 7 day moist curing compared to the continuously moist cured ones until testing (see figure 2.5b). It is worth noticing that the moisture conditions at testing and the explanations for the behaviour are not stated.

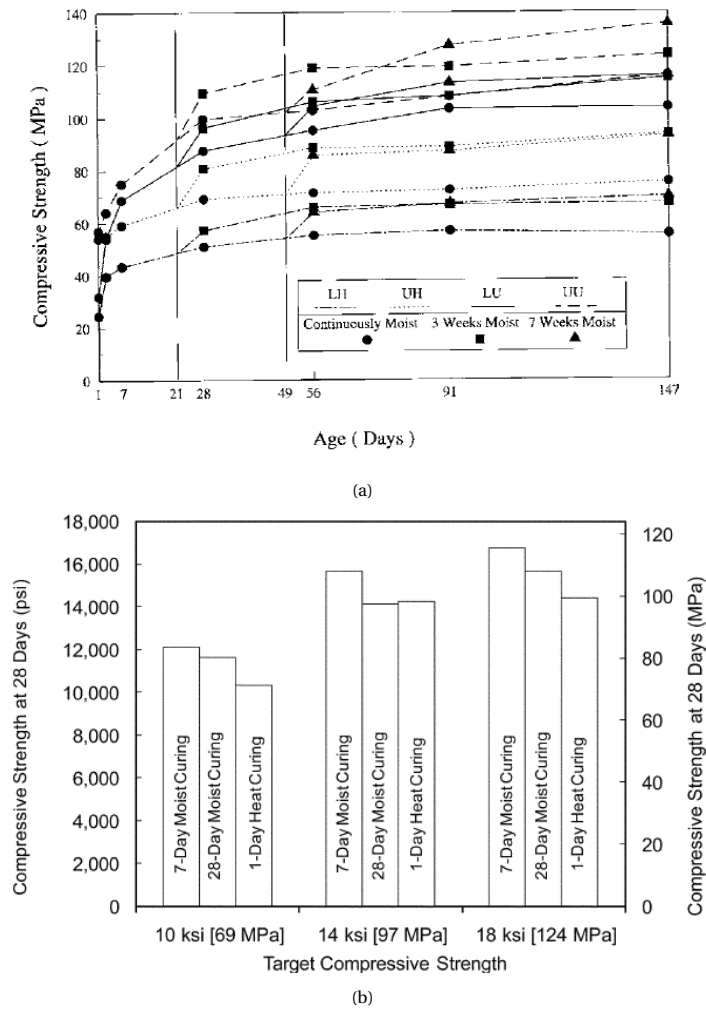


Figure 2.5: (a) Trend of compressive strength with age based on different curing conditions for High Strength concrete (LH and UH: Lower bound mix of HSC and UHSC without silica fume , LU and UU : Upper bound mix of HSC and UHSC (with silica fume) [19] (b) Compressive Strength of 100x200 mm specimen at 28 days based on different curing regimes [24]

From the results of Iravani [19] and Logan et al. [24], the importance of specifying the moisture state of the specimen before testing is observed. It can be possible that the testing conditions influence the observed values of the compressive strength. Interestingly, this issue has been addressed a long time back by Popovics [34]. In his study, the influence of different curing regimes on the compressive strength of a normal strength concrete tested until 28 days is studied and it is reported that the highest compressive strength is found for the specimens exposed initially to moist curing followed by 3 days finishing air curing before testing and not for the ones exposed to continuous water curing (as shown in table 2.4 and 2.6). Also, the specimens exposed to continuous air curing have higher strength compared to the ones exposed to air curing initially followed by 3 days finishing water curing before testing. With this, it is seen that the method of curing especially during the last days before testing of the compressive strength is really crucial.

Table 2.4: Compressive strength of concrete based on various curing conditions at various ages [34]

Mix No.	Age, days	3		7				28							
		CA	CM	CA	CM	A + 3	M + 3	CA	CM	A + 3	M + 3	A + M	M + A	A + W	W + A
A1.10	—	4470	4540	4720	5280	4570	6320	5690	6240	4520	7350	5740	6710	5820	6500
A1.9	—	5550	5750	6140	7060	5660	8070	6200	7950	5430	9920	—	—	—	—
A1.2	Epoxy	4550	4350	5820	5630	5340	6280	6870	6230	6020	6580	6020	6300	6340	6350
A1.7	20 percent	6360	5710	7670	7060	7520	8030	9440	7620	8340	8990	—	—	—	—
B1.8	Epoxy	4630	4480	5790	5060	4940	5100	6320	6300	5970	6520	—	—	—	—
B1.7	31 percent	4220	4350	7030	6160	5670	6710	8710	8040	7850	7940	—	—	—	—

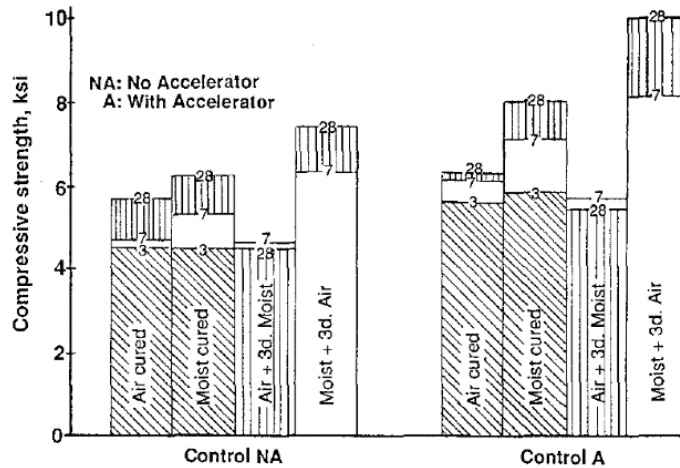


Figure 2.6: The influence of varying curing regime-s on the compressive strength [34]

The explanation is given on the basis of development of moisture gradient as a result of non uniform drying, which influence the obtained strength of concrete. It is explained that drying the specimen causes the outer surface to shrink, but since it is internally restrained by the core (inside part), eigen stresses are developed which increases the compressive strength of the specimen. The opposite effect happens on swelling i.e the compressive strength is reduced.

Moreover, Bartlett and MacGregor [6], in their review paper, mention about the effect of moisture condition on the concrete strength. They report that the provisions of ASTM C42-90 and ACI 318-89 standards are too extreme to cause a uniform change in the entire volume of the specimen. Moreover, it is highlighted that if there is a uniform increase in the moisture content (across the entire volume), it can result in the reduction of compressive strength, and vice versa. However, when there is non-uniform increase/decrease of moisture content, then moisture gradient is created and a similar effect occurs as stated by Popovics [34].

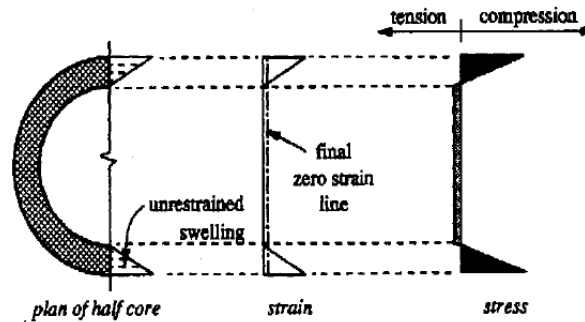


Figure 2.7: The eigen stresses due to soaking (circumferential swelling) [6]

As observed until now, the compressive stresses induced at the core due to the non uniform drying is benefi-

cial for the compressive strength. However, at the surface, there exists eigen stresses which leads to reduced tensile capacity of the concrete. If these tensile eigen stresses generated surpass the tensile strength of concrete, there could be microcracking (discussed further in section 2.4.2).

2.2.3. Influence of specimen size

Traditionally, based on the size effect theories by famous researchers like Weibull and Bazant, it is believed that the strength increases with decreasing specimen size. This is consistent with the results of Irvani [19] and Carrasquillo et al. [9] who report that the compressive strength of cylindrical specimens (100 mm diameter and 200 mm height) exposed to 100% RH conditions are 6-10% more than the larger cylinders (150 mm diameter and 300 mm height) of the same mix.

However, the traditional size effect is not directly valid when the specimens are exposed to drying as highlighted by the study of Soroka and Baum [37]. In their study, the influence of specimen size (70mm, 120mm, 200mm and 250mm cubes) on the effect of curing regime on the compressive strength of a normal strength concrete ($w/c = 0.75$) at 28 and 91 days is studied. The samples are tested in air dried conditions. Additionally, the variable moisture condition of the specimens at the time of testing is also accounted for by incorporating saturated surface dry conditions, although no such differences are found. It is reported that air cured samples have lower compressive strength relative to the water cured ones, particularly in smaller sized specimens. This effect is explained by the slow hydration and internal cracking that takes place in the outer layers leading to the reduction in strength.

Moreover, it is also reported that the influence of specimen size on the strength would depend on the curing conditions exposed and the resulting influence of the two opposing phenomena- (a) the intrinsic size effect (as mentioned before, "traditional size effect theory") and the effect of drying (reduction of strength for smaller specimens). From the figure 2.8, it can be observed that at 28 days, for the curing regimes A and B, the effect of drying is more dominant than the intrinsic size effect, thus the concrete strength increases with increasing size. At 90 days, the effect is even more prominent probably due to the larger drying period. However, for regime D, there is a reduction in the compressive strength with increasing cube size. Thus, the intrinsic size effect is dominant over the drying effect in this case (as now there is no drying effect). Also for curing regime C, as there is an initial moist curing for 6 days, it follows almost the same pattern as regime D at 28 days. However at 90 days (due to more drying), the two opposing effect somehow balances out and the strength is almost constant.

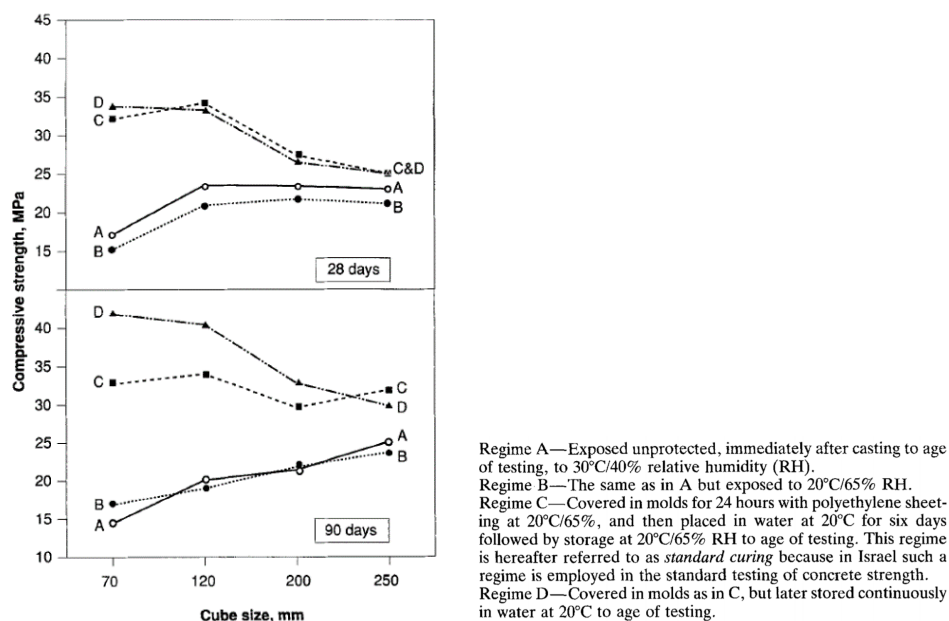


Figure 2.8: Variation of compressive strength with different cube sizes at 28 and 90 days [37]

Moreover, Hameed [16], in his study, observed the influence of specimen size (100 mm and 150mm cubes) on the compressive strength of 4 mixes (Mix 1,2,3,4 with specified strength of 40,50,70 and 80 MPa respectively) under three types of curing regimes- initial 7 days moist cured followed by air curing in lab conditions (26 – 30° C) till test day (Group A), continuously moist cured until testing (Group B), and high temperature curing (Group C). The test is done at 7,28 and 90 days. From table 2.5, it can be seen that irrespective of the curing regimes, the strength of 100mm sized cube is always greater than 150mm ones, thus following the traditional size effect theory. The results indicate that the effect of drying does not reduce the strength for smaller specimens which is in contradiction to what Soroka and Baum [37] reported (if a comparison is made of Mix 1 Regime A of Hameed [16], with Regime C of Soroka and Baum [37]). However, since the testing conditions are not mentioned specifically in the study of Hameed [16], there can be possible discrepancies. Moreover, in the study of Aitcin et al. [3], the effect of varying cylindrical specimen size (diameter of 100,150 and 200mm) on the trend of compressive strength of three grades of concrete (35,90 and 120 MPa) are studied under air curing conditions. It is reported that for the 35 and 90 MPa samples, the 100mm samples have the largest compressive strength followed by the 150mm and 200mm ones, after a period of 1 year (as shown in figure 2.9). Although, it might not be fair to compare cubes and cylinders, still the results are in contradiction to what Soroka and Baum [37] reported. However, the 120 MPa samples are not dependent on size as the others. It is also stated that the lower strength concrete showed more variation in the strength at the period of 1 year. This is attributed to the larger porosity of the lower strength concrete (35 MPa), which makes it more prone to drying compared to the higher strength ones, thus ceasing the hydration in the outer part of the specimen. Interestingly, it is stated that due to drying shrinkage, the surface cracks will be deeper for larger specimen sizes causing reduction in the compressive strength, especially for more porous concrete (35 MPa).

Table 2.5: Values of compressive strength for various mixes exposed to different curing regimes at 7,28 and 90 days [16]

Age day	Curing type	Mix No. 1		Mix No. 2		Mix No. 3		Mix No. 4	
		fcu150 (MPa)	fcu100 (Mpa)						
7	A	35.60	37.00	44.2	53.3	50.44	61.00	66.00	70.4
	B	35.60	37.00	44.5	53.5	50.45	61.00	66.00	70.4
	C	39.30	44.40	43.15	57.4	62.0	68.9	70.00	73.2
28	A	49.73	51.80	63.3	71.25	67.77	73.87	78.00	85.2
	B	52.54	56.50	64.4	78.57	68.2	77.77	82.00	88.00
	C	56.53	59.50	71.00	79.00	75.56	82.7	85.00	93.65
90	A	54.80	59.60	77.3	85.8	73.00	78.00	82.2	88.00
	B	57.70	64.83	78.6	85.57	84.4	85.00	84.3	92.2
	C	59.00	64.70	80.5	86.6	74.3	81.35	71.6	80.42

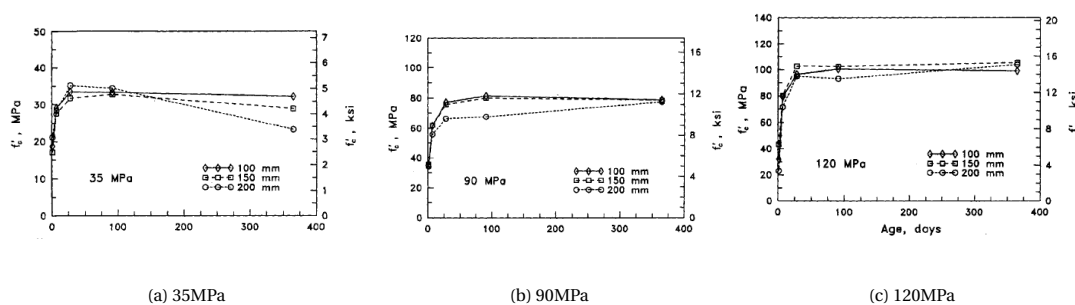


Figure 2.9: Variation of compressive strength for 3 mixes with age for different sized specimens [3]

2.3. Elastic Modulus

The compressive strength is not the lone parameter which decides the criteria for designing the concrete structures. It is equally important to understand the stiffness properties like Elastic Modulus of concrete to ensure that the deflection of member is within the serviceability requirements [21]. Moreover, the elastic

modulus has a strong correlation with creep and shrinkage which could affect the prestress losses in pre-stressed structures [4].

Generally, it is believed in literature that there is a strong inter-dependency between the modulus of elasticity and the compressive strength of concrete. Some of the equations collected from the literature are summarized in table 2.6

Table 2.6: Predictive empirical equations collected from literature relating Elastic Modulus with the compressive strength of concrete

Committee/ Researcher(s)	Equation proposed	Additional Remark
(Pauw, 1960)	$E_c = 0.043 W_c^{1.5} \sqrt{f_c}$	Specimen - Cylinder $2.5MPa < f_c < 40MPa$ $1500kg/m^3 < W_c < 2500kg/m^3$
(Parrott, 1979)	$E_{28} = C_o + 0.2f_{28}$	C_o = factor related to modulus of elasticity of aggregate $20MPa < f_{28} < 70MPa$
(ACI 318M-89, 1989)	$E_c = 4730\sqrt{f_c}$	$f_c \leq 41.4MPa$ NSC, $1440 \leq \lambda \leq 2480 kg/m^3$
(ACI 363 R-92, 1992)	$E_c = (3321\sqrt{f_c} + 6895) \left(\frac{\lambda}{2300} \right)^{1.5}$	HSC, $f_c \leq 83MPa$
(Iravani, 1996)	$E_c = 4700 C_{ca} \sqrt{f_c}$	$55 MPa < f_c < 125 MPa$ C_{ca} = empirical coarse aggregate coefficient.
(Eurocode 2, 2004)	$E_{cm}(f) = 22 \left(\frac{f_{cm}}{10} \right)^{0.3}$	Valid upto C90/105
(Takafumi Noguchi, 2009)	$E_c = 33500k_1 k_2 \left(\frac{\lambda}{2400} \right)^2 \left(\frac{f_c}{60} \right)^{1/3}$	$40 MPa < f_c < 160 MPa$ k_1 -> factor accounting for type of coarse aggregate used k_2 -> factor accounting for type of SCMs used
(Graybeal, 2012)	$E_c = 4069\sqrt{f_c} MPa$	UHSC, $97 MPa < f_c < 179 MPa$
(Ali Alsalman, 2017)	$E_c = 8010 (f_c)^{0.36} MPa$	$31 MPa < f_c < 235 MPa$
NS 3473	$E_c = 9500 (f_c)^{0.3} MPa$	$25 MPa < f_c < 85 MPa$
Ma et al.	$E_c = 19 \left(\frac{f_{cm}}{10} \right)^{0.3}$	$150 MPa < f_{cm} < 180 MPa$
Kollmorgen	$E_c = 11800 (f_c)^{1/3} MPa$	$34 MPa < f_c < 207 MPa$

2.3.1. Development with age

It is observed that the elastic modulus is generally determined from the compressive strength by the use of various empirical equations. Although, the relation is not always precise due to the numerous choices available while designing the mix of various grades, but the equations are modified in order to closely predict the actual results.

It has been reported in Mehta and Monteiro [28] that the trend of compressive strength and the elastic modulus of concrete are not affected in the same manner by the age. Instead, it is found that when different

strength of concrete are considered, the compressive strength increases at a lower rate than the elastic modulus as clear from figure 2.10

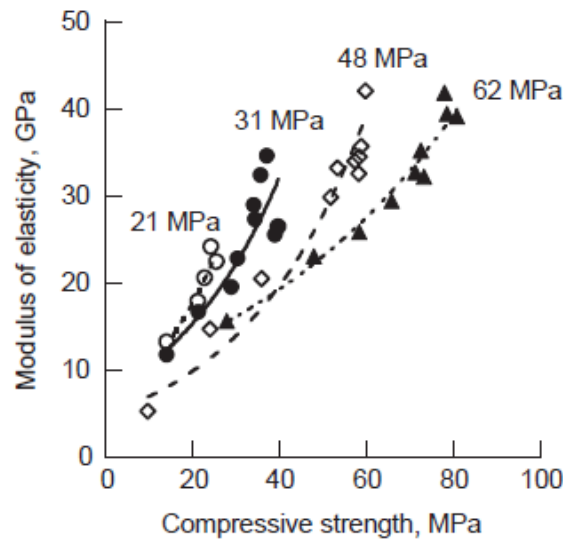


Figure 2.10: Relation between Modulus of Elasticity and Compressive Strength for different strength of concrete [28]

According to Eurocode 2 [2], at any age "t", the Elastic Modulus is predicted by equation 2.4. However, it is clear that equation 2.4 is a modification of equation 2.1

$$E_{cm}(t) = E_{cm} \left(\frac{f_{cm}(t)}{f_{cm}} \right)^{0.3} \quad (2.4)$$

where,

E_{cm} is the elastic modulus at 28 days

f_{cm} is the compressive strength at 28 days

$f_{cm}(t)$ is the compressive strength at any age "t".

Parrott [33] also proposed an equation especially to predict the elastic modulus of concrete at any age "t" :-

$$E_t = E_{28}(0.4 + 0.6 f_t / f_{28}) \quad (2.5)$$

where,

E_{28} is the elastic modulus at 28 days

f_{28} is the compressive strength at 28 days

" f_t " is the compressive strength at any age "t".

With regard to the other relations in the table 2.6, it is not mentioned exclusively whether these empirical relations hold true with increasing age of the concrete. In other words, it is not clear whether the elastic modulus varies with a predictable trend as compared to the compressive strength as the concrete ages.

2.3.2. Influence of curing conditions

The type of curing conditions (temperature, age, humidity) can influence the elastic modulus of concrete to a large extent. The protection of the concrete from rapid evaporation of water is very important as it can lead

to shrinkage which often results in the microcracking of concrete. These microcracks can affect the elastic modulus of concrete. As already mentioned, the testing conditions play a huge role in case of compressive strength with higher values for air dried samples compared to wet ones. However in the case of elastic modulus, the wet tested concrete specimens have around 15 % higher Elastic modulus than their dry counterparts. The reduction of E-modulus in case of dry samples is reported to be due to the increase in the microcracking in the Interfacial Transition Zone (ITZ) [28].

Asselanis et al. [5] carried out a study to understand the influence of curing conditions on elastic modulus of very high strength concrete. The continuous moist curing is at 100% RH in a fog room at 20° C, continuous air curing is in lab air at 20° C and 50%RH. From the results (as shown in table 2.7) for high strength concrete, the importance of moist curing (at least for 7 days) can be observed. The specimens moist cured for only 1 day (Group 2,6,9) have lower elastic modulus as compared to specimens moist cured for 7 days and above (Groups 4,5,7,8). Moreover, it is mentioned that the wet tested specimens have higher elastic modulus values than the dry tested ones. This is vivid from Group 8 & 4 concrete compared to Group 7 & Group 5 concrete respectively. However, it is clear that 7 days of moist curing is a good enough for getting satisfactory value of elastic modulus.

Table 2.7: Comparison of Elastic Modulus for different curing conditions [5]

G R O U P No	CURING CONDITIONS	Weight Changes (g)	Compressive strength	Elastic modulus
			MPa (psi)	GPa (10^6 psi)
1	1 d	—	38.4 (5570)	—
2	7 d	- 36.9	62.8 (9100)	30.3 (4.4)
3		+ 12.9	77.5 (11240)	37.2 (5.4)
4	28 d	- 11.6	99.2 (14 390)	40.7 (5.9)
5		+ 16.1	98.8 (14 330)	41.4 (6.0)
6		- 53.4	81.2 (11,780)	35.2 (5.1)
7	56 d	+ 0.9	105.2 (15 260)	42.1 (6.1)
8		+ 17.9	97.6 (14 160)	43.4 (6.3)
9		- 57.2	82.3 (11 930)	35.2 (5.1)



Moreover, Kocab et al. [21] did a study on the influence of curing regimes on the trend of both static and dynamic Elastic Modulus of a normal strength concrete (C30/37). For the mixtures, CEM-I 42.5 R is used and the curing conditions employed start right from the day of demoulding. It is reported that the air cured samples always have lower values as compared to the moist cured ones with increasing age (as shown in the figure 2.11). The reduction is said to cause due to insufficient hydration. Further, due to sharp evaporation of the water, there is shrinkage which results in volume changes and hence microcracks, thereby reducing the elastic modulus. At 730 days, it is mentioned that the difference of Elastic modulus between the two regimes is 29% (dynamic) and 19.8% (for static).

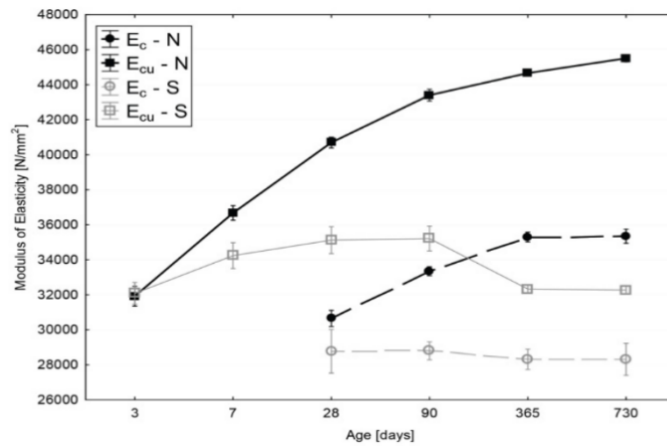


Figure 2.11: Development of Static (E_c) and Dynamic Modulus (E_{cu}) of Elasticity for air (S) and moist cured (N) specimens [21]

2.3.3. Influence of specimen size

It is observed from the literature that not much importance is given to the influence of specimen size on the elastic modulus of concrete. It has been mentioned in Iravani [19] that the effect of size on the elastic modulus is not significant and can be just 5% for a high strength concrete mix.

Lee et al. [22] did an investigation on the effects of cylinder size (150x300mm and 100x200mm) on the static elastic modulus of concrete for concretes with compressive strength of 30, 35 and 40 MPa. The specimens are initially cured in water (till 1 day before testing), and then left in air at a constant temperature and humidity room in the final day until testing. The static elastic modulus tests are carried out at 4,7,14 and 28 days and the results are compared with the database obtained from the literature. They report that the two considered specimen sizes are highly correlated at lower ranges of elastic modulus (10 to 15 GPa) i.e for normal strength concrete upto compressive strength of 30 MPa (as clear from figure 2.12). Although, for higher strength concrete, range greater than 30 MPa (elastic modulus > 25 GPa), the static elastic modulus of 150mm sized specimens is greater than 100 ones. It is however mentioned that due to the lack of data at higher strength range (>50 MPa), a definite conclusion cannot be made and more research is further needed.

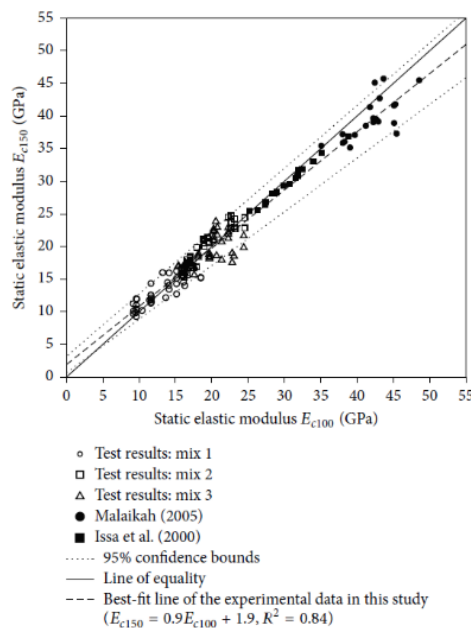


Figure 2.12: Correlation between static modulus of elasticity of 100mm and 150mm sized specimens [22]

Moreover, Chen et al. [10] did a study on the effect of size (varying diameters) on the compressive behavior of cylindrical specimens until failure. The specimens are cured at 20° C (defined as lab conditions) until the test age. A part of this study also focused on the elastic stage wherein the influence of varying specimen diameters on elastic modulus is studied. From figure 2.13, it can be seen that the elastic modulus of both C60 and C45 grades remains more or less constant with varying diameters. The results are explained by the fact that the determination of elastic modulus is done by only taking the elastic stage into account and it is not affected by the concrete fracture (which actually is linked to the size effect).

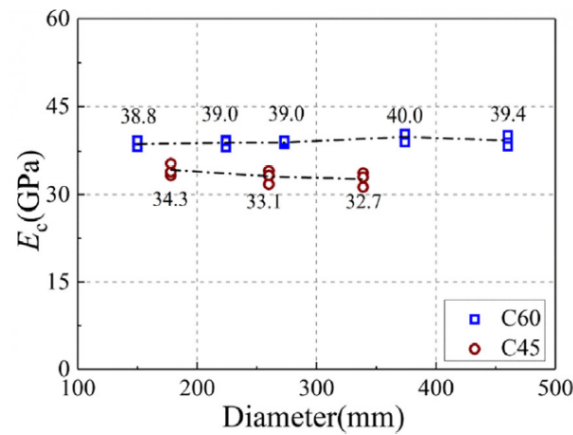


Figure 2.13: Variation of modulus of elasticity of C45 and C60 specimens for different diameters [10]

2.4. Splitting Tensile Strength

Although, the structures made of concrete are not designed primarily to carry loads in tension, but understanding the behaviour of concrete under tension is necessary especially when it comes to crack control. The tensile strength is usually important when it comes to mitigating cracking in prestressed concrete and countering shear forces in concrete sections with no reinforcement [36]. The tensile strength of concrete can be determined using direct and indirect testing methods. However, the direct tension tests are not usually preferred due to the difficulty in carrying out the test. Thus, the indirect methods like splitting tensile and flexural tests are carried out. However, these methods overestimate the true tensile strength than under uniaxial loading. In this section, the focus will be more on splitting tensile strength, with a discussion on the direct tension and flexural test wherever necessary.

In cases where the tensile tests cannot be carried out, it could be predicted with the use of empirical relations. It is reported in Mehta and Monteiro [28] that just like in the case of elastic modulus, the tensile strength (direct) is also closely linked to the compressive strength. The tensile strength is said to increase with the increase of compressive strength, but at a decreasing rate (as shown in figure 2.8).

Table 2.8: Relation between Compressive and Direct Tensile strength of concrete [28]

Strength of concrete (MPa)			Ratio (%)		
Compressive	Modulus of rupture	Tensile	Modulus of rupture to compressive strength	Tensile strength to compressive strength	Tensile strength to modulus of rupture
7	2	1	23.0	11.0	48
14	3	1	18.8	10.0	53
21	3	2	16.2	9.2	57
28	4	2	14.5	8.5	59
34	5	3	13.5	8.0	59
41	5	3	12.8	7.7	60
48	6	4	12.2	7.4	61
55	6	4	11.6	7.2	62
62	7	4	11.2	7.0	63

In the literature, there exists several equations correlating the compressive strength and the splitting tensile

strength. These relations are summarized in figure 2.9 below :-

Table 2.9: Predictive equations of Splitting tensile strength from Compressive strength

Committee/ Researcher(s)	Equation proposed	Additional Remark
(Eurocode 2, 2004)	$f_{ctm} = 0.3 f_{ck}^{(2/3)}$ $f_{ctm} = 2.12 \ln \left(1 + \frac{f_{cm}}{10} \right)$ $f_{ctm} = 0.9 f_{ct,sp}$	for strength class \leq C50/60 for $>$ C50/60
(ACI 318M-89, 1989)	$f'_{sp} = 0.56 \sqrt{f'_c}$	
(ACI 363 R-92, 1992)	$f'_{sp} = 0.59 \sqrt{f'_c}$	for 21 MPa $<$ $f'_c <$ 83 MPa
(Iravani, 1996)	$f'_{sp} = 0.57 \sqrt{f'_c}$	for 50 MPa $<$ $f'_c <$ 100 MPa
(Gardner, 1988)	$f'_{sp} = 0.47 f_c^{0.59}$ $f'_{sp} = 0.46 f_c^{0.60}$	for 3 MPa $<$ $f'_c <$ 46 MPa for 13 MPa $<$ $f'_c <$ 72 MPa
(Carino, 1982)	$f'_{sp} = 0.272 f_c^{0.71}$	No range stated
(Raphael, 1985)	$f'_{sp} = 0.313 f_c^{0.667}$	Normal Strength concrete $f'_c <$ 40 MPa
(Ahmad, 1985)	$f'_{sp} = 0.462 f_c^{0.55}$	for 15 MPa $<$ $f'_c <$ 84 MPa
(Oluokun, 1991)	$f'_{sp} = 0.294 f_c^{0.69}$	for 3.5 MPa $<$ $f'_c <$ 63 MPa
(Arıoglu, 1995)	$f'_{sp} = 0.321 f_c^{0.661}$	for 15 MPa $<$ $f'_c <$ 120 MPa
(Nihal Arıoglu, 2006)	$f'_{sp} = f_c * 0.387 f_c^{-0.37}$	for 4 MPa $<$ $f'_c <$ 120 MPa

2.4.1. Development with age

As seen in the table 2.9, the splitting tensile strength can be determined from the compressive strength by the use of various empirical equations. According to Neville and Brooks [30], just like the compressive strength, the tensile strength also increases with age, but at a much lower rate. It is to be pointed out that the validity of the empirical relations in figure 2.9 is not stated exclusively at higher ages.

However, in Eurocode 2 [2], an expression is given which could be taken as a first guess to predict the mean tensile strength at any time. Accordingly, the splitting tensile strength can be determined.

$$f_{cm}(t) = (\beta_{cct})^\alpha \cdot f_{ctm} \quad (2.6)$$

$$f_{ctm} = 0.9 f_{ct,sp} \quad (2.7)$$

where,

$$\beta_{cct} = \exp \left\{ s \left\{ 1 - \left(\frac{28}{t} \right)^{0.5} \right\} \right\}$$

f_{ctm} is the 28 day mean tensile strength in [MPa]

$f_{ct,sp}$ is the equivalent splitting tensile strength

$\alpha=1$ for $t<28$ and $2/3$ for $t>28$.

However it is suggested to carry out the tensile tests specifically considering the curing conditions and the size of the specimen in order to get accurate results.

2.4.2. Influence of curing conditions

The curing of concrete is important for ensuring that the concrete has gained sufficient tensile strength. As mentioned before, the curing conditions can be varied in terms of temperature, relative humidity, moisture condition, duration, etc.

Weerheijm [40], in his study, highlighted that moist curing only has a beneficial effect on the tensile strength if there is no moisture gradient across a cross section. As already discussed in 2.3.2, the moisture gradient creates differential shrinkage and eigenstresses which does apparently increase the compressive strength of the concrete. However, due to the generation of tensile eigen stresses at the surface, the tensile capacity of the concrete is reduced. Moreover, if the tensile eigen stresses generated exceed the concrete's fairly low tensile strength, there could be microcracking .

It is reported in the study by Bonzel as mentioned in Hordijk and Reinhardt [18] that a strong reduction in the uniaxial tensile strength can be observed if specimens stored in water are dried for some time before testing. This reduction is also attributed to the eigen stresses as a result of the moisture gradient. However, as shown in figure 2.14, after few days, the tensile strength starts to increase again (indicating that the eigen stresses did not exceed the tensile strength). A probable explanation could be because of the fact that once there is uniform moisture distribution in the specimen with time, the eigen stresses disappear. Additionally, it is mentioned in the PhD thesis of van Vliet [39] that the eigen stresses has greater effect on the behaviour of smaller specimens because of their larger specific area (a larger part of the specimen will dry out as compared to the larger specimens).

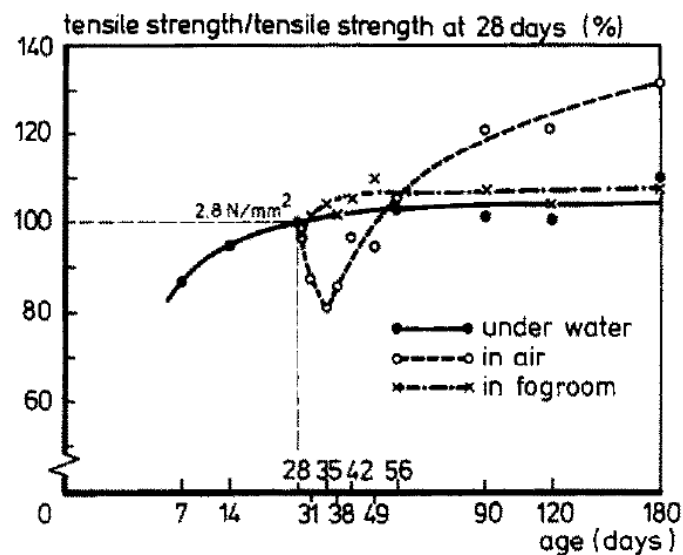


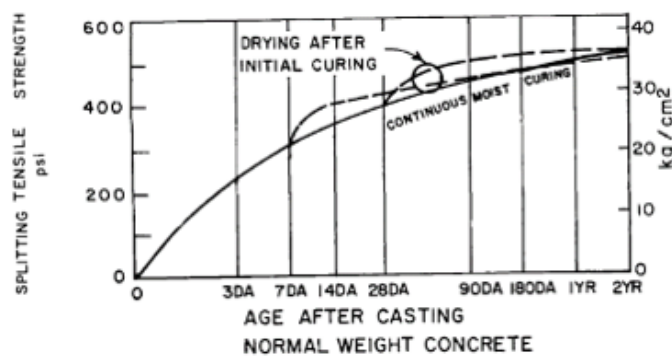
Figure 2.14: Development of tensile strength/tensile strength at 28 days with age for different curing conditions [18]

However, it is important to note that the above trend is for the specimen tested for uniaxial tensile strength. It is reported in a study by Bonzel cited in [18] and Vliet [39] that as compared to uniaxial and flexural tensile strength test, the splitting strength is not affected by drying because of the fact that there is a biaxial compressive region under the application of load which is in the same region of the tensile eigenstresses.

However, few researchers in the past have shown that drying could have an effect on the the splitting tensile

strength too. Way back in the late 1960s, Hanson [17] did a study on the importance of curing environments on the splitting tensile strength of cylindrical concrete specimens made up of normal weight and light weight aggregates. The focus will be on the normal weight concrete. In the experimental set up, the effect of varying the starting moist curing period (3,7,14 and 28 days) followed by exposure to and 50% RH on the splitting tensile strength is studied for the normal weight concrete, as shown in figure 2.15. The mix is designed for achieving a 28th day compressive strength of 31 MPa.

From the figure 2.15, it can be seen that for the normal weight concrete, drying at 50% RH after moist curing period of 7 and 28 days increases the splitting tensile strength as compared to the continuously moist cured specimens and at the end of 2 years the strength from all the curing regimes are almost the same. The reason for the increase in the splitting tensile strength after drying is not stated. However, it is noticed that the increase in strength coincided in the period when the moisture gradient was the highest in the specimen.



(a)

Moist cured, 7 days

¼ (6 mm)	100	89	84	77	68	59	57	56	52	50
¾ (19 mm)	100	97	93	88	81	67	61	59	55	52
1¾ (44 mm)	100	100	98	94	89	76	69	63	57	53
3 (75 mm)	100	100	99	96	92	78	72	65	59	55

Moist cured, 28 days

¼ (6 mm)	100	85	82	76	69	58	57	55	52	50
¾ (19 mm)	100	98	94	87	80	68	64	61	55	52
1¾ (44 mm)	100	100	97	94	90	76	70	66	58	54
3 (75 mm)	100	100	99	96	92	78	73	69	61	56

(b)

Figure 2.15: Development of splitting tensile strength with age for Normal weight concrete and (b) Relative Humidity profile across the width of the specimen [17]

Conroy-Jones and Barr [11] did a study on the effects of water and air curing (20° and 60 % RH) regimes on the tensile strength of medium to high strength concrete range (with 28 day compressive cube strength ranging from 40 to 110 MPa). The tensile strength tests are measured in saturated surface dry conditions at 28, 84 and 365 days using three indirect tests namely flexural, splitting and torsional. The discussion will mostly be focused on the splitting tensile strength.] It is reported that the positive and negative effects

caused by the air and water curing regimes is complicated in reality. While, the positive effect of air curing is the creation of moisture gradient and differential shrinkage resulting in prestressing the specimen, however, the negative effects are damage induced due to microcracks on the surface. For the water curing regime, the positive effect is increased hydration thereby increasing strength, however the negative effect is the reduction of intermolecular bonding between cement particles causing a reduced strength. It is reported that although the splitting tensile test is an internal failure test, but the failure is still controlled by the concrete region close to the surface implying that air curing has quite a significant impact. This is confirmed in the table shown in 2.10, wherein the air cured split cylinder show strength loss as compared to the water cured counterparts. This means that the negative influence of air drying (microcracks due to differential shrinkage) dominates

over the positive effects (prestressing on the specimens). Moreover, it can also be seen that the strength loss due to air curing is lower in the case of higher strength mixes, although the difference is minute.

Table 2.10: Splitting tensile strength for water and air cured specimens at 84 and 365 day [11]

Curing condition	28-day cube strength: N/mm ²	Split cylinder	
		84	365
		Water cured 20°C	42.1
	60.5	0.96	1.10
	70.9	1.01	1.10
	86.9	0.98	1.03
	108.7	1.00	0.98
Air dried 60% RH 20°C	42.1	1.18	1.03
	60.5	1.11	1.19
	70.9	1.09	1.17
	86.9	1.03	1.00
	108.7	0.97	1.12

An interesting study by Lin et al. [23] on the effect of splitting tensile strength on the varying degree of drying gives a different perspective. For their study, two types of concrete mixes containing limestone (LS-Mix) and sandstone aggregate (SS-Mix) respectively, along with a mortar mix (M) for comparison, is opted. The cylindrical specimens (100x200mm) are used and cured in water upto 1 year at constant temperature of 20° C. After that small sections of the cylinder (100x9mm) are cut and dried under varying RH % value and tested for splitting tensile strength once there is almost no weight change.

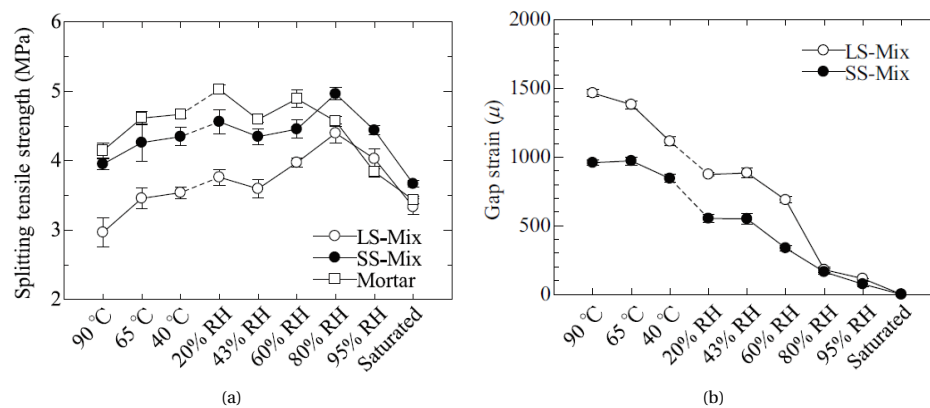


Figure 2.16: (a) Variation of splitting tensile strength with change in relative humidity for concrete and mortar. (b) Variation of Gap strain with change in relative humidity for two concrete mixes [23]

It can be observed from 2.16a that the variation of the splitting tensile strength of all the three mixes are not uniform. From 80% RH until 43% RH, there is a difference in behaviour between the mortar mix and the two concrete mixes. It is reported that this is due to the damage caused around the aggregate as a result of the restricting effect of the coarse aggregate and the cement paste. The damage around the aggregates is also supported by the plot shown in 2.16b where the gap strain (defined as difference of strain between concrete and mortar) is seen to increase sharply between 80% and 43% RH. This behavior is similar to the research by Maruyama et al. [27] for the compressive strength, as discussed in Chapter 1.

2.4.3. Influence of specimen size

As mentioned before, according to the size effect theories by famous researchers like Weibull and Bazant, it is believed that the strength increases with decreasing specimen size. It is indeed confirmed by Malhotra [26], where the splitting tests on 100x200mm specimens yields 7.5% higher strength than 150x300mm specimens.

As a part of a larger study, Carmona [8] summarized the results obtained in the literature, which had a lot of variation. In the figure 2.17, the splitting tensile strength as a ratio of splitting tensile strength corresponding to diameter 150mm f_n/f_{n150} is plotted for various diameters sizes. It can be observed from figure 2.17 that while Sabnis y Mirza reported a continuous decrease in the splitting strength for the considered diameter range (25 mm to 150mm), Chen y Yuan reported increase in the strength (from 76mm to 152mm). A wide range of diameter (100 to 3000mm) is also studied by Hasegawa who report that the strength initially declined with increasing diameter but then after reaching minimum strength rose at larger diameter range. Bazant did testing on the splitting tensile strength (diameter range from 20 to 500 mm) and report that for diameters less than 150 mm, the strength declined with increasing size, although the trend reversed for diameter exceeding 150mm.

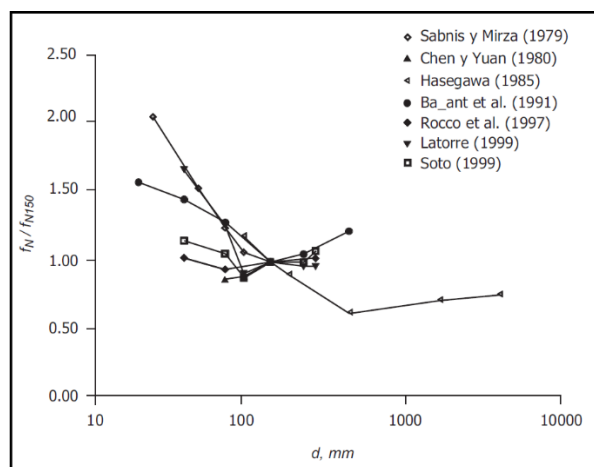


Figure 2.17: Variation of f_n/f_{n150} for different diameter sizes according to various authors [8]

Lin et al. [23] also checked the splitting tensile strength for different specimen sizes. The diameter of the specimen is fixed as 100mm whereas the length of the specimen was changed. From the figure 2.18, it can be seen that there isn't much variation in the splitting tensile strength with change in the specimen length.

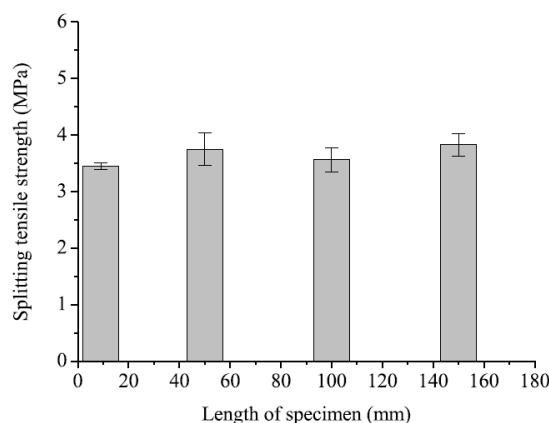


Figure 2.18: Variation of Splitting tensile strength with length of the specimen [23]

As observed, testing the splitting tensile strength using cylinders is quite popular in the literature. However, according to NEN-EN 12390-6, if cubes are used for splitting tests, it gives roughly 10% higher values com-

pared to cylinders. Also, it is mentioned that 150mm cubes would give lower tensile strength as compared to 100mm cubes, which is in line with the traditional size effect theories. With regard to the influence of size on the splitting tensile strength based on drying conditions, there is not much research done in the past.

2.5. Drying Shrinkage

When a hardened concrete specimen is exposed to a dry environment, it tries to reach equilibrium with that environment. In the process of reaching equilibrium, it loses moisture due to evaporation. The rate of evaporation would depend on external factors like the temperature, relative humidity, wind speed and internal factors like the permeability of concrete. Initially, the moisture (free water) is lost from the large capillary pores, and this loss of water does not cause a remarkable volume change and therefore it is not accompanied by any shrinkage. However, with the process of further drying, there is a loss of moisture (adsorbed water) from the smaller capillary pores and gel pores [28]. It is learnt that the removal of adsorbed water from the smaller capillary pores generates an under-pressure in the pore system, and to balance this under-pressure, compressive stresses acts on the solid material, which leads to the contraction of the cement paste successively leading to drying shrinkage [28].

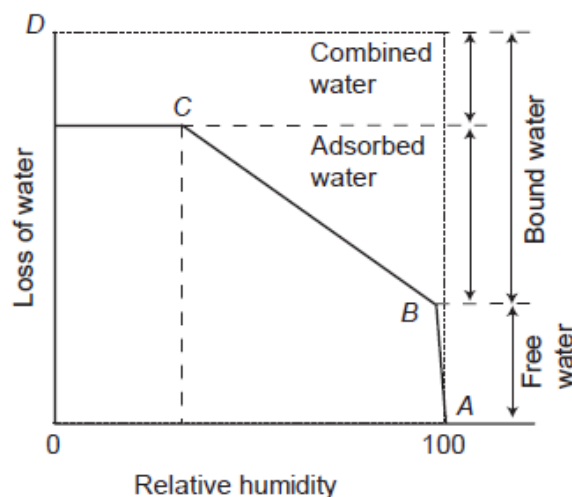


Figure 2.19: Loss of water with varying relative humidity [28]

As mentioned before, the rate of water removal and successively the magnitude of drying shrinkage also depends on the internal factors like the permeability of concrete. The permeability of concrete is dependent on parameters like the water cement ratio, the cement content and the degree of hydration. The drying shrinkage is believed to be higher for the concrete mix having high cement content and higher water cement ratio (as shown in figure 2.20a). This implies that the higher strength concrete mixes have considerable lower drying shrinkage than the lower strength ones. This is even more evident when Ultra High Strength concrete is considered. The drying shrinkage is almost negligible when compared to the total shrinkage (as shown in figure 2.20b). Thus, in higher strength mixes, autogenous shrinkage is a greater issue compared to drying shrinkage.

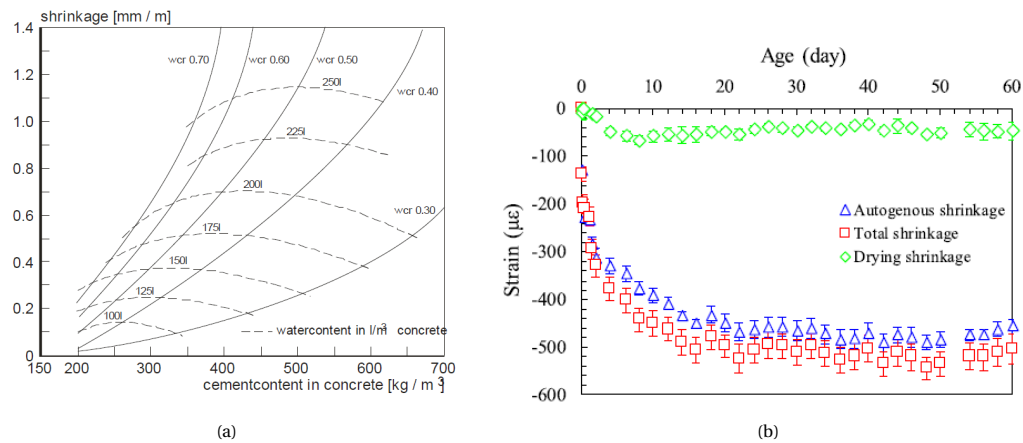


Figure 2.20: (a) Relation between shrinkage strain, water cement ratio, and cement content [38] (b) Comparison of Drying, Autogenous and Total Shrinkage of UHFRC with age

As a matter of fact, if the concrete specimen/structure is unrestrained, drying shrinkage is not a problem. However, if there are any sort of restraints, then the situation might be different. On a larger scale, the restraint could be "external". An example could be a concrete repair layer on an existing subgrade. On smaller scales, the restraint could also be "internal" which can further be either due to "aggregate restraint" or due to "self restraint" (induced by moisture gradient). In the Eurocode 2 [2], the drying shrinkage is calculated based on the assumption that the shrinkage strain is distributed uniformly across the entire cross section. However, it is mentioned in the pink book [38] that in case of a thick concrete structure, the drying shrinkage of the specimen is not uniform in the cross section. As a result, the surface region dries out rapidly relative to the core and due to the internal restraint, tensile stresses are generated at the surface and if it exceeds the fairly low tensile strength of concrete, there could be cracking at the surface. Thus, even though the average shrinkage strain might be low, there could be a chance of cracking at the surface. Usually, the shrinkage cracks are discontinuous and a typical pattern is shown in the figure 2.21.

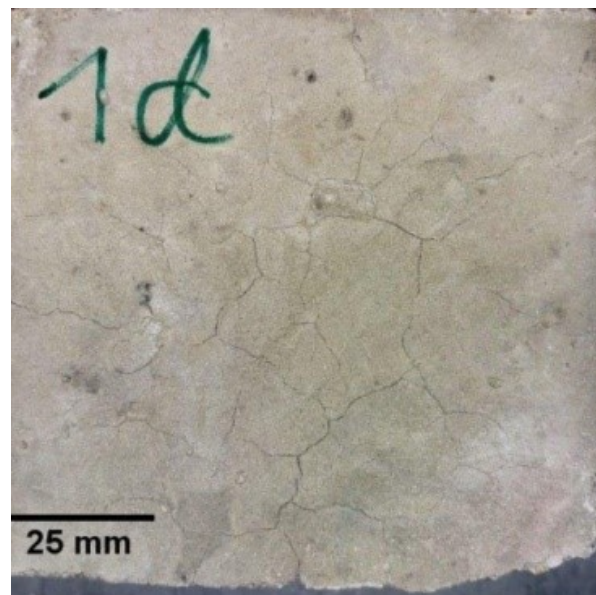


Figure 2.21: Shrinkage cracks on concrete surface

2.6. Conclusion

The key motivation of carrying out the literature study was to get an idea of the current research outlook on influence of the parameters like the curing conditions, specimen size and the type of concrete on the devel-

opment of mechanical properties of ordinary concrete with time. It can be observed that there is some uncertainty with respect to understanding the trend of the studied mechanical properties of ordinary concrete with time. It is also clear that the inter-dependency involving the different parameters makes it challenging to understand the behavior explicitly.

With respect to the development with age, for the compressive strength, it is seen that the renowned codes like the Eurocode and ACI model predicts the trend of compressive strength development in time but only for standard conditions (moist curing at 20° C). In the case of Elastic Modulus and Splitting tensile strength, it is often empirically related to the compressive strength. However, it is mentioned that both these properties do not increase at a certain predictable rate with the compressive strength and the validity of the empirical relations at higher ages is questionable.

The parameter which seems to influence the mechanical properties to a large extent is the type of curing conditions employed. It is observed that in the case of compressive strength, there is still no consensus with regard to the understanding of the trend based on the application of different curing conditions. While, researchers such as Carrasquillo et al. [9] and Hameed [16] conclude that moist curing gives the higher compressive strength especially for higher concrete strength mixes, researchers such as Irvani [19] and Logan et al. [24] believe otherwise i.e they conclude that drying at lab conditions after a certain moist curing period gives higher strength as compared to continuously moist cured specimens. Interestingly, the research by Popovics [34] and Bartlett and MacGregor [6] threw some light in explaining the uncertainty involved. The importance of mentioning the testing conditions is evident from their research. It is understood that the non uniform drying of the concrete specimen can lead to a moisture gradient which apparently increases the compressive strength.

Although, the development of moisture gradient is understood to increase the compressive strength, it seems to be not the case with tensile strength. Due to the moisture gradient and internal restraint, tensile stresses are present at the surfaces, which reduces the tensile capacity. This is evident from the research by Bonzel as mentioned in Hordijk and Reinhardt [18] where the uniaxial tensile strength is seen to reduce for a certain period after being taken out of water. However, once the moisture gradient vanishes, it results in an increased strength (if there is no microcracking), even more than the continuously moist cured samples. It is also mentioned that drying after initial moist curing would not negatively affect the splitting tensile strength due to the biaxial compressive zone underneath the point load which corresponds to the same region of the tensile eigen stresses. The research of Hanson [17] confirms it by showing a positive effect of drying for the splitting tensile strength after a certain moist curing period. Moreover, the research of Conroy-Jones and Barr [11] cites the complexity in understanding the drying phenomenon due to the presence of both positive and negative effects. On one hand, drying can lead to a moisture gradient, which can result in prestressing the specimen creating a positive effect. On the other hand, the negative effect of drying can be development of cracks due to the tensile strength being exceeded. It is also highlighted that although splitting failure is an internal failure test, but the ultimate failure is governed by the surface underneath the point load. Thus, the negative influence due to air curing affects the splitting tensile test too in addition to the surface failure tests like flexural and direct tensile tests. The dependence on the different grades of concrete is not entirely concluded due to complexity in understanding the net effect between the positive and negative influences. For E-modulus, it is shown by authors like Asselanis et al. [5] and Kocab et al. [21] that the continuously moist cured samples gives higher values than the air cured ones. Although, the study by Asselanis et al. [5] conclude that for a higher strength concrete mix, 7 days of moist curing is sufficient to gain almost the same strength as the continuously moist cured over a duration of 56 days.

With regard to the "specimen size" effect, it is imperative to combine the effect with the varying curing regimes, in order to understand the phenomenon better. In case of standard conditions, the traditional size effect is prominent wherein smaller specimens have increased tensile and compressive strength, as observed by many researchers like Carrasquillo et al. [9] and Irvani [19]. But, with the introduction of air curing/combination of air and water curing, understanding the trend becomes slightly complicated. This is evident from the research of Soroka and Baum [37] and Aitcin et al. [3] whose results on the compressive strength are contradictory. While Soroka and Baum [37] depict that the negative effect of drying dominated the smaller size specimens, Aitcin et al. [3] prove otherwise concluding that larger sized specimens have wider surface cracks due to drying. In case of splitting strength, the results are quite limited, especially for varying drying conditions. With regard to the E-modulus, there is no such major size dependency observed in the

literature.

In case of drying shrinkage, it is reported to be higher for the high water cement ratio mixes, with almost negligible value for the ultra high strength concrete mix. Moreover, the drying shrinkage is only an issue when there is some kind of external or internal restraint present in a concrete specimen/structure. In that case, it can lead to cracking if the tensile stresses at the surface exceed the tensile strength of concrete. It is also pointed out by van Breugel [38] that the Eurocode assumes uniform shrinkage throughout the entire concrete section which could lead to underestimation of the tensile stresses generated at the edges as a result of the internal restraint leading to surface cracking.

In a nutshell, it can be observed that a lot of researchers have tried to understand the development of mechanical properties of cement based concrete with time based on the various parameters like the curing conditions, specimen size and type of concrete (based on strength). However, it is noted that the complex interdependency of the parameters involved makes it challenging to get a clearer picture on the development of properties in time. In this regard, it is believed that a further research into understanding the parameters involved along with their inter-dependency would help to get a better insight on understanding the trend of the mechanical properties with time.

3

Methods

3.1. Introduction

Based on the motivation highlighted in Chapter 1, an initial hypothesis is formulated wherein a similar reduction in the trend of mechanical properties due to drying, as observed by Prinsse [35] for a Geopolymer concrete, is expected to occur for ordinary concrete. It is assumed that if drying does have a huge influence on the properties, the effect could vary for different specimen sizes. Moreover, it is assumed that the effect could also vary for the different strength of ordinary concrete mixes designed. Subsequently, an extensive literature survey is carried out where it is understood that there is some uncertainty involved in the trend of mechanical properties of the ordinary concretes with time which is further aggravated due to the interdependency of various parameters mentioned above. Thus, an extensive experimental program is set up in order to understand the development of properties in time for the ordinary concrete mixes based on the above mentioned parameters and verify if a similar reduction in the trend of mechanical properties due to drying occurs, as observed by Prinsse [35] for the Geopolymer concrete.

Additionally, from the literature survey, it is evident that a major parameter influencing the trend of particularly compressive and tensile strength with time is the non uniform drying that occurs across the concrete specimen. Due to this effect, eigen stresses are generated (compressive stresses inside and tensile stresses outside) and they play a significant role in the development of compressive and tensile properties of concrete with time. These eigen stresses are only present temporarily as long as there is sufficient moisture gradient across the specimen. During this period, they seem to increase the compressive and splitting tensile strength while reducing the direct tensile strength. In case, these (tensile) eigen stresses on the surface exceed the tensile capacity of concrete, there could be microcracking and thus permanent decrease of all the strength properties. Moreover, from the literature study it is noted that majority of the experiments are performed (also in the current experimental regime) at a larger frequency (for example at 28, 56, 90 days and so on..). Thus, there is a tendency to miss out the period during which the eigen stresses might have been present (as shown in red in figure 3.1)

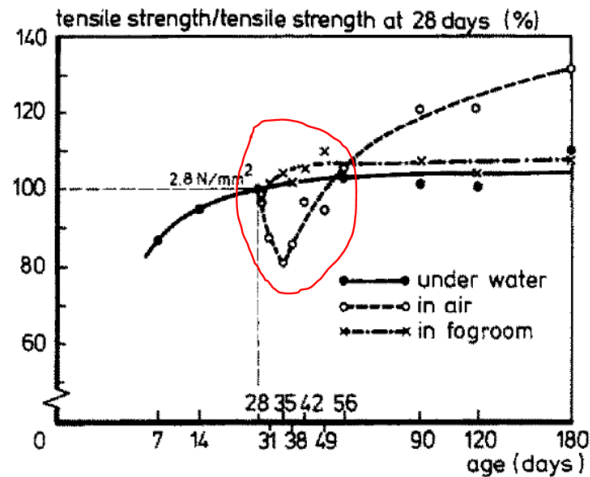


Figure 3.1: Figure depicting the region of influence of tensile eigen stresses

In this regard, a finite element tool can be useful in order to capture the effect due to the eigen stresses which is being missed out in the experiments. For this purpose, a specialized concrete material FEM tool known as "FEMMASSE" is used in this study. This model can also be used to reproduce the results obtained in the experimental study and help understand the results at a greater depth.

Accordingly, with a clear motivation in mind, the research objectives and the research questions are framed. Furthermore, the research strategy and methodology is also looked upon.

3.2. Research Objectives

1. To investigate the development of mechanical properties of ordinary concrete mixes in time.

The main idea is to investigate if drying after a certain moist curing period does cause reduction in the development of the mechanical properties of the ordinary concrete mixes (viz. compressive strength, splitting tensile strength and elastic modulus) with time as reported by Prinsse [35] for a Geopolymer concrete. Additionally, the goal is also to understand the effect of specimen size, strength grade and curing conditions on the observed trend.

2. To understand the trend of the mechanical properties obtained experimentally at greater depth using numerical simulations.

The idea is to use a numerical simulation tool "FEMMASSE", designed for concrete material specialists, in order to simulate the experiments and help understand the results obtained experimentally at a greater depth.

3.3. Research Questions

The research objectives stated will be achieved by answering the following research questions during the course of the thesis.

1. Do the reduction in the trend of the mechanical properties in time also occur for the ordinary concrete mixes of different strength casted here at TU DELFT? If yes, what are the reasons for such behaviour?

a) Does the observed behaviour depend specifically on the strength of concrete mix considered? If yes, how can it be explained?

b) If the type of curing regime and testing conditions does cause sharp variations in the development of properties in time, how can it be explained? Is the observed behaviour only temporary (as a result of eigen

stresses), or is it permanent (as a result of microcracking) ? Is the observed behaviour more dominant on the smaller sized samples? If yes, how can it be explained?

2. Can the numerical concrete material FEM tool " FEMMASSE" help in understanding the experimentally obtained results at a greater depth?

3.4. Research Strategy

The first research objective is fulfilled by answering the first research question. The major strategy followed is the Experimental based approach, wherein the results of the various experiments is used for study/comparison with the literature data and the database in Stevin II lab.

In order to address the first research question , an experimental set up is arranged. For that, three mixes of portland cement mixes are considered based on strength (Normal Strength, High Strength and Ultra High Strength concrete). For all the concrete mixes, only CEM-I cement type is used. Accordingly, these mixes will be exposed to the two curing conditions (similar to the one used by Prinsse [35]) :-

1. Continuous moist curing (CM) (fog room, 20° C and 99% RH) until testing
2. 28 day moist curing (28 DM) , followed by exposure to lab conditions (20° C and 55%RH) until testing.

It is observed from the literature that there is not much importance given to the testing conditions. However, in this study, NEN 12390 standards are followed. As in the standards, it is only mentioned to keep the surface dry (no specific duration), it is decided use the knowledge of previously conducted experiments at TUD by Prinsse [35] and Lukovic [25] where the specimens are kept in the lab conditions (20° C and 55%RH) for 2 hours before testing. It is assumed that the effect of drying for 2 hours does not give rise to a large moisture gradient within the specimen. For the mixes exposed to 28DM regime, the compressive strength, elastic modulus and splitting tensile strength are determined at the age of 28, 56 and 91 days. For the ones exposed to CM regime, the above properties are only determined at 91 days to see the difference caused by continuous moist curing.

The parameters investigated and mechanical properties tested is schematically shown below :-

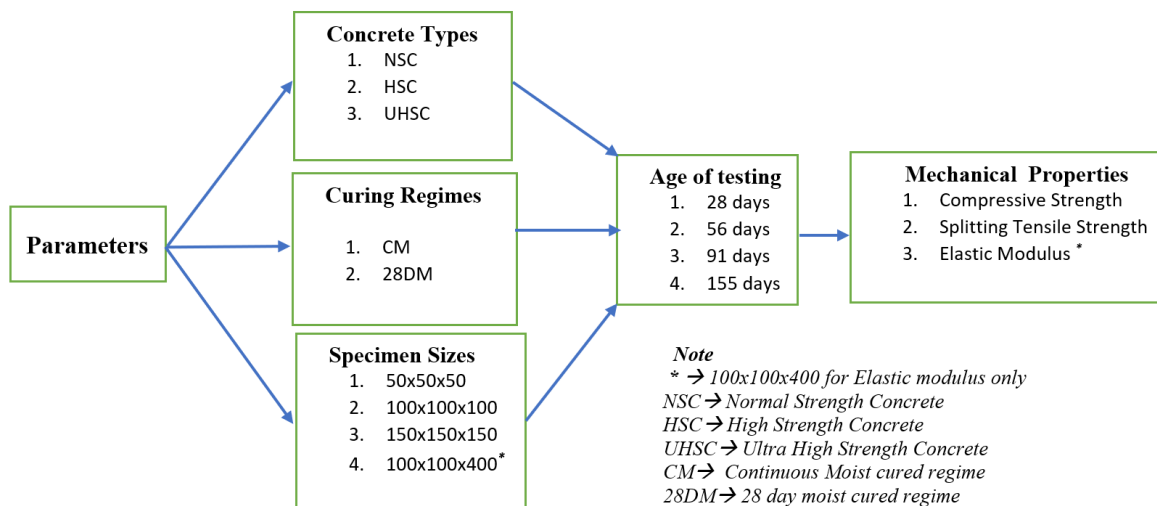


Figure 3.2: A schematic representation of the parameters investigated and mechanical properties tested

Additionally, testing of drying shrinkage and inspection of possible surface cracking using a portable microscope is also planned as part of the experimental set up.

For the experimental set up, the total number of prisms and cubes are schematically planned.

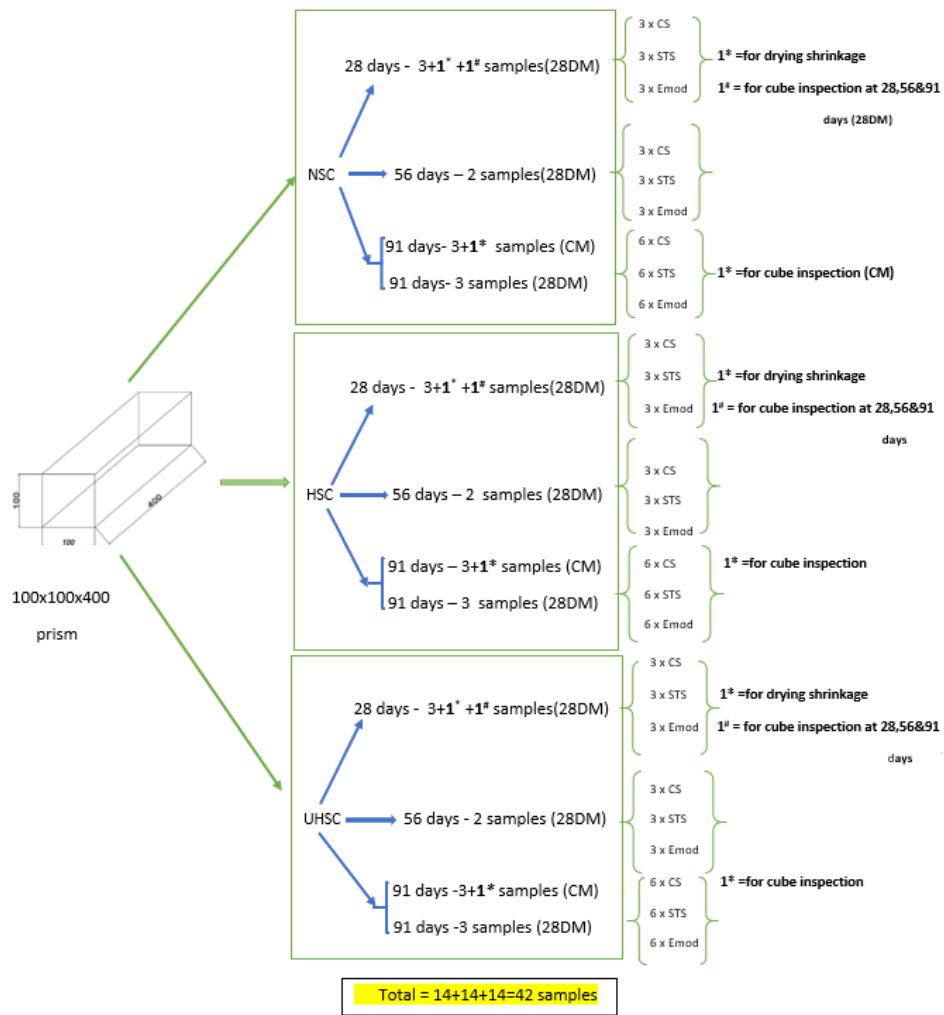


Figure 3.3: A schematic representation of number of prism specimens

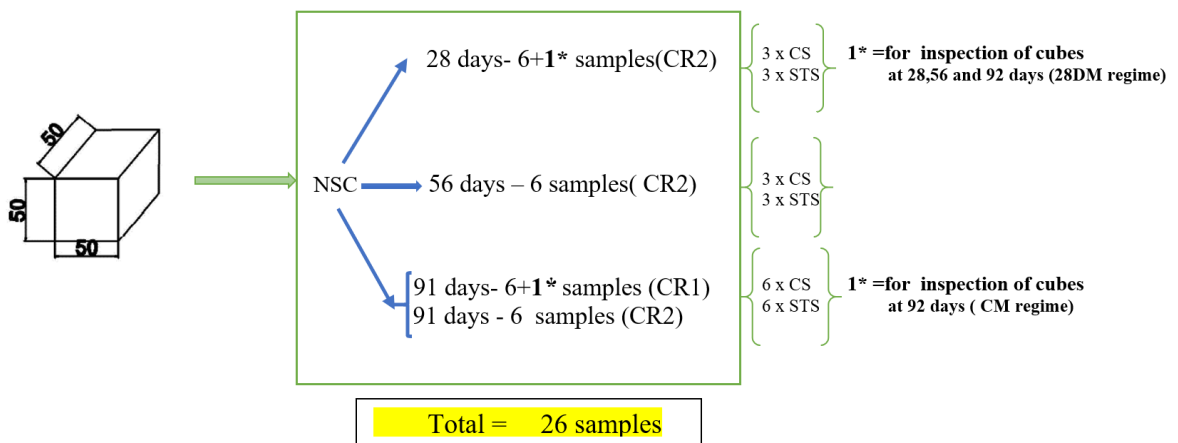


Figure 3.4: A schematic representation of number of 50mm cubes

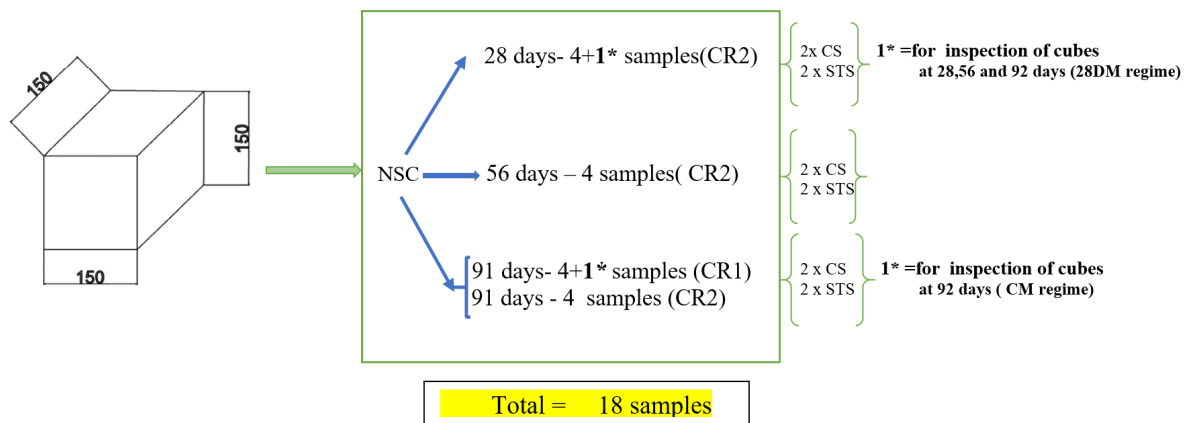


Figure 3.5: A schematic representation of the number of 150mm cubes

Thus, the results of the various mechanical properties tested in time is analyzed along with the help of information from the inspection of cubes and drying shrinkage tests. With this, the first research objective is fulfilled.

The second research objective is fulfilled by answering the second research question. For this case, a "Numerical Modelling based approach" is carried out by using the FEM tool known as "FEMMASSE" designed specifically for concrete material specialists. The basic strategy is to simulate the experiments as realistically as possible by taking into account the effects of hydration as well as hygral behaviour.

3.5. Research Methodology - Experimental

3.5.1. Materials and Mix Design used

For this study, CEM-I class of cement (CEM-I 42.4N and CEM-I 52.5R) is used for the design of all concrete mixes. Accordingly, three types of cement concrete mixes are designed based on strength from the existing database. The NSC, HSC and UHSC mixes have a specified (cube) strength of 25, 67 and 120 MPa respectively at 28 days. The ingredients used for NSC and HSC are the same except for the cement type (a rapid hardening cement (CEM I 52.5R) is used for the HSC mix. The UHSC mix is characterised by the addition of Blast Furnace Slag (BFS), silica fume and steel fibers. The details of the mix design is shown in the tables 3.1, 3.2 and 3.3.

For the NSC mix, the casting is done in two batches of 100 L each. For the HSC mix, the existing mix design was modified as the superplasticizer considered in the planned mix design was not available. As an alternative, a superplasticizer with a brand name "Glenium 51" is used. However, on using the same quantity as the planned mix design, the resulting mixture turned out to be watery and not workable indicating that the quantity of superplasticizer was not adequate. Finally, instead of 350 mL, only 20 mL is used and the corresponding quantity of water is adjusted.

Table 3.1: Mix Design for NSC

Normal Strength Concrete (NSC) w/c : 0.6 Casting date : 10th April 2019		Volume	
		Batch A : 100L	Batch B : 100L
Ingredients	Density (kg/m³)	(in kg)	(in kg)
CEM I 42.5 N	260	26	26
water	156	15.6	15.6
sand 0.125-0.25mm	78.83	7.883	7.883
sand 0.25-0.5mm	256.2	25.62	25.62
sand 0.5-1mm	256.2	25.62	25.62
sand 1-2mm	157.661	15.766	15.766
sand 2-4mm	98.538	9.854	9.854
gravel 4-8mm	394.152	39.415	39.415
gravel 8-16mm	729.181	72.918	72.918
superplasticizer	0.26	0.026	0.026

Table 3.2: Mix Design for HSC

High Strength Concrete (HSC) w/c : 0.45 Casting date : 15th April 2019		Volume=65L	
Ingredients	Density (kg/m³)	Planned mix design (in kg)	Modified mix design (in kg)
CEM I 52.5 R	166.667	24.93	24.93
water	366.667	11.33	11.04
sand 0.125-0.25mm	75	5.1	5.1
sand 0.25-0.5mm	93.333	6.35	6.35
sand 0.5-1mm	150	10.2	10.2
sand 1-2mm	223.333	15.19	15.19
sand 2-4mm	300	20.4	20.4
gravel 4-8mm	373.333	25.39	25.39
gravel 8-16mm	653.333	44.42	44.42
Superplasticizer	5.133	0.349	0.02

Table 3.3: Mix Design for UHSC

Ultra High Strength Concrete (UHSC) w/c : 0.23 Casting date : 23rd April 2019		Volume=65L
Ingredients	Density (kg/m³)	(in kg)
CEM I 52,5 R	800.4	52
CEM I 42,5	69.6	4.5
Blast furnace slag	104.4	6.8
Silica fume	43.8	2.9
Water	204.6	13.3
Superplasticizer	26.6	1.7
Sand 0,5-1,0	529.1	34.4
Sand 0,25-0,5	318.7	20.7
Sand 0.125-0,25	213.3	13.9
Fibers (13 mm)	125	8.1

3.5.2. Casting, demoulding and curing procedures

The overall casting and demoulding process is spread over 3 weeks, with each type of mix casted and demoulded in a particular week. In general, the casting procedure of HSC and NSC are similar. However, there is a slight difference while casting the UHSC specimens. The typical steps followed while casting, demoulding and curing the specimens are depicted in the following steps.

STEP 1 : *The ingredients are placed in buckets, weighed according to the mix design and kept ready for mixing. In case of UHSC, the extra ingredients include Silica fume, Blast Furnace slag and steel fibers.*

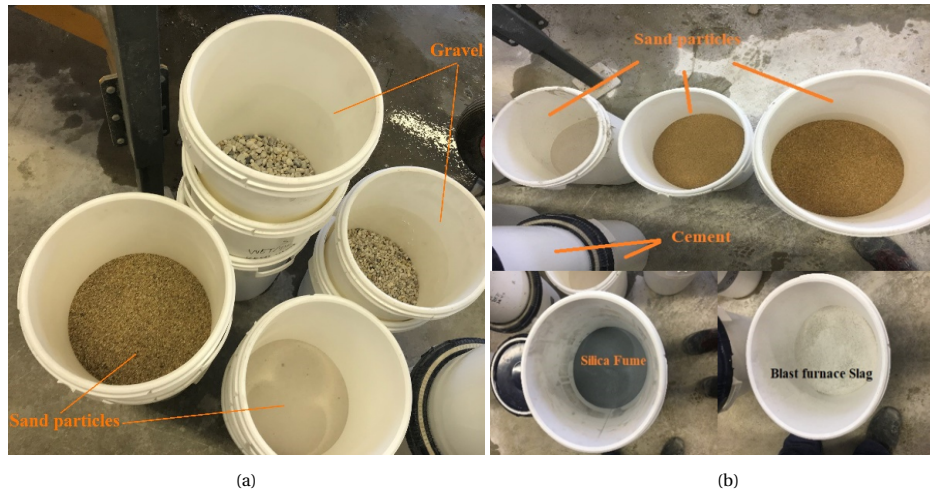


Figure 3.6: (a) Ingredients used for NSC and HSC mix (b) Ingredients used for UHSC mix

STEP 2 : *The sand and gravel particles are dry mixed for roughly 3 minutes and then the cement is added and mixed for additional minute. In case of UHSC, all the ingredients including silica fume and Blast furnace slag are added and mixed for a minute. For the mixing, a concrete mixer with 100 L capacity is used*

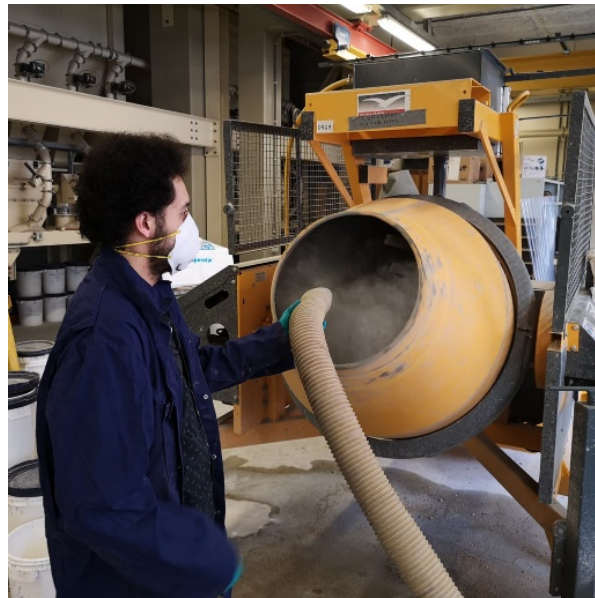


Figure 3.7: A 100L Concrete mixer for mixing the ingredients

STEP 3 : *The superplasticizer is mixed with water and added to the mixture (roughly 3/4th is added first). After about a minute, the remaining 1/4th is added. The mixing process is carried out for about four minutes. In case of UHSC, after the addition of superplasticizer, the fibers are added (in two halves) and mixed for 1 minute.*



Figure 3.8: (a) Adding of water mixed with superplasticizer (b) Adding of fibres in case of UHSC mix

STEP 4 : *If the mixture is well mixed, the concrete is poured in a wheelbarrow and taken near to the location where the moulds are ready to be filled. For convenience, the moulds are already pre-oiled and kept on the vibrating table.*



Figure 3.9: Prepared mix for (a) NSC (b) UHSC

STEP 5 : *The concrete mixture is then poured in both the cube and prism moulds in approximately 3 layers. After each layer, the vibration machine is turned on and the mixture is vibrated for about 20 seconds. After filling, the top surface is levelled.*

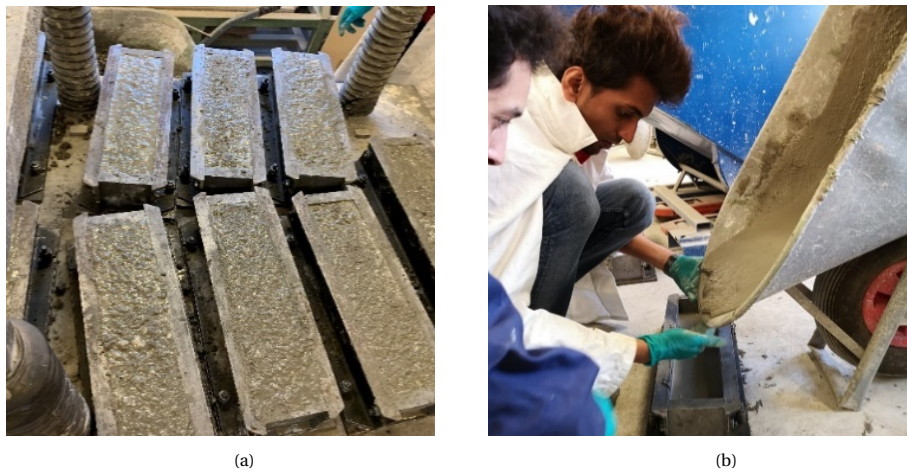


Figure 3.10: (a) Pouring of NSC mix in prismatic moulds NSC (b) Pouring of UHSC mix

STEP 6: *Immediately after levelling the top surface, the moulds are covered with plastic sheets to prevent evaporation of water. To ensure that the plastic sheets remain intact, wooden blocks are placed in the sides for of the mould. The moulds are clearly labelled for future use*



Figure 3.11: Covering of moulds with plastic sheets

STEP 7: *The demoulding is done after 24 hours after the mix has sufficiently hardened. All the specimens are placed in the fog room which was maintained at (22° C and 99% RH) until 28 days. After the curing period, some of the specimens are taken out and kept in laboratory conditions , which is maintained at 20° C and 55% RH.*



Figure 3.12: (a) Demoulding of UHSC prism (b) NSC specimens taken to the fog room

3.5.3. Testing Procedures

Elastic Modulus test

The determination of Elastic Modulus is done according to the ISO 1920-10 2010 standards. The following steps/instructions are followed :-

- a) The prism specimens (100x100x400) used has the length/width ratio equal to 4 and it is within the limit of the standards. The specimens are taken out from the fog room and brought to the lab. It is important to note that the specimens are not re immersed in water for 12 hours before testing.
- b) It is ensured that the setting up of the apparatus is done as quickly as possible before testing. The strain measuring apparatus is set up by first identifying the reference points with the help of a plastic mask (as shown in figure 3.13a), then carving the surface identified, followed by gluing the metallic devices on those carved surfaces (as shown in figure 3.13b).



Figure 3.13: Preparation for E-modulus test (a) labelling of reference points with plastic mask (b) specimen after gluing of metallic devices

c) The test is performed using the TONI-BANK machine in Stevin II lab. The specimen along with the metallic devices attached is placed centrally with the casting side facing the back wall of the machine (see figure 3.14). After that four LVDTs are used to measure the vertical displacement.



Figure 3.14: Specimen with LVDTs attached placed in the Toni Bank machine

d) The specimen is initially loaded under displacement control until a basic stress of 0.5 MPa is reached. After that the machine is turned to Load controlled mode with the speed of 1.6 kN/s until one third of the maximum compressive strength of the specimen is reached. The specimen is then unloaded and this completes one cycle. The specimen is loaded and unloaded again for 2 more cycles.

e) Then, the output file is exported and it contains displacement values obtained by the four LVDTs along with the force and time data. Using these data, stress vs strain plots are made, from which E-modulus can be obtained by using linear regression equations between the two stress levels (basic stress of 0.5 MPa and stress corresponding to one third of compressive strength).

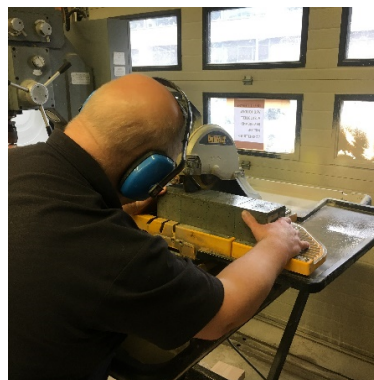
Compressive Strength Test

The compressive strength test is done according to the NEN-EN 12390-3 standards. The following steps are followed :-

a) Firstly the cubes are made ready for testing purpose. For the 150mm and 50mm sized cubes, they are directly taken out of the curing /controlled room. In case of the 100mm cubes, they are wet sawed from the prisms (100x100x400mm). All the cubes sizes comply with the NEN-EN 12390-1 standards.



(a)



(b)

Figure 3.15: Preparation for Compression Testing - (a) Marking of lines before wet sawing , (b) Wet sawing process

b) The continuously moist cured and the wet sawed specimens are dried for about 2 hours before testing (assuming that the excess moisture at the top surface is evaporated till then).

c) The testing is done using CYBERTRONIC machine in Stevin II lab. The cubes are centred and positioned such that the load applied is perpendicular to the direction of the casting. The rate of loading is kept constant and adjusted according to the standards which considers the dimensions of the cubes. The maximum load sustained is then recorded.



Figure 3.16: Testing of Compressive Strength of cube

d) Finally, the compressive strength (f_c) is calculated by dividing the maximum load sustained (F) with the cross sectional area (A_c).

$$f_c = \frac{F}{A_c} \quad (3.1)$$

where, "F" is the maximum load sustained in [N] and A_c is the cross sectional area in [mm^2]

Splitting Tensile Strength

The Splitting Tensile test is carried on using NEN-EN 12390-6 standards. Instead of cylindrical specimens, cubes are used. It is mentioned in the standards that the cube specimens have approximately 10% higher values than cylindrical specimens. The following procedure is followed :-

a) Firstly the cubes are made ready for testing purpose. For the 150 mm and 50 mm sized cubes, they are directly taken out of the curing /controlled room. In case of the 100 mm cubes, they are wet sawed from the prisms (100x100x400mm).

b) Similar to the Compression Testing, the wet sawed cubes and the continuously moist cured specimens are dried two hours prior to testing.

c) The testing is done using the same CYBERTRONIC machine in Stevin II lab. The specimen is centred and is kept in between two wooden strips, making sure that the load is distributed and perpendicular to the direction of casting, as shown in figure 3.17



Figure 3.17: Testing of Splitting tensile strength of cube specimen

d) The loading rate is again set according to the standards considering the specified dimensions. As soon as the crack is appeared, the machine is stopped and the maximum load sustained is recorded.

e) Finally the Splitting tensile strength (f_{spt}) is calculated using the formula below :-

$$f_{spt} = \frac{2P}{\pi \cdot l \cdot d} \quad (3.2)$$

where, "F" is the maximum load sustained in [N], "l" is the length of line of contact of the specimen in [mm] and "d" is the cross section dimension in [mm]

Drying Shrinkage

The Drying Shrinkage test is carried out in accordance to ISO 1920-8. After demoulding, the prism specimen (100x100x400) is placed in the fog room (20° C and 99 % RH) until 28 days. After that, the specimen is taken out and kept in a room under lab conditions (20° C and 55 % RH), where the arrangement is made for the drying shrinkage test. The drying shrinkage test consists of length change and weight loss measurements. The length change measurements, which yields the magnitude of the shrinkage, is done by attaching a clock at a distance of 100mm from the top (as shown in the figure 3.18). It has a measuring length of 20cm and an accuracy of 1 micrometre. The weight loss measurement is done by weighing the prisms on an electric weighing machine with an accuracy of 0.1 gram. Both the weighing and length change measurements are done every day in the earlier days with increasing frequency as both the parameters stabilize.

Initially one prism for each of the three types of concrete mixes is opted. However, due to the successive inaccuracy in the results of NSC and HSC mixes due to temperature and RH fluctuations in storage room, four prisms (2 each for NSC and HSC mix) are casted again to measure the drying shrinkage.



Figure 3.18: (a) Test setup for measuring Drying Shrinkage.(b) Overview of the prisms used for drying shrinkage measurement

Inspection of cubes for surface cracking

As already mentioned before, due to the non uniform drying of the specimen, a moisture gradient is developed across the cross section leading to tensile eigen stresses at the surface. There is a possibility of cracking even before loading the specimen, if these tensile eigen stresses exceed the concrete's tensile strength. In order to check for the surface cracking, a portable microscope is used. For each of three sizes - 50, 100 and 150 mm, one cube is set aside for inspection which is exposed to the same curing regime (28DM) as the ones used for testing. On the surface of the cubes, square grid lines are drawn in order to mark and track the growth of the crack(in case there is one) over time. The arrangement for the cube inspection is shown in figure 3.19

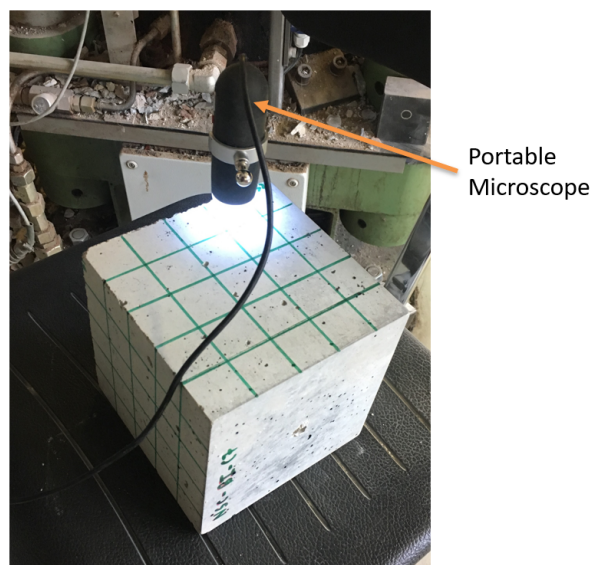


Figure 3.19: Inspection of surface cracking using portable microscope

3.6. Research Methodology - Numerical Modelling

As discussed before, the goal of using the modeling approach is to simulate the experimental tests in order to understand the results at greater depth. The idea is also to understand the influence of eigen stresses on the trend of strength development by modelling the experimental tests at smaller intervals which otherwise is being missed out in the experimental tests. During the course of the thesis, it is realized that the model has its limitation in predicting the compressive behaviour. Thus, it is decided to focus on the tensile behaviour by simulating the direct tension, flexural and splitting tests. In order to meet the stated goals using FEMMASSE, the following steps are followed.

- a) Setting up of Geometrical and Material properties of the model.
- b) Setting up of the hygral properties for simulating the effect of drying.
- c) Setting up of the loading and support conditions for the experimental tests.
- d) Validation of the model for simulating the hygral behaviour and the splitting tensile tests.
- e) Applying the analytical concept mentioned in the pink book [38] to understand stresses due to shrinkage deformations.
- f) Simulating the current experimental set up of splitting tensile test and also simulating the direct tension and flexural strength test.

3.6.1. "FEMMASSE" : An Introduction

FEMMASSE stands for Finite Element Modules for MAterials Science and Structural Engineering and it is specifically designed for concrete material specialists. The software is based on the heat and moisture models developed by the collaboration of researchers namely Peter Roelfstra from EPFL and Erik Schlangen from TU DELFT. This software works only in a 2D environment and can simulate the experimental tests by using the state parameter approach. In this approach, the various material properties are a function of the state of the material. The user has control over the choice of the state of the material which could be the relative humidity, temperature, degree of hydration, maturity and moisture content.

3.6.2. General Description of the model used

In this study, FEMMASSE-MLS version 8.5 is used for all the simulations. As already mentioned, the corresponding tasks using FEMMASSE are to model the drying behaviour and simulate the tensile tests. Accordingly, the model is configured to take into account the effect of hydration and the hygral behaviour. The hydration is incorporated in terms of the strength of the material property considered as a function of maturity based on standard conditions (20° C and moist cured conditions). The hygral behaviour is incorporated by defining a hygral boundary and then imposing the value of the moisture potential at experimental conditions. Additionally, the diffusion and film coefficients are also taken into account in order to simulate the flow of the moisture from/within the concrete specimen. Finally, the tensile can be simulated by making use of the experimental set up and the corresponding conditions used. It is important to note that the effects of self desiccation and relaxation are not taken into account in the model.

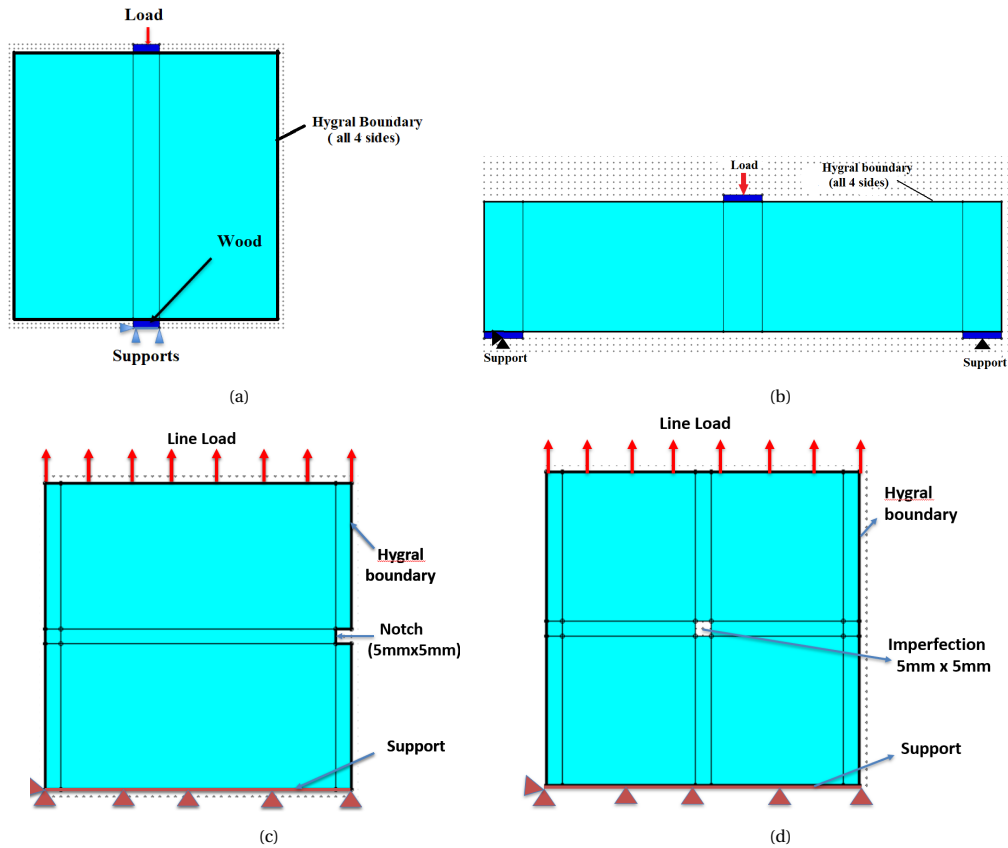


Figure 3.20: General Model used for - (a) Splitting Tensile test (b) Flexural strength test (c) Direct tension test using a notch (d) Direct tension using an imperfection

3.6.3. Geometry of the model

In the current study, all the models used in FEMMASSE are based on 2D environment using regular plane stress elements. All the models have a thickness of 1mm. The shape and dimensions of the specimens are based on the types of tests.

For simulating the splitting tensing test, a 2D model is made corresponding to the experimental set up for the different sizes of the cubes used (50,100 and 150mm). The dimensions of the wooden strip is in accordance to the experiments performed according to NEN standards. In case of the flexural strength, a standard beam of cross sectional size 100x400mm is modelled along with the steel plate of size 25mmx5mm underneath the two point supports and at the application of point load at the centre. In case of direct tension test, two models are proposed , one with a notch(5mmx5mm) at the side and other with an imperfection (5mmx5mm) at the centre. The dimensions of the specimen used is 100mm. A typical model used for both the tests are shown in the figure 3.20

3.6.4. Material properties

Strength and Stiffness properties

In this study, the major focus is on simulating the tensile tests of the cement based concretes of various strength grades. Thus the development of tensile strength in time along with the softening behaviour of concrete in tension are the most important material properties. The other properties which are relevant include the compressive strength, elastic modulus, poissons ratio, etc. The development of tensile, compressive strength and Elastic modulus in time is inputted in the model based on the experimental value at standard conditions (20° C and moist cured conditions). In the current experimental set up, the tensile, compressive and Elastic modulus tests based on standard conditions are only performed until 91 days. Thus, for

simulations at further ages, there is no experimental data. An option was to use Eurocode to predict the strength/stiffness after 91 days. However, it is noticed that Eurocode leads to underestimation of the value even at 91 days and if the size effect is to be taken into consideration, it becomes even more complicated. Thus, for simulations post 91 days, the trend for strength and stiffness with time is taken as constant. In case of poisson's ratio, a constant value of 0.2 is opted. The wood and steel used in the splitting and flexural tests are modelled as linear isotropic members.

Tensile softening behaviour

In case of the tensile softening behaviour for the NSC and HSC, Hillerborg's bilinear curve defined in FEM-MASSE is used. The parameters are based on values obtained by [41] for mixtures of similar w/c ratio.

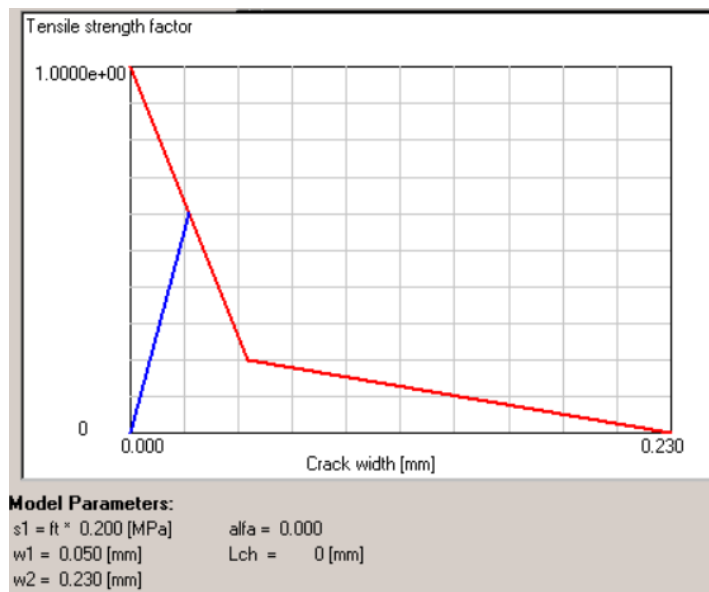


Figure 3.21: Tensile softening curve defined for both NSC and HSC mixes

3.6.5. Hygral properties

The hygral boundary is defined on all four sides of the specimen in case of both flexural and splitting tests. The specimens are exposed to relative humidity of 50%, similar to the experimental conditions. The important hygral properties taken into account are the film, diffusion and the shrinkage coefficient.

Film coefficient

In order to depict the rate of evaporation, a film coefficient is given depending on the type of concrete mix. For the NSC mix, a film coefficient of 3.5mm/day is chosen (after the sensitivity study done as discussed later in 4.2.1). In case of HSC mix, a five times lower value of the film coefficient is chosen (0.7mm/day) based on logical assumptions from the NSC mix.

Diffusion coefficient

The diffusion coefficient of Normal strength concrete is based on the research by Bazant and Najjar [7] for similar w/c ratio. In case of HSC, due to the lack of data, a logical assumption is made and the value is reduced by 5 times.

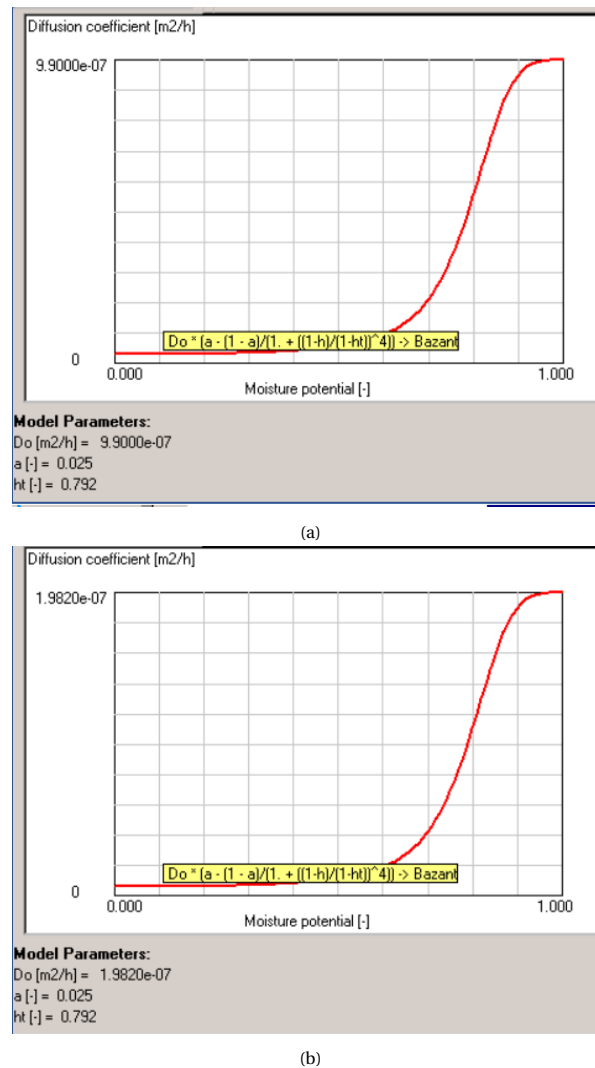


Figure 3.22: Diffusion curve as defined for (a) NSC mix and (b) HSC mix

Shrinkage coefficient

There is no consensus in the literature for the value of shrinkage coefficient even for the normal strength concrete mixtures. As a benchmark, a value of 0.001 is chosen as opted in the PhD thesis of Lukovic [25]. For the higher strength mixtures, limited data is available. Thus, as an assumption, the same shrinkage coefficient used for NSC is chosen.

3.6.6. Loading and Support conditions

In case of the splitting test, the load is applied at the centre of the wooden block placed at the centre of the specimen. The loading rate is in accordance to the NEN standards used in the experiment. The supports are given at the base of the wooden block consisting of two point supports in the vertical direction and a horizontal point support to closely depict the experimental set up. In case of flexural test, a point load is applied at the centre of the steel plate with a loading rate of 0.0277 N/sec. Two vertical point supports are given at the two bottom steel plates along with a horizontal point support only in the middle of the bottom right steel plate. Finally, for the direct tension tests, a line load is applied at the top with the same loading rate as used in the flexural tests. A vertical line support is used at the bottom surface with a point support at the extreme left node.

3.6.7. Meshing and Analysis

With regard to meshing fully integrated element type is chosen with the size of the element depending on the size of the specimen. Generally, a comparatively finer mesh is used for regions underneath the point loads. The typical mesh arrangement for all the specimen used in the respective tensile tests are given in the figure

With regard to analysis, all the simulations are performed using Load controlled analysis method. The computations are performed until there is a failure of the specimen governed by the convergence limits set in the model. The convergence limits set are the same for all the models and is depicted in the table below :-

Convergence parameters	
Number of Iterations	100
Displacement increment	0.01 mm
Displacement improvement	0.01 mm

3.6.8. Validation of FEMMASSE

It is important to ensure that FEMMASSE can be used to simulate the drying behaviour and the corresponding tensile tests of the current experimental set up. For this matter, the experimental results published by Hanson [17] are used. As already mentioned in the literature study, this research deals with firstly observing the humidity profile across the cross section of the hardened concrete specimen and then understanding the trend of splitting tensile strength based on different curing conditions for a long period of 2 years.

Initially, the idea is to check if FEMMASSE can be used to model the specimen and obtain similar humidity profile by Hanson [17] across the cross section of the hardened concrete specimen. In doing so, all the relevant material properties are given in the paper and can be directly inputted in the model. The trend of the tensile strength and compressive strength is given for standard conditions and they are inputted in the model to account for hydration. With regard to studying the hygral behaviour, the diffusion parameters published by Bazant and Najjar [7] for the same experiment are used. The film coefficient is unknown and there is no consensus in the literature about the value to be used. As a starting point, a value of 0.7mm/day is used based on the PhD thesis of Lukovic [25]. However, there is an important issue which needs to be addressed. The published experimental results are for cylindrical specimens and it is found out during the course of thesis that FEMMASSE has its limitation while simulating splitting tests on cylinders. As a solution, it is proposed to compare the humidity profile in both the cylindrical and cubical specimens and it is found that there are no major differences. The results are discussed in the next chapter.

Moreover, while using the combination of the diffusion coefficient published by Bazant and the assumed film coefficient of 0.7mm/day, it is observed that the humidity profile obtained are not exactly comparable to the experimental results especially at early age. It is hypothesized that the film coefficient is causing the difference and a sensitivity study is done in order to come up with a value which gives the humidity profile closest to the experimental results. Once the film coefficient is finalised, the diffusion coefficient published by Bazant is also verified based on a similar sensitivity study. After choosing the most favourable film coefficient and diffusion coefficient published by Bazant, it is seen that the humidity profile obtained is the closest to the experimental results. Finally, after validating the drying behaviour, the model is extended to simulate the splitting tensile tests and compare with the experimental results. The details of the results of the validation are discussed in the next chapter.

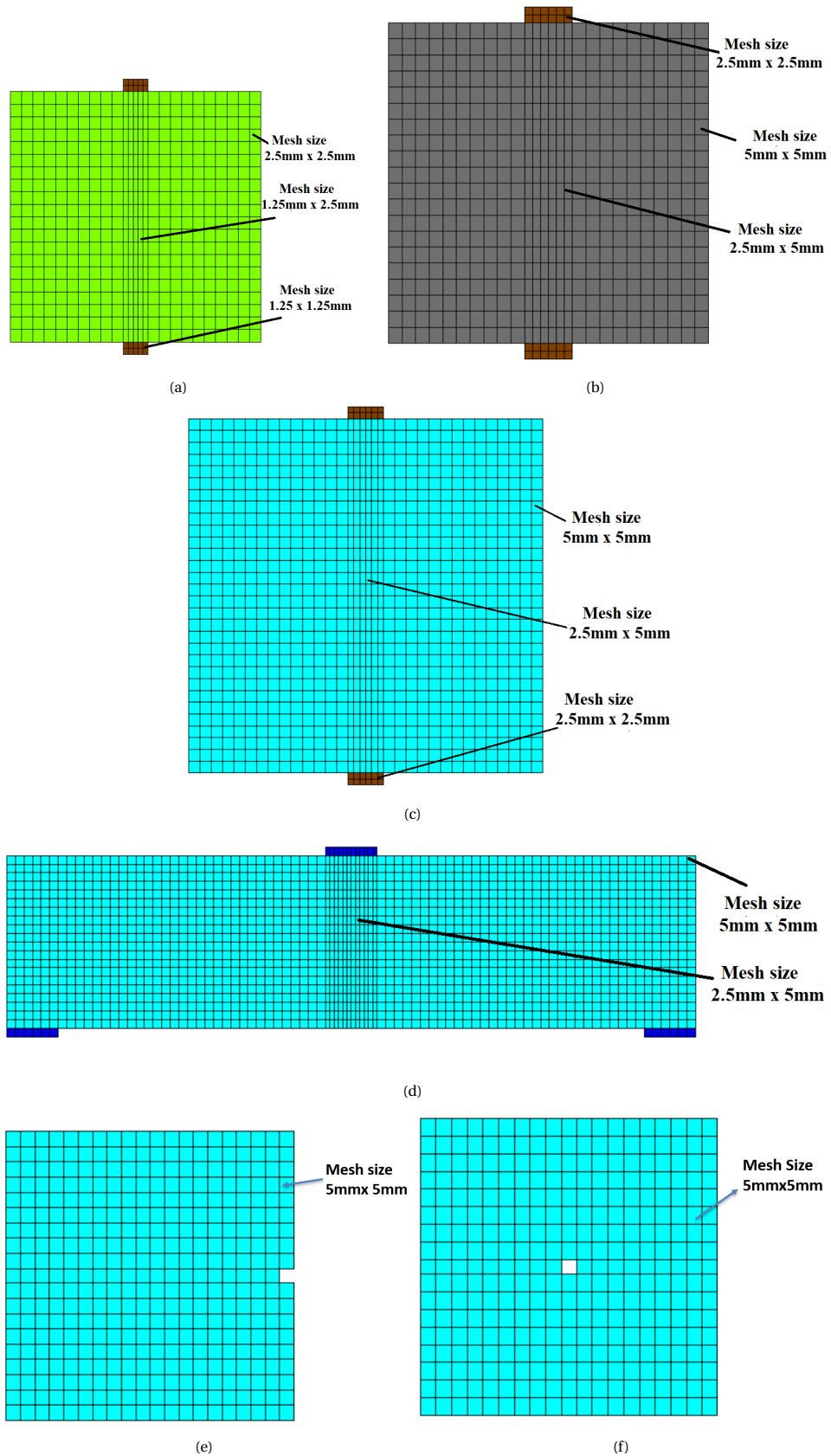


Figure 3.23: Meshing layout for the splitting test for (a) 50mm (b)100mm (c) 150mm specimen and for the (d) flexural test of 100x100x400 prisms (e) direct tensile test with a notch (e) direct tensile test with an imperfection

3.6.9. Analytical approach of understanding drying profile

As stated earlier in chapter 2, in Eurocode 2 the drying shrinkage is calculated assuming uniform distribution of the drying profile across the entire specimen. However, on exposure to atmosphere of lower relative humidity, there is non uniform drying with more drying on the outside compared to the inside and due to the internal restraints, there could be chances of surface cracking.

Thus, in this section, the analytical approach as mentioned in the pink book by van Breugel [38] for temperature profile, is extended to the shrinkage profile using the following steps :-

a) Analogous to the temperature profile, the non linear shrinkage profile (can be given in terms of relative humidity) is broken down into its mean, gradient and eigen/non linear components.

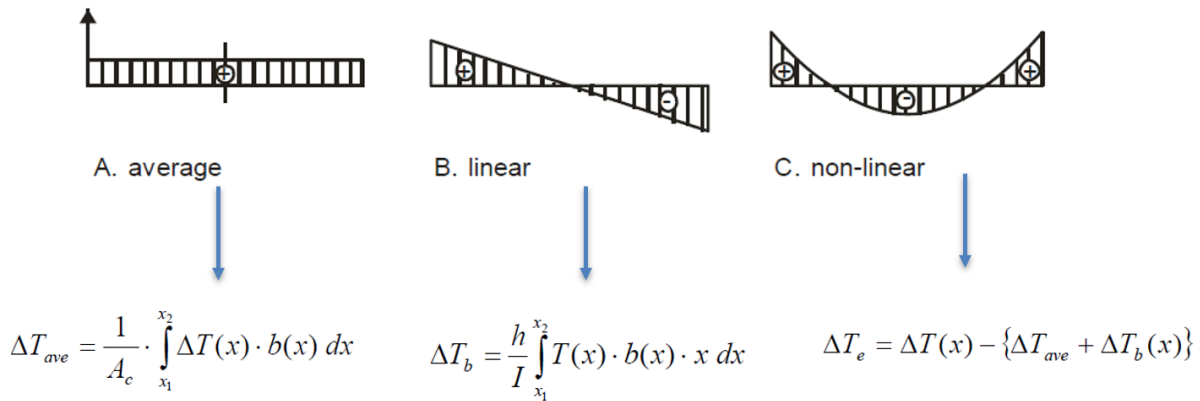


Figure 3.24: Subdivision of shrinkage profile into its mean, gradient and eigen components

b) The shrinkage strain (ϵ_{sh}) is computed corresponding to each of these components by using equation 3.3 and if there are any restraints, the stresses can be determined using equation 3.4.

$$\epsilon_{sh} = \alpha_{sh} \cdot \Delta H \quad (3.3)$$

$$\sigma_{sh} = E \cdot \epsilon_{sh} \quad (3.4)$$

Generally, for an unrestrained(external) concrete specimen exposed to dried atmosphere, there would be no stresses due to mean component. However, due to the eigen component coupled with internal restraint, there could be tensile stresses generated at the surface. This approach is tried on the cube specimens used in the study and the results are given in the next chapter.

4

Results

4.1. Experimental Results

The experimental results of the various tests conducted are presented in this section.

4.1.1. Compressive Strength

Table 4.1 and figure 4.1 shows the compressive strength for the three types of concrete mixes. It is to be noted that all the values are for the 100 mm sized cubes. It can be observed from the figure 4.1 that for the 28 day moist (28DM) cured samples, the trend for the UHSC mix increases continuously with time with an increase of 24% at 155 days relative to 28 days. In case of the NSC and HSC mixes, the trend looks quite similar with both the mixes showing an increasing trend followed by a drop in strength within the period of 91 to 155 days. It is to be noted for both the mixes that at the period of 155 days, the value is still larger than the value at 28 days. Moreover, from table 4.1, it can clearly be seen that at 91 days, there is not much difference between the values of CM and 28DM samples for HSC and UHSC specimens. However, for NSC specimens, CM samples give 16.8 % higher results than 28DM ones.

Table 4.1: Compressive Strength values for the three types of concrete mixes. Note: CM - Continuously Moist cured until test age and 28DM - 28 day moist cured and then exposed to controlled lab conditions until test age

Compressive Strength (in MPa)										
Days	Curing Regime	NSC			HSC			UHSC		
		Value	Mean	SD	Value	Mean	SD	Value	Mean	SD
28	28DM	24.7	27.8	2.9	70.5	64.4	5.4	145.5	131.6	29.75
		29.6			62.7			151.8		
		29.3			60.1			97.4		
56	28DM	34.4	34.1	0.4	62.8	70.6	6.7	139.9	151.2	9.85
		33.9			73.9			157.8		
		33.8			75.1			155.8		
91	28DM	35.3	35.6	1.5	72.4	70.0	2.9	141.9	154.4	11.7
		37.2			66.5			156.2		
		34.2			72.4			165.2		
91	CM	38.1	41.6	3.1	66.3	70.1	4.3	155.9	160.3	4.3
		42.6			69.3			164.5		
		43.9			74.8			160.5		
155	28DM	36	32.8	2.9	61.2	66.1	5.7	152.0	163.0	9.6
		32			64.8			168.9		
		30.4			72.3			168.2		

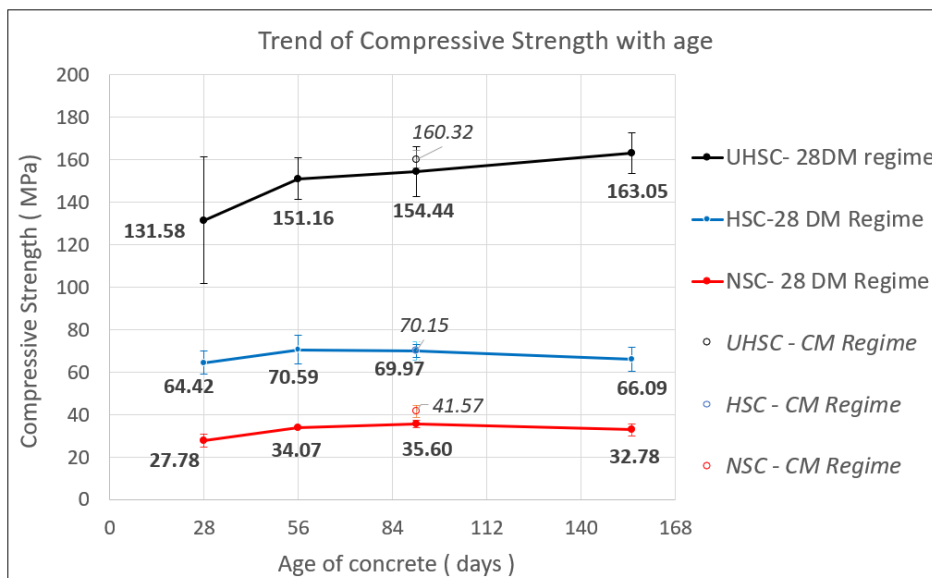


Figure 4.1: Trend of the Compressive Strength with time for different cement based concrete mixes. Note: CM - Continuously Moist cured until test age and 28DM - 28 day moist cured and then exposed to controlled lab conditions until test age

Table 4.2 and figures 4.2- 4.3 show the compressive strength of Normal Strength concrete based on different sized specimens. From the figure 4.2, it is observed that for CM samples, there is a clear traditional size effect seen at both 28 and 91 days. However, for the 28DM samples, there is some ambiguity in understanding the trend as clear from the figure 4.3. Until the period of 56 days, there is a clear traditional size effect seen. However, at the period of 91 and 155 days, the 50mm samples and the 150mm samples have the highest strength respectively, with the value of 100mm dropping continuously within this period.

Table 4.2: Compressive strength values for NSC of different specimen sizes. Note: CM - Continuously Moist cured until test age and 28DM - 28 day moist cured and then exposed to controlled lab conditions until test age

Days	Curing Regime	Compressive Strength [in MPa]								
		150mm			100mm			50mm		
		Value	Mean	SD	Value	Mean	SD	Value	Mean	SD
28	28DM	29.5	29.2	0.4	24.7	27.8	2.9	36.3	33.5	4.3
		29.4			29.6			38.8		
		28.7			29.3			28.2		
				34.1						
				30.2						
56	28DM	30.4	31.5	2.6	34.5	34.1	0.4	41.5	40.4	1.8
		34.5			33.9			37.8		
		29.7			33.8			41.5		
				40.7						
91	28DM	42.4	41.6	2.8	35.3	35.6	1.5	46.5	45.9	0.73
		38.6			37.2			45.4		
		44.0			34.2			-		
91	CM	38.0	38.4	1.0	38.1	41.6	3.1	41.6	42.1	1.4
		39.5			42.6			40.5		
		37.6			44.0			44.0		
				42.3						
155	28DM	45.9	46.4	0.6	36.0	32.8	2.9	46.0	43.9	2.9
		46.8			32.0			41.8		
		-			30.4			-		

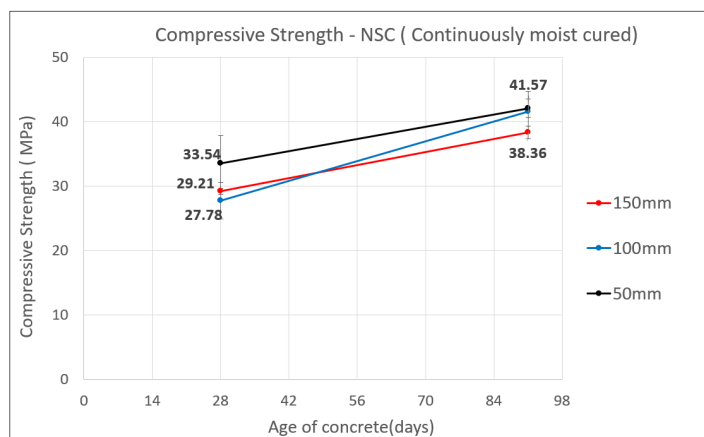


Figure 4.2: Trend of the Compressive Strength of different specimen sizes with time : Continuous moist cured regime. Note: CM - Continuously Moist cured until test age and 28DM - 28 day moist cured and then exposed to controlled lab conditions until test age

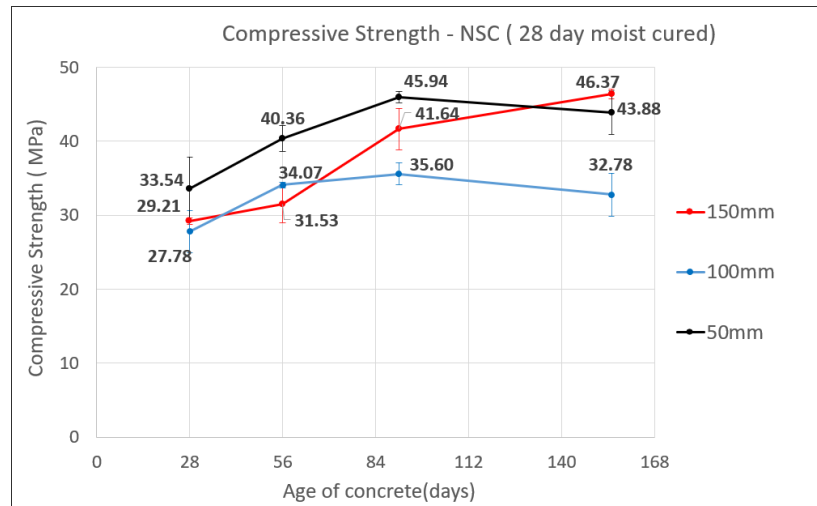


Figure 4.3: Trend of the Compressive Strength of different specimen sizes with time : 28 day moist cured regime. Note: CM - Continuously Moist cured until test age and 28DM - 28 day moist cured and then exposed to controlled lab conditions until test age

4.1.2. Splitting Tensile Strength

Table 4.3: Splitting tensile strength values for the three types of concrete mixes. Note: CM - Continuously Moist cured until test age and 28DM - 28 day moist cured and then exposed to controlled lab conditions until test age

Splitting Tensile Strength (in MPa)										
Days	Curing Regime	NSC			HSC			UHSC		
		Value	Mean	SD	Value	Mean	SD	Value	Mean	SD
28	28DM	3.07	2.98	0.09	5.63	5.23	0.39	20.13	21.66	1.65
		2.96			4.84			21.43		
		2.89			5.22			23.41		
56	28DM	3.66	3.59	0.06	5.05	5.26	0.29	22.02	23.12	1.12
		3.55			5.13			23.07		
		3.57			5.60			24.26		
91	28DM	3.51	3.64	0.15	5.44	5.47	0.11	22.04	21.35	0.62
		3.61			5.59			21.19		
		3.80			5.39			20.83		
91	CM	3.76	3.79	0.02	5.35	5.39	0.08	21.59	19.40	1.91
		3.79			5.34			18.56		
		3.80			5.47			18.06		
155	28DM	3.68	3.71	0.03	5.26	5.22	0.03	19.9	19.6	0.31
		3.71			5.20			19.3		
		3.75			5.21			19.6		

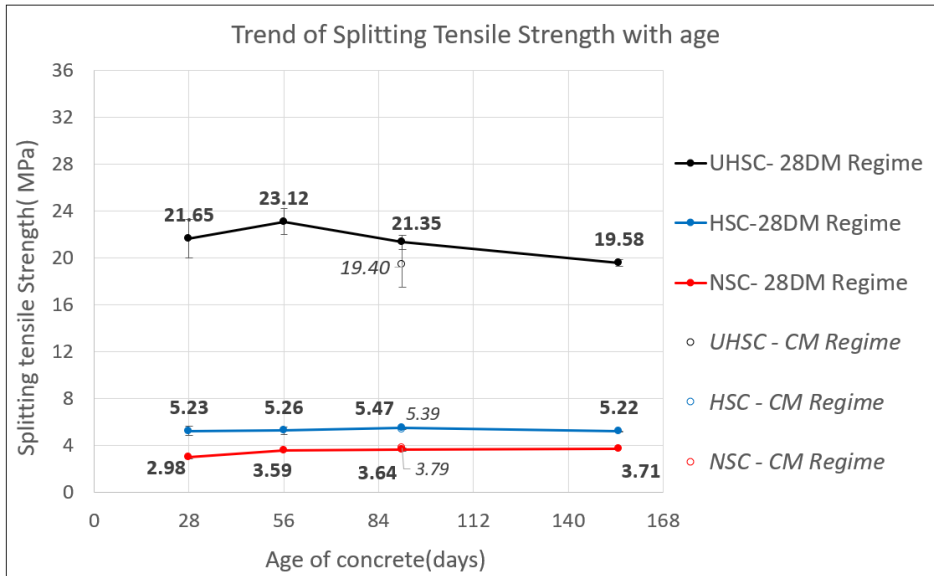


Figure 4.4: Trend of the Splitting Strength of different specimen sizes with time : 28 day moist cured regime. Note: CM - Continuously Moist cured until test age and 28DM - 28 day moist cured and then exposed to controlled lab conditions until test age

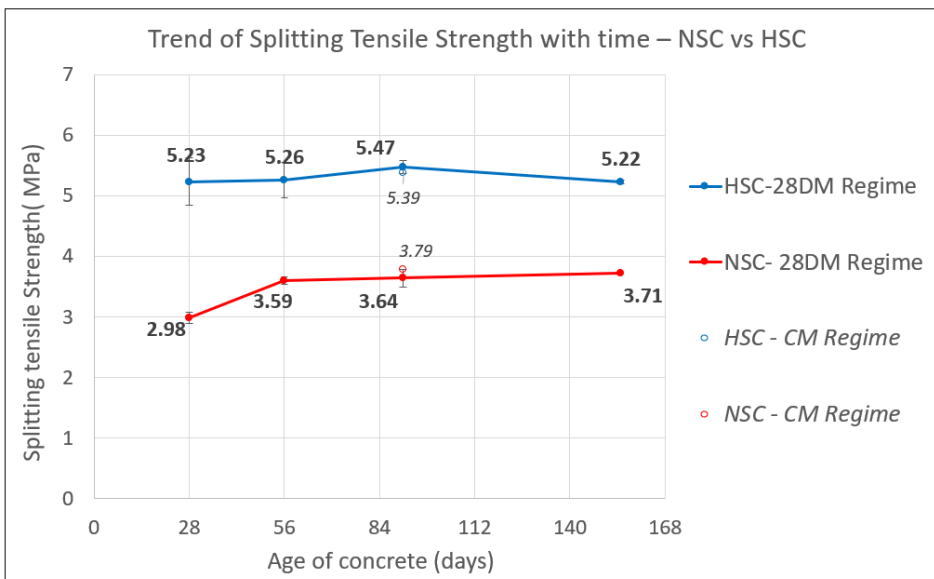


Figure 4.5: Comparison of the trend of the Splitting Strength of NSC and HSC specimens. Note: CM - Continuously Moist cured until test age and 28DM - 28 day moist cured and then exposed to controlled lab conditions until test age

Table 4.3 and figure 4.4 shows the trend of the splitting tensile strength with age for the three types of concrete. Figure 4.5 shows the trend of splitting strength of NSC and HSC mixes. It can be observed from the figure 4.4 that for the 28DM cured samples, the trend for NSC specimens are increasing throughout with age, with the increase of 24.4 % (relative to 28 days) at 155 days. In case of the HSC specimen, the trend is more or less constant with a slight decrease of about 4% within the period of 91 to 155 days. However, for the UHSC specimens, there is a downward trend observed within the period from 56 to 155 days with a decrease of around 9% relative to the 28 day value. Moreover, from the table 4.3, it can be seen that at 91 days, there is not much difference between the values of CM and 28DM samples for NSC and HSC specimens. However, for UHSC specimens, 28 DM samples gives 10% higher results than CM ones.

Table 4.4: Splitting tensile strength values for NSC mix of different sizes. Note: CM - Continuously Moist cured until test age and 28DM - 28 day moist cured and then exposed to controlled lab conditions until test age

Days	Curing Regime	Splitting tensile Strength [in MPa]								
		150mm			100mm			50mm		
		Value	Mean	SD	Value	Mean	SD	Value	Mean	SD
28	28DM	2.33	2.36	0.10	3.07	2.98	0.09	3.15	3.62	0.66
		2.28			2.96			4.09		
		2.47			2.89			-		
56	28DM	2.77	2.97	0.23	3.66	3.59	0.06	5.24	5.07	0.25
		3.22			3.55			4.90		
		2.93			3.57			4.99		
								5.14		
91	28DM	3.32	3.41	0.23	3.51	3.64	0.15	3.60	4.05	0.63
		3.24			3.61			4.49		
		3.68			3.80			-		
91	CM	3.26	3.23	0.04	3.76	3.79	0.02	4.59	4.59	0.01
		3.18			3.79			4.59		
		3.26			3.80					
155	28DM	3.56	3.69	0.18	3.68	3.71	0.03	3.99	4.16	0.24
		3.82			3.71			4.33		
		-			3.75			-		

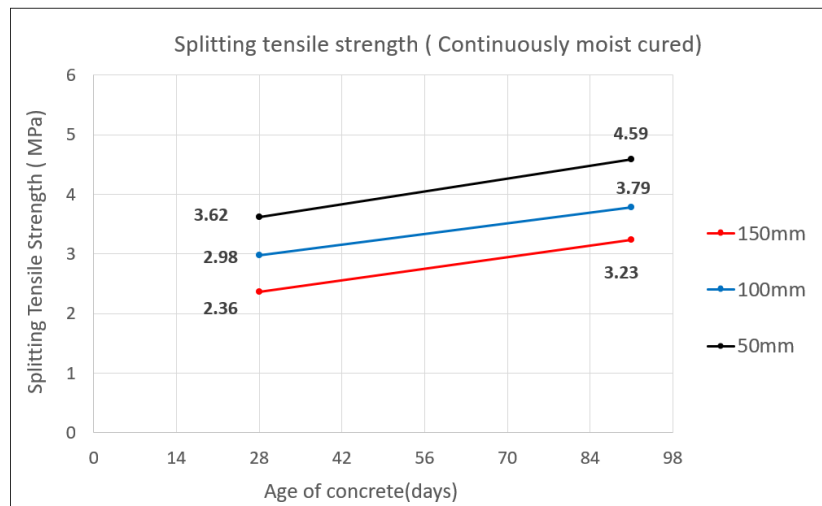


Figure 4.6: Trend of the Splitting Strength of different specimen sizes with time : Continuous moist cured regime. Note: CM - Continuously Moist cured until test age and 28DM - 28 day moist cured and then exposed to controlled lab conditions until test age

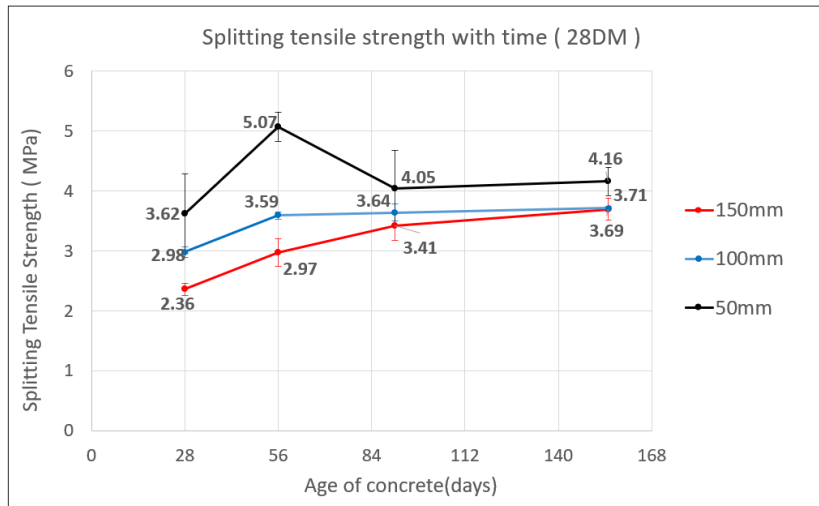


Figure 4.7: Trend of the Splitting Strength of different specimen sizes with time : 28 day moist cured regime.
 Note: CM - Continuously Moist cured until test age and 28DM - 28 day moist cured and then exposed to controlled lab conditions until test age

Table 4.4 and figures 4.6-4.7 show the splitting tensile strength of Normal Strength concrete based on different sized specimens. As similar to the compressive strength, it is observed from figure 4.6 that for the CM samples, there is a clear traditional size effect seen throughout the age. In case of the 28DM samples too, there is a traditional size effect observed with 50mm size having the highest strength at all measured days followed by 100mm and 150mm samples. Interestingly, there is a somewhat similar trend of increasing period accompanied by the stabilizing period observed for all the specimen sizes, except that this trend takes place at varying period of time for the respective specimen sizes.

4.1.3. Elastic Modulus

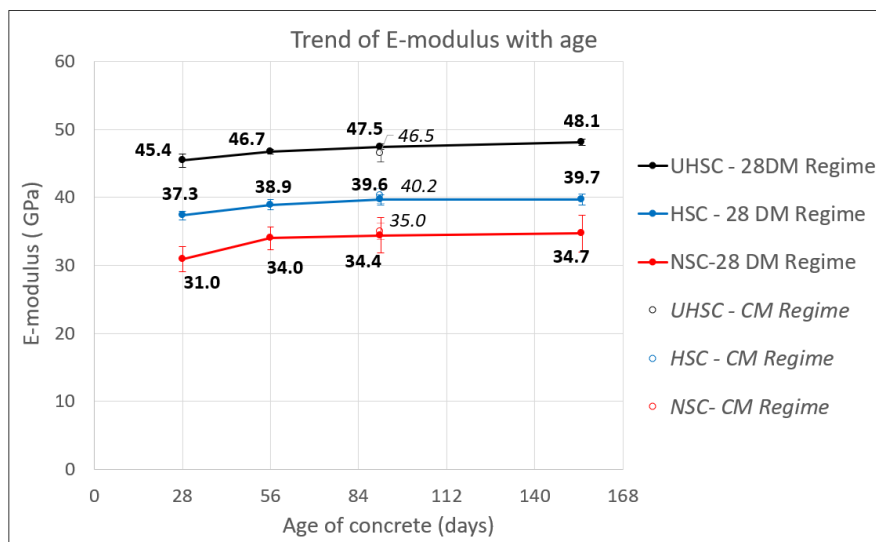


Figure 4.8: Trend of the Elastic Modulus of different types of concrete with time. Note: CM - Continuously Moist cured until test age and 28DM - 28 day moist cured and then exposed to controlled lab conditions until test age

Table 4.5: Elastic modulus values for the three types of concrete mixes. Note: CM - Continuously Moist cured until test age and 28DM - 28 day moist cured and then exposed to controlled lab conditions until test age

Days	Curing Regime	Elastic Modulus [in GPa]								
		NSC			HSC			UHSC		
		Value	Mean	SD	Value	Mean	SD	Value	Mean	SD
28	28DM	29.0	31.0	1.9	36.7	37.3	0.7	44.6	45.4	1.0
		32.6			37.3			45.1		
		31.3			38.0			46.5		
56	28DM	32.2	34.0	1.7	38.1	38.9	0.7	46.6	46.7	0.4
		35.5			39.6			46.4		
		34.3			39.0			47.2		
		-			-			-		
91	28DM	32.6	34.4	2.6	38.7	39.6	0.8	47.4	47.5	0.4
		36.3			40.2			47.1		
		-			40			47.9		
		-			-			-		
91	CM	36.3	35.0	1.2	39.0	40.2	1.1	48.0	46.5	1.3
		34.7			40.9			46.0		
		34.1			40.8			45.5		
155	28DM	36.6	34.7	2.7	38.8	39.7	0.8	48.0	48.1	0.5
		32.8			40.4			47.7		
		-			39.9			48.6		

Table 4.5 and figure 4.8 shows the trend of the Elastic Modulus for the three types of concrete. In general, it can be observed that for the 28DM cured samples, the trend for all the concrete types is generally increasing with age. At 155 days, the highest increase is seen for the NSC mix (12%) followed by HSC mix (6%) and UHSC mix (5%), relative to 28 days. Moreover, from the table 4.5, it can clearly be seen that at 91 days, there is not much difference between the values of CM and 28DM samples for all the concrete types.

4.1.4. Drying Shrinkage

The figures 4.9 and 4.10 show the variation of the drying shrinkage strain and the weight loss expressed as a % of initial value, with time. It can be observed that in general, the NSC mixes are shrinking more followed by the HSC and UHSC ones, which is as expected in the literature. As also observed, there is quite a huge difference among the three NSC mixes casted successively, although their weight loss pattern is the same.

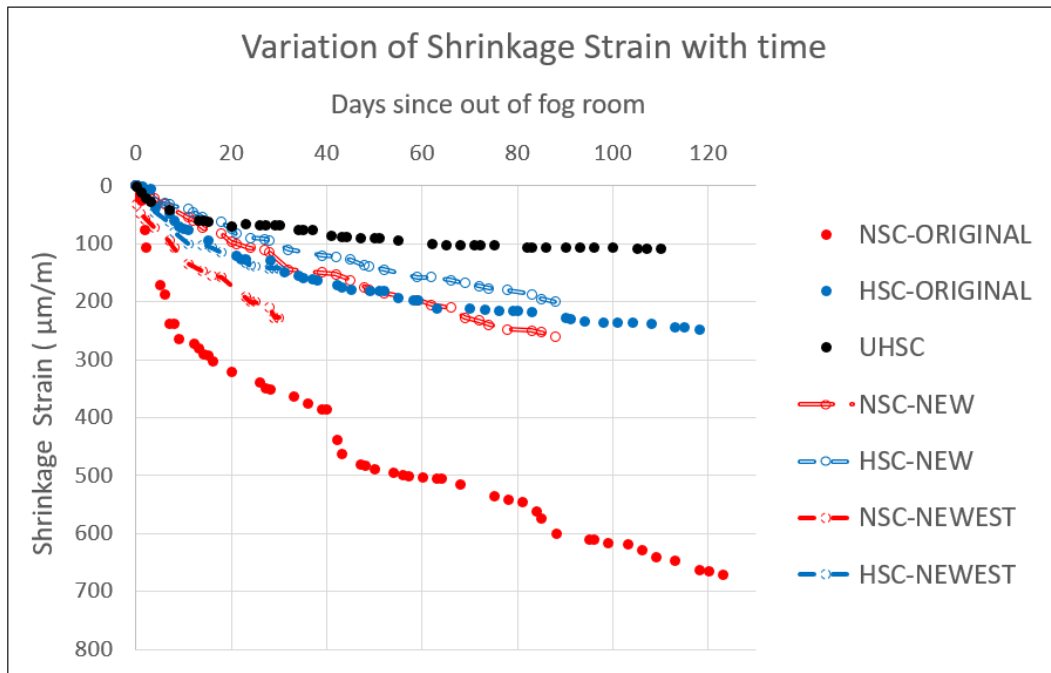


Figure 4.9: Drying Shrinkage strain with time for different concrete mixes

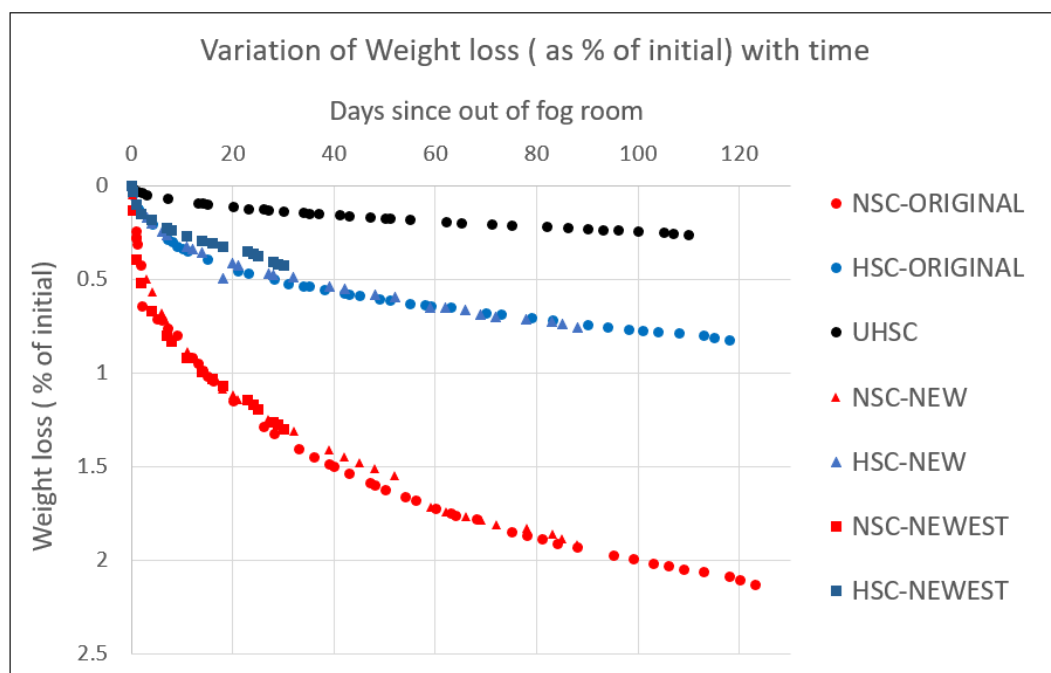


Figure 4.10: Variation of the Weight loss expressed as a % of initial value with age for the different cement based mixes

4.2. Modelling Results

4.2.1. Validation for hygral behaviour

For the validation of hygral behaviour, the humidity profile across the concrete specimen based on the experimental results published by Hanson [17] is simulated using FEMMASSE. As already stated in the previous chapter, owing to the use of cylindrical specimens in the experiments by Hanson [17], it becomes important to first compare the humidity profile of the cubical and cylindrical specimens before using the cubical specimens for simulating splitting tests. It is stated that in the experiment, the cylindrical specimen is dried throughout the periphery except at the ends. The simulation of the cylindrical specimen in FEMMASSE is carried out using the axisymmetric option and in order to keep the drying conditions same, in case of cubes too, drying is allowed on all 4 sides (see figure 4.11b).

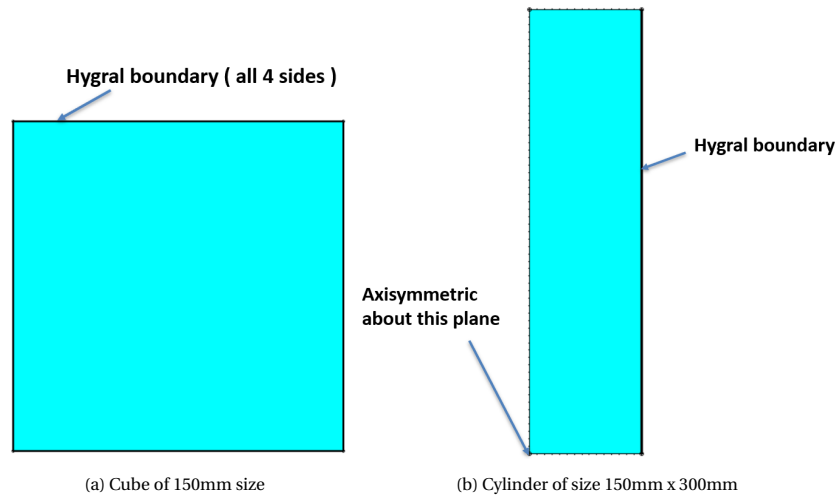


Figure 4.11: Hygral boundaries of the cubes and cylinder profile used for simulation

For the simulation of humidity profiles, the diffusion parameters published by Bazant are used and a film coefficient of 0.7mm/day is used as an initial approximation as stated in the previous chapter. As stated in chapter 3, it is important to recollect that since the experimental data was for the hardened concrete, the effect of self desiccation is turned off in these simulations. It can be observed from the humidity plots as shown in the figure 4.13 that the model seems to depict the drying behaviour with the gradual loss of relative humidity from the edges with increasing age. Moreover, the relative humidity distribution of both the cylinder and cube specimens look quite identical. In order to compare in more detail, a cross section cut is made in the specimens (as shown in the figure 4.12) and accordingly, the humidity profile of both the cylindrical and cubical specimens is plotted until the age of 3 years (see figure 4.14).

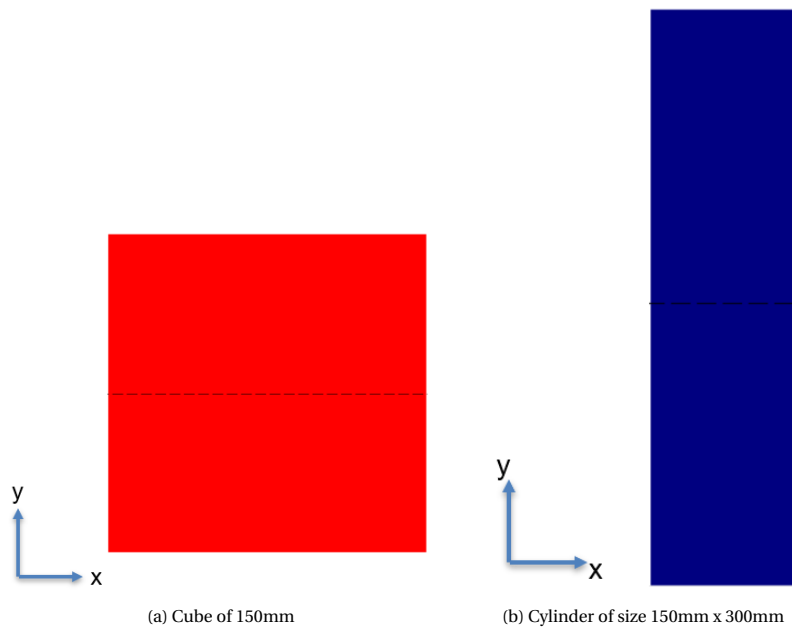


Figure 4.12: Cross section cut on cylinder and cube specimen

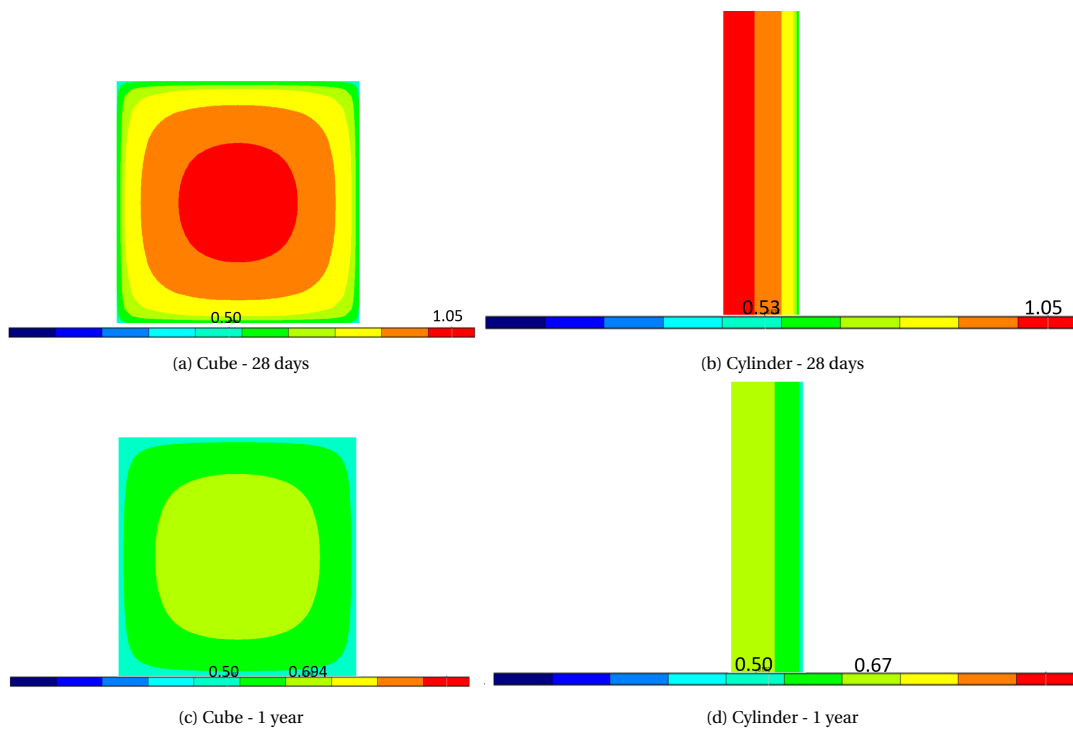


Figure 4.13: Humidity contour plots simulated by using FEMMASSE

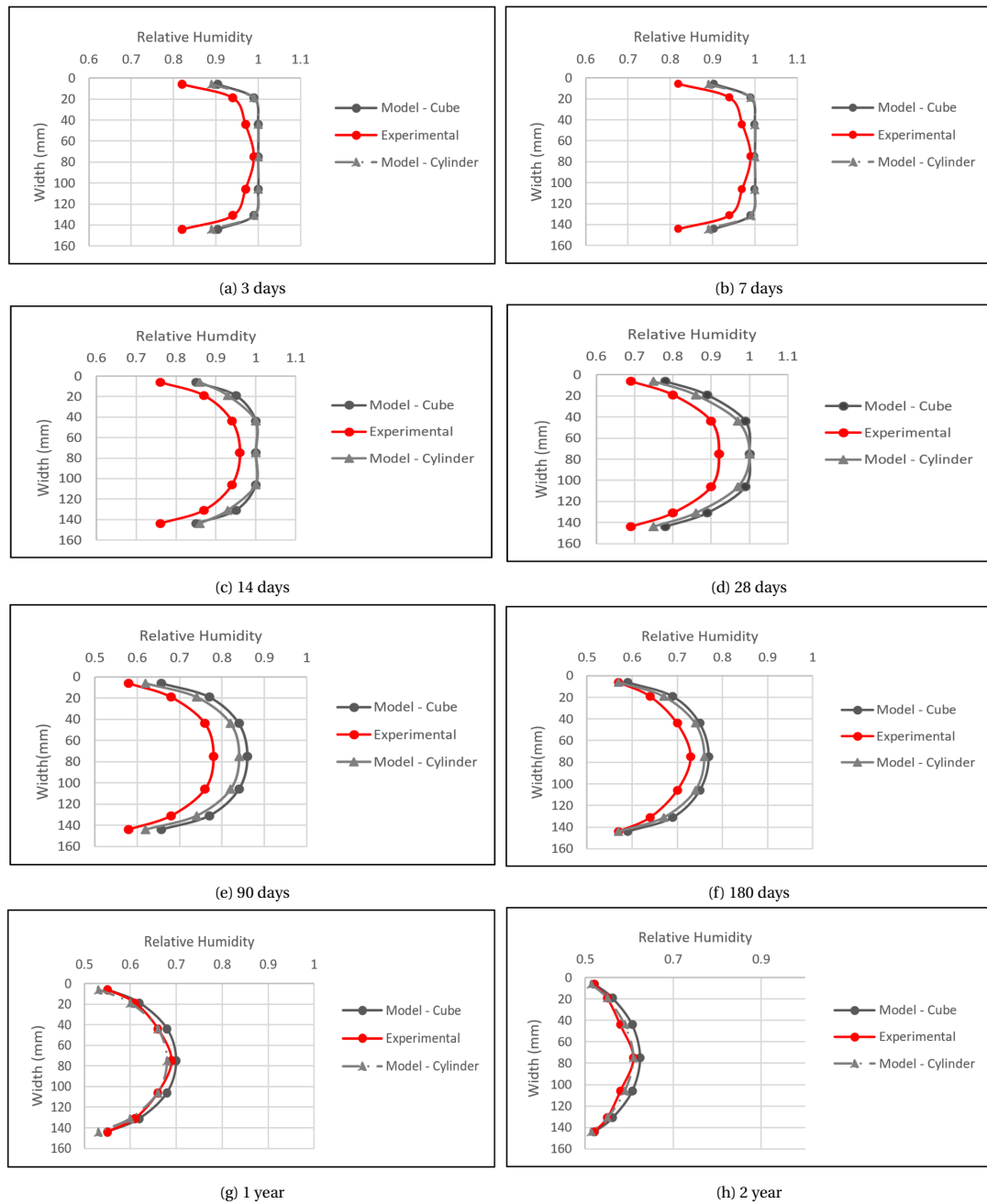


Figure 4.14: Comparison of humidity profile of cubical and cylindrical specimens

It can be observed from figure 4.14 that the relative humidity profile across the width of both cylinder and cube specimens are quite similar and it cubical specimens are used for further simulations of experimental tests. However as stated before, it is quite evident now that for the chosen diffusion and film coefficient, there is still some discrepancy in the relative humidity profile as compared to the experimental values especially at early ages (when drying is dominant). Accordingly, a sensitivity study of the film coefficient is done in order to obtain the humidity profile closely comparable to the experimental results (as shown in figure 4.15). It is important to note that for all the plots, the diffusion coefficient published by Bazant is used.

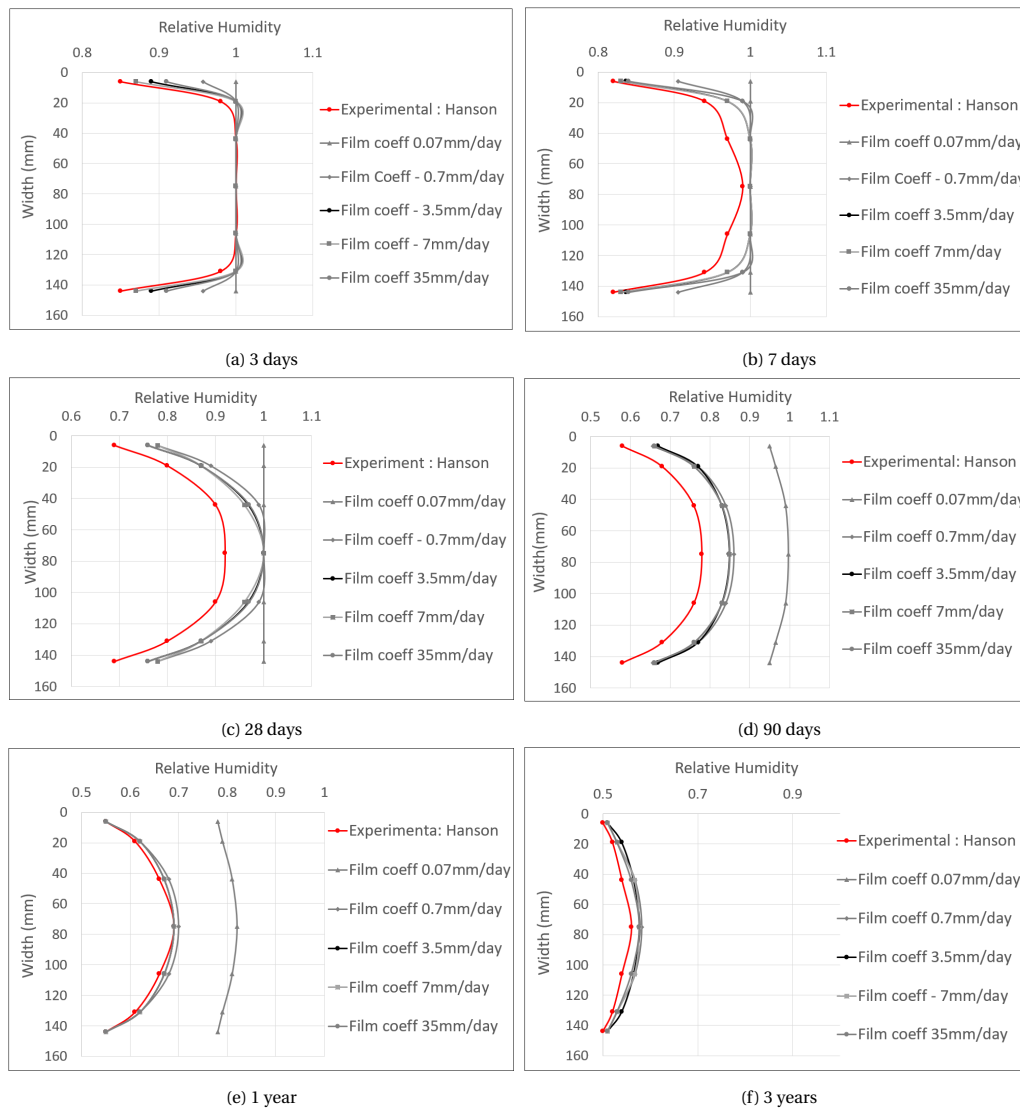


Figure 4.15: Humidity profile across the concrete cross section based on the different values of film coefficient

Accordingly, the best fit film coefficient is chosen (3.5mm/day) and then the diffusion coefficient given by Bazant is critically reviewed by varying around the original value. It is observed that at the age of 3 years, the diffusion coefficient given by Bazant gives the closest drying profile, as shown in the figure 4.16.

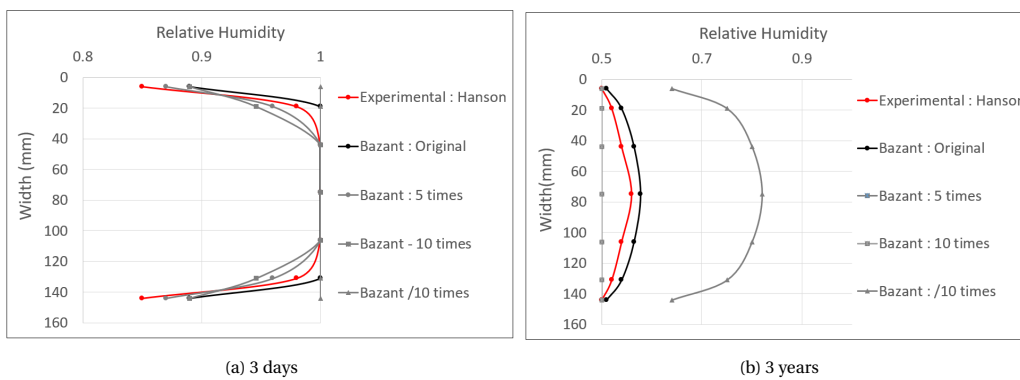


Figure 4.16: Variation in the humidity profile based on different diffusion coefficients

4.2.2. Stress profile and comparison with Analytical approach

At the cross section of the cube specimen as shown in the figure 4.12, the major stress profile is plotted and compared with the analytical approach as discussed in the literature study. For the sake of brevity, only the stress distribution at 28 days and 1 year are shown. It can be observed that both these models do predict a similar stress distribution on drying across the cross section with tensile stresses at the edges and compressive stresses at the core. However, the magnitude of the stresses are not comparable probably due to the linear elastic behaviour assumed in the analytical model.

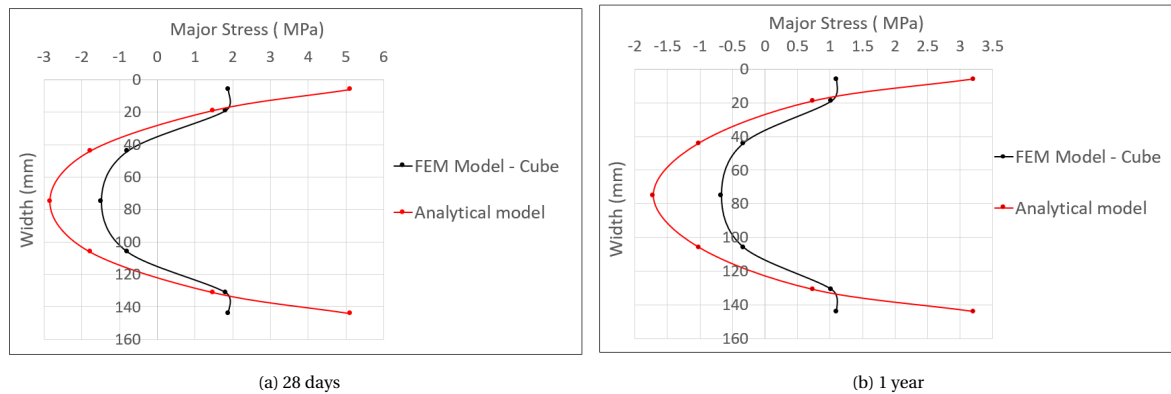


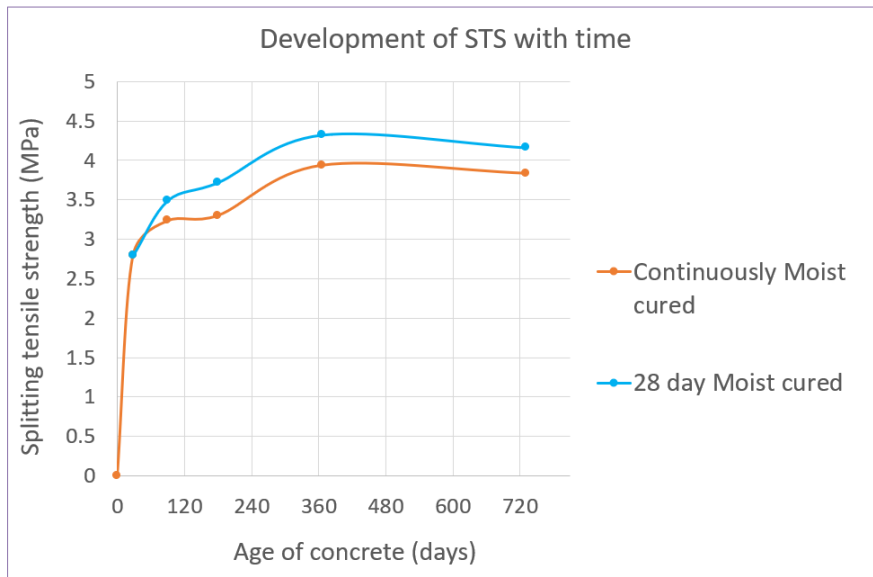
Figure 4.17: Stress profile across the concrete section

4.2.3. Validation for Splitting tests

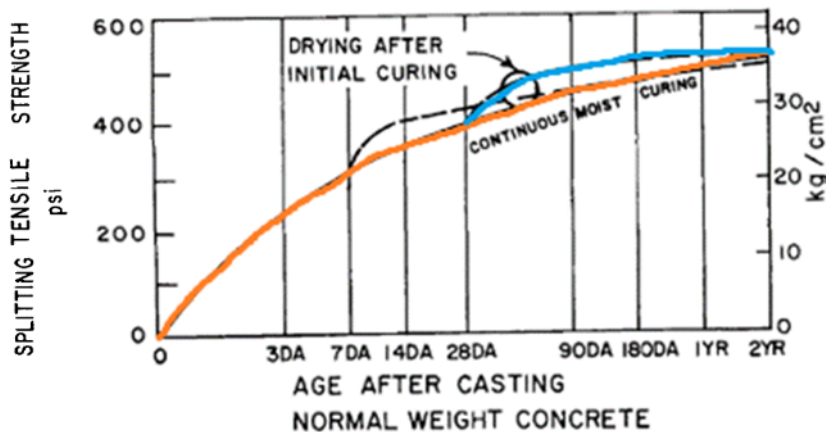
Initially, the model is validated for obtaining the splitting tensile strength without incorporating any drying conditions. As an input, a constant value of direct tension strength is used and the splitting tensile strength is calculated corresponding to the ultimate load. After few successive trials, it is found out that the ratio of direct tensile strength to splitting tensile strength varies from 0.85-0.88, which is close to the value of 0.9 as given in Eurocode 2.

In order to check if FEMMASSE can simulate the splitting tests by taking into account the effect of drying, the experimental data of Hanson [17] is used. The use of the cube specimens for the simulation is justified on the basis of almost similar relative humidity profile obtained as discussed in the previous section. For simulation using FEMMASSE, the effect of hydration is incorporated using the experimental data for the splitting tensile strength obtained at standard conditions. However, as the experimental data for the splitting tensile strength is given for the cylinders, a shape factor of 1.1 (as stated in NEN standards) is used in order to get equivalent splitting strength in the cubes and a conversion factor of 0.85 is used to convert the splitting to direct tensile strength which is then fed in as input. The effect of drying is taken into account using the diffusion and film coefficient as mentioned in the previous section. Finally, the splitting tensile test is simulated until the period of 2 years for the two curing regimes described in the experiment - the 28 day moist cured and the Continuous moist cured regime.

It is found that FEMMASSE is able to replicate the similar trend of the splitting tensile strength observed in the experiments, as indicated by the blue and orange lines in the figure 4.18.



(a)



(b)

Figure 4.18: Development of Splitting tensile strength (STS) with age : (a) Results of FEMMASSE (b) Experimental results by Hanson [17]

4.2.4. Simulation of Hygral Behaviour : Current Experiment

After validating the model for depicting the hygral behaviour by comparing the profile of the relative humidity with the experimental data of Hanson [17], the model is extended to study the hygral behaviour of the concrete strength mixes used in the study. Moreover, the influence of the varying specimens sizes is also observed in case of the NSC mixes. For all the simulations, the input parameters stated in the chapter 3 are used. The contour plots of relative humidity profile and the major stresses corresponding to the NSC mix of three different specimen sizes - 150mm, 100mm and 50mm after the period of 28 days and 1 year of drying (at 50% RH) are shown in the figures 4.19-4.20. It can be seen that from the humidity plots that at the period of 28 days and 1 year, the 150mm cubes have the highest moisture gradient followed by the 100mm ones and the 50mm ones. Consequently, the magnitude of the major stresses are also higher for respective cube sizes. Additionally, it can be observed that for the 50mm cubes, hygral equilibrium is reached at 1 year period. However, in case of the 100mm cube, it takes almost 3 years to reach the same while the 150mm cube does not even reach equilibrium at a period of 3 years.

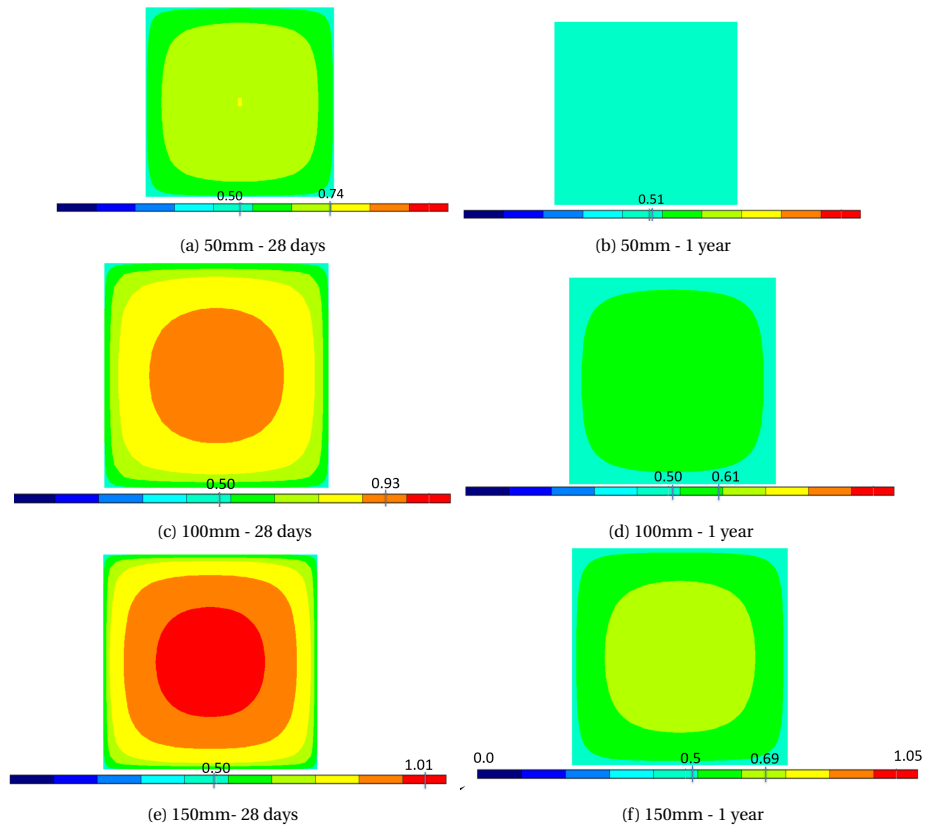


Figure 4.19: Contour plot of relative humidity of NSC mix for various specimen sizes

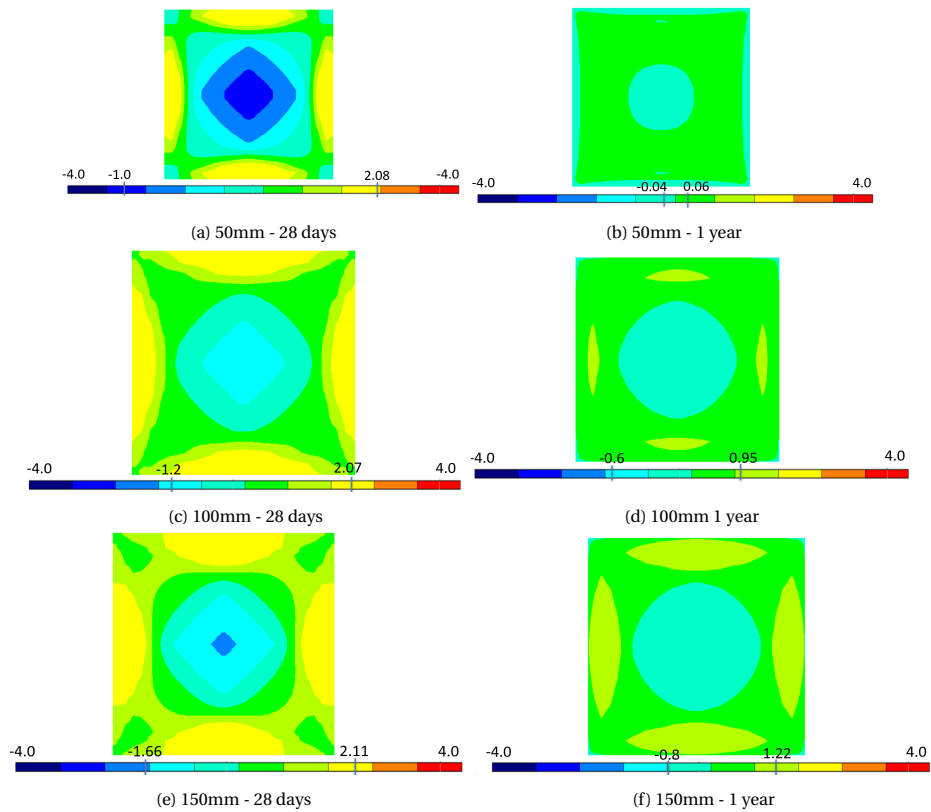


Figure 4.20: Major Stress contour plot for NSC mix of various specimen sizes

In the case of HSC mix, only the 100mm cubes are studied similar to the experimental regime. It is observed that compared to the 100mm cube of NSC mix, there are higher moisture gradient at 28 days leading to high tensile stresses at the surface. Moreover, it is seen that even after a period of 3 years, the 100mm HSC specimen does not find hygral equilibrium unlike the 100mm NSC ones, as shown in the figure 4.22.

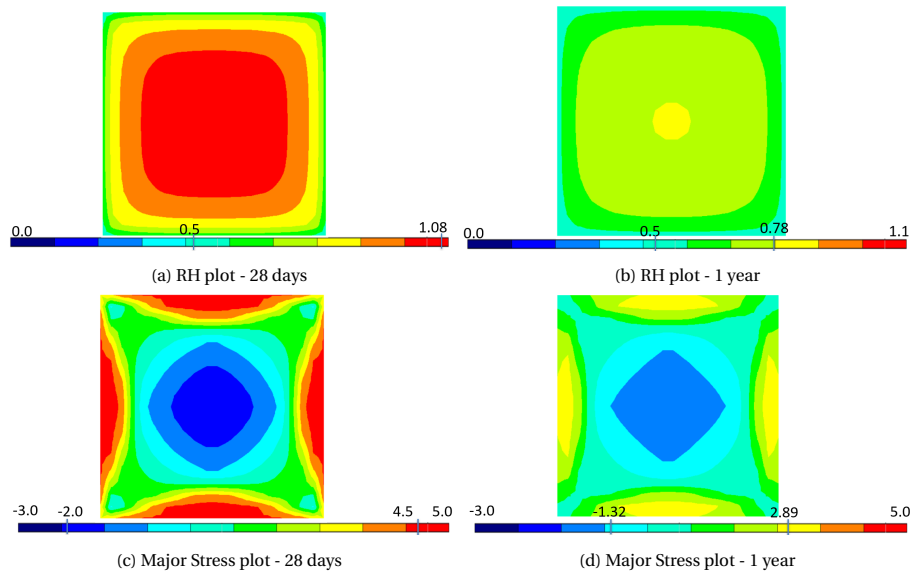


Figure 4.21: Relative Humidity and Major Stress contour plots for HSC mix

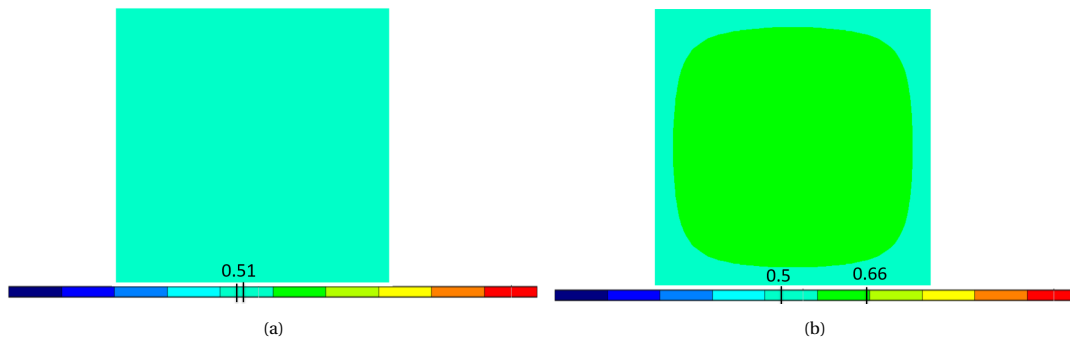


Figure 4.22: Relative humidity contour plot for 100mm cube at 3 years for (a) NSC mix (b) HSC mix

4.2.5. Simulation of Splitting Strength results : Current experiment

A similar approach is followed as mentioned in 4.2.3 in order to simulate the splitting test for the NSC and HSC mixes of the current experimental regime. The splitting tensile tests are simulated for the three specimen sizes - 150mm, 100mm and 50mm for both the NSC and HSC mixes. However, in case of HSC mixes, since the experimental data for continuously moist cured specimens is only available for 100mm size, it is assumed to be similar in case of 150mm and 50mm in order to study the trend. The curing regimes followed are the same as opted in the experiments - Continuously Moist cured (CM) and 28 Day Moist cured (28DM). The relevant material and hygral properties used are stated in the chapter 3. As shown in the figure 4.23, the positive effect of drying after the initial 28 day moist curing period on the splitting strength is clear for all the specimen sizes and it is similar to the one obtained for the experiment of Hanson [17]. It is worth noticing that the drying seems to immediately affect the 50mm cube resulting in a steep increase at a period of 91 days. However, there is a quick stabilizing effect seen after the period of a year. In case of the 100mm and 150mm specimen sizes, there is relatively higher increase on drying for the 100mm specimen observed clearly at the period of 1 year. However, they seem to stabilize from the period of 5 years onward.

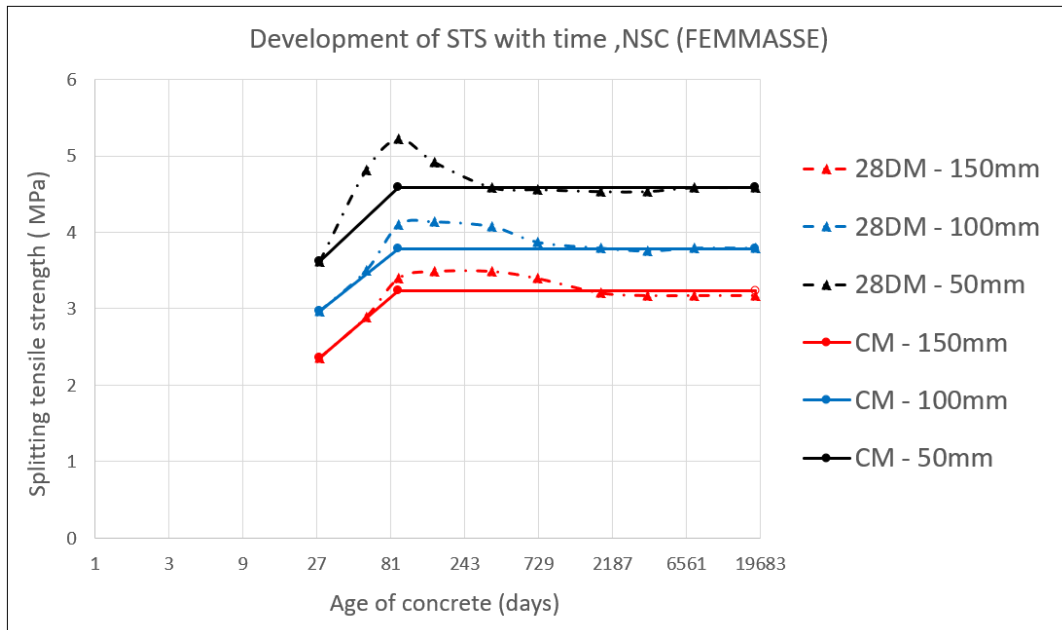


Figure 4.23: Simulation of the splitting tensile strength for the NSC specimens of different sizes

In case of the HSC mix, drying seems to have a completely different effect on the splitting tensile strength as compared to the NSC mixes. As shown in the figures 4.24, 4.25 and 4.26, for all the specimen sizes, there is a more or less similar pattern observed. However, the difference lies in the timing and magnitude of the fluctuations in the trend.

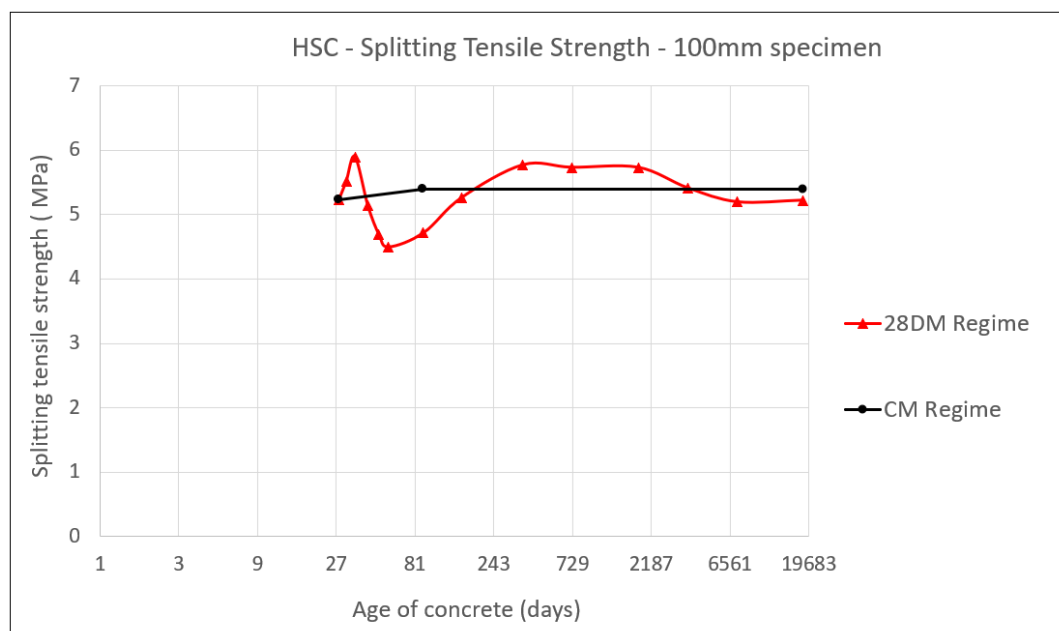


Figure 4.24: Simulation of the splitting tensile strength for the HSC specimen-100mm

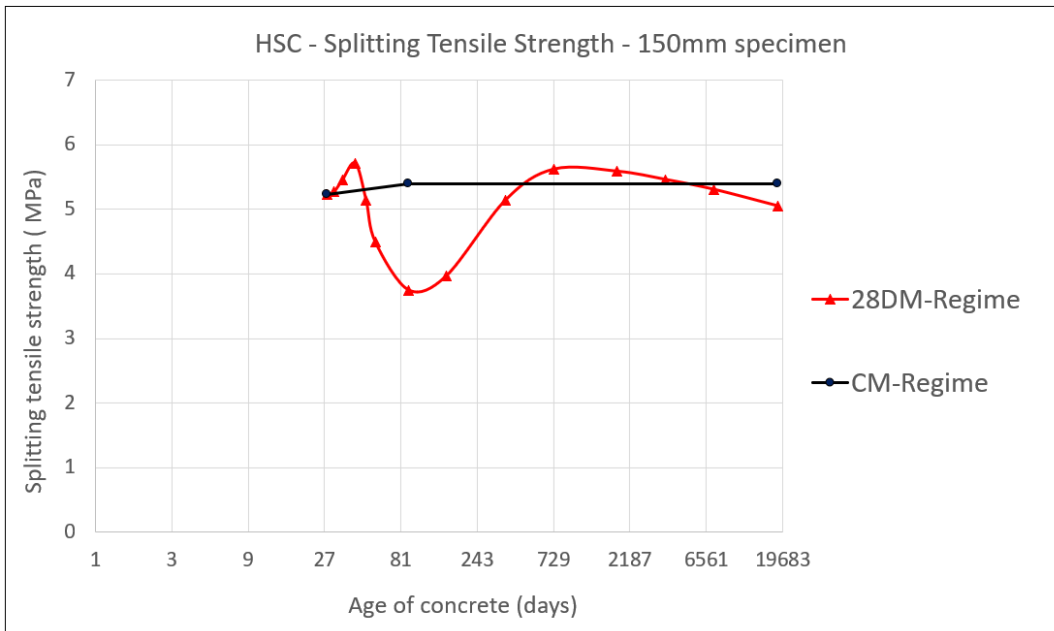


Figure 4.25: Simulation of the splitting tensile strength for the HSC specimen-150mm

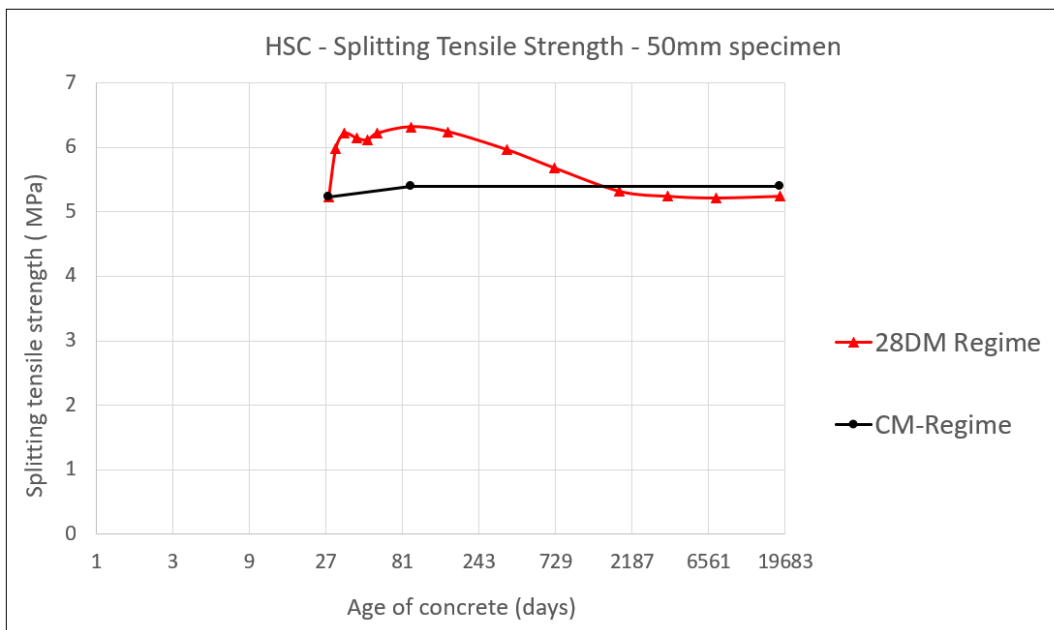


Figure 4.26: Simulation of the splitting tensile strength for the HSC specimen-50mm

4.2.6. Simulation of the Direct Tensile Test

Similar to the splitting tensile tests, initially the model is checked for the determination of direct tensile strength without any drying conditions. A constant value of the direct tensile strength is inputted in the model and the corresponding output is verified with the input. Subsequently, the material and hygral properties stated in chapter 3 is incorporated and the trend of the direct tensile strength is simulated for both the concrete mixes - NSC and HSC until the period of 50 years. It can be observed from the figure 4.27 and 4.28 that a similar trend is obtained for both the mixes. In case of the NSC mix, it is observed that drying after

28 days reduces the direct tensile strength, however the trend starts to increase immediately after 38 days contrary to the HSC mix where the decrease is for a longer period until 56 days.



Figure 4.27: Simulation of the direct tensile strength for the NSC specimen

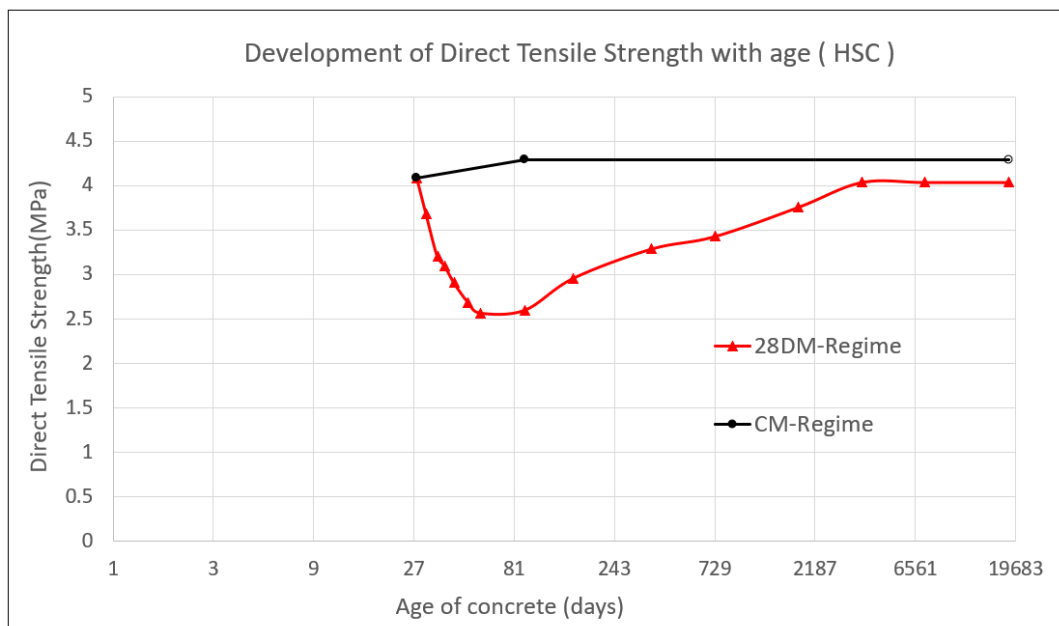


Figure 4.28: Simulation of the direct tensile strength for the HSC specimen

4.2.7. Simulation of the Flexural Strength test

Using the similar procedure as splitting and direct tensile tests, initially the model is checked for the determination of flexural strength without any drying conditions. A constant value of the direct tensile strength is inputted in the model and the corresponding flexural tensile strength is calculated and verified. Subsequently, the material and hygral properties stated in chapter 3 is incorporated and the trend of the flexural

strength is simulated for both the concrete mixes - NSC and HSC until the period of 50 years. It can be observed from the figures 4.29 and 4.30 that just like the direct tensile strength, a similar trend is obtained for both the mixes. In case of the NSC mix, it is seen that drying after 28 days reduces the flexural strength, however the trend starts to increase immediately after 35 days contrary to the HSC mix where the decrease is for a longer period until 90 days. Moreover, a slender specimen of NSC mix (50x50x400mm) is also simulated (see figure 4.31) in study to see the effect of size on the flexural strength trend. It is observed that as compared to the larger specimen (100x100x400mm), the slender specimen (50x50x400mm) has a smaller decreasing period with the trend showing an upward trend right after 31 days.

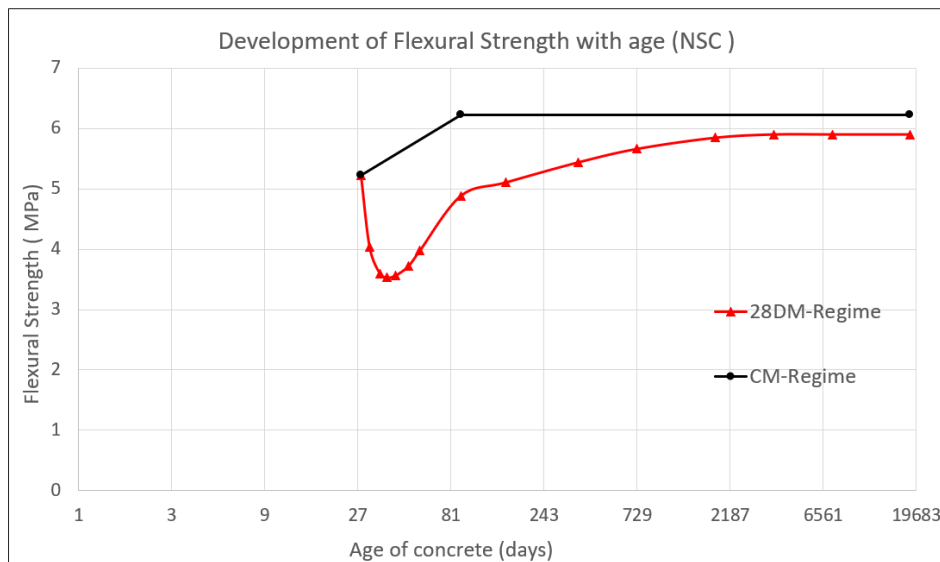


Figure 4.29: Flexural strength development with time for NSC specimen - 100x100x400mm

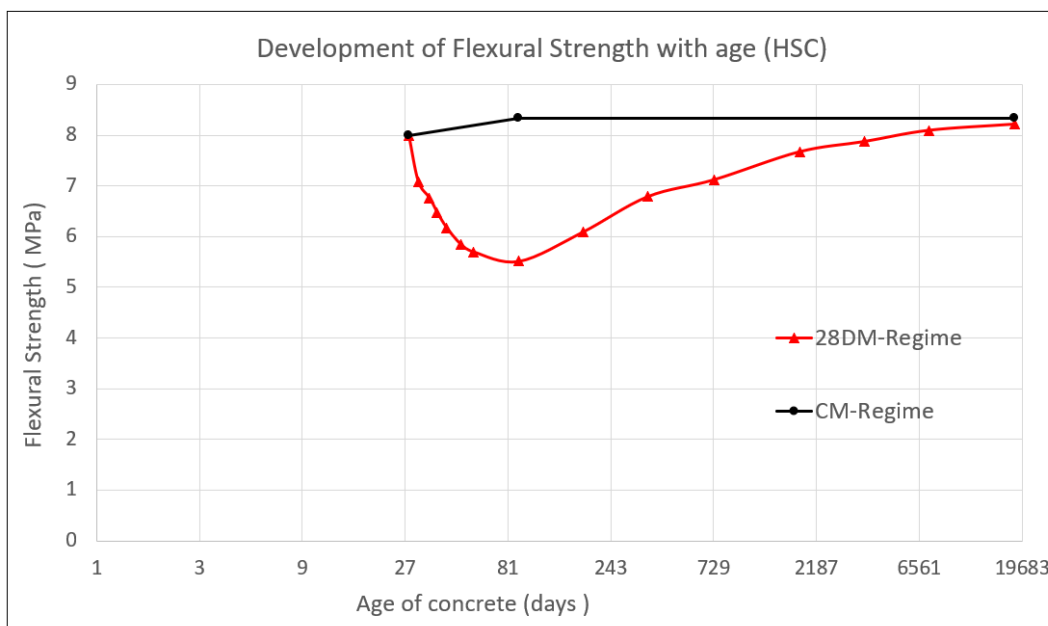


Figure 4.30: Flexural strength development with time for HSC specimen - 100x100x400mm

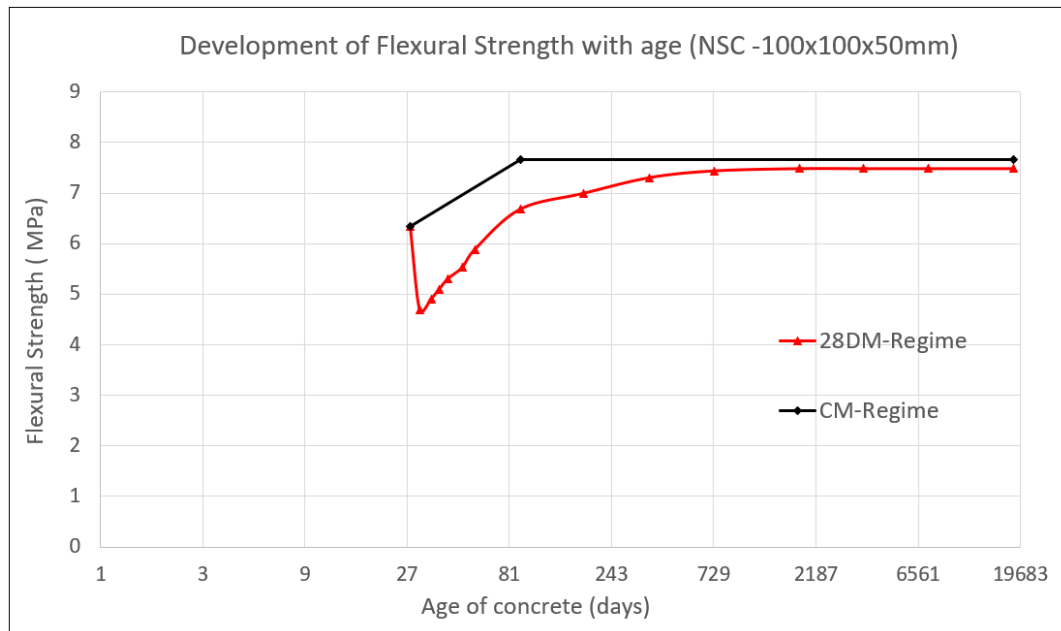


Figure 4.31: Flexural strength development with time for NSC specimen of size 50x50x400mm

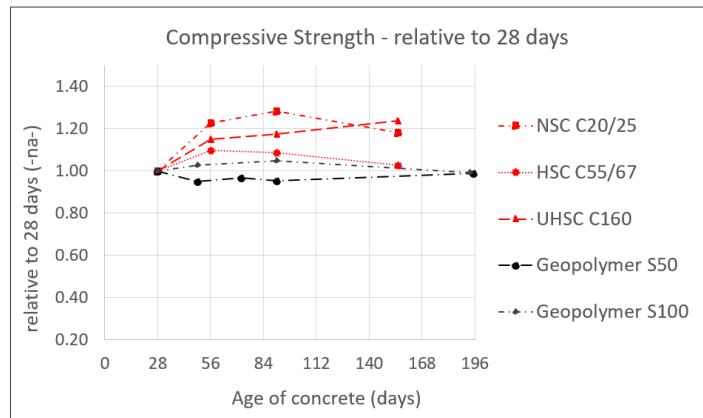
5

Discussion

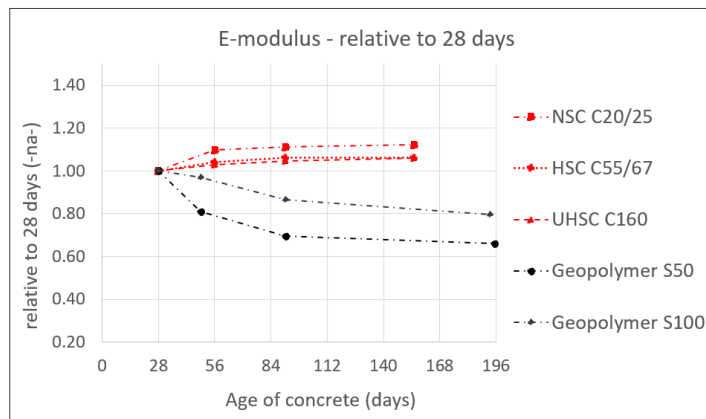
In this chapter, the obtained experimental and modelling results are discussed with respect to the research objectives and research questions.

5.1. Comparison with Geopolymer concrete

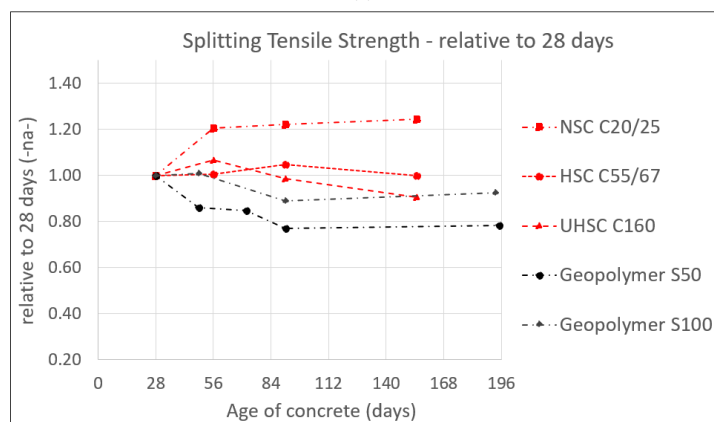
One of the prime objective of this study was to see if a similar reduction in the trend of the strength and stiffness properties as observed in the Geopolymer concrete mix designed by Prinsse [35], also occurs for the ordinary concrete mixes of varying strength grades. It can be observed from the results shown in the previous chapter that, in general, no such major reduction is observed in the trend.



(a)



(b)



(c)

Figure 5.1: Comparison of mechanical properties of cement based concrete mixes with the Geopolymer mix prepared by Prinsse [35] (a) Compressive Strength (b) Elastic Modulus (c) Splitting Tensile Strength

Generally, from the initial impression in figure 5.1, it is observed that for all the studied mechanical properties - compressive strength, splitting tensile strength and Elastic modulus, the ordinary concrete mixes show an increasing trend as compared to the two Geopolymer mixes - S50 and S100, which shows a decreasing trend. On looking further in more detail, it is noticed that for the ordinary concrete mixes, the trend of the mechanical properties with time stabilizes during the period of 91 to 155 days with the values approaching the 28 day value. The only exception is the splitting tensile strength of the UHSC mix, where the trend seems to decline within the same period (a reduction of 9% relative to 28 days). In case of the two Geopolymer mixes, the stabilizing behaviour is seen specifically for the compressive strength within the period of 91 to 196 days. In case of the elastic modulus and splitting tensile strength, although the trend seems to stabilize with respect to

the 91 day value, the decrease is still alarming (34% and 22% for elastic modulus and splitting tensile strength respectively) when compared to the 28 day value.

Thus, it is clear that except for the decrease of splitting tensile strength of UHSC mix at 155 days, there is no major reduction in the trend of the strength and stiffness properties of ordinary concrete mixes as compared to the Geopolymer concrete. In case of the Geopolymer concrete mix, it is reported by Prinsse [35] that the S50 mix loses more moisture than slag rich S100 mix and there is a strong influence of the weight loss on the Elastic modulus. However, it can be observed from the figure 5.2 that the weight loss of S50 and S100 Geopolymer mix is comparable to the HSC and NSC mix respectively and yet no reduction in the Elastic modulus is observed in both these concrete mixes. This implies that the moisture loss does not negatively impact the elastic modulus of the ordinary concrete mixes as compared to the Geopolymer ones used by Prinsse [35] and that the reduction in case of Geopolymer concrete might be due to its intrinsic chemistry.

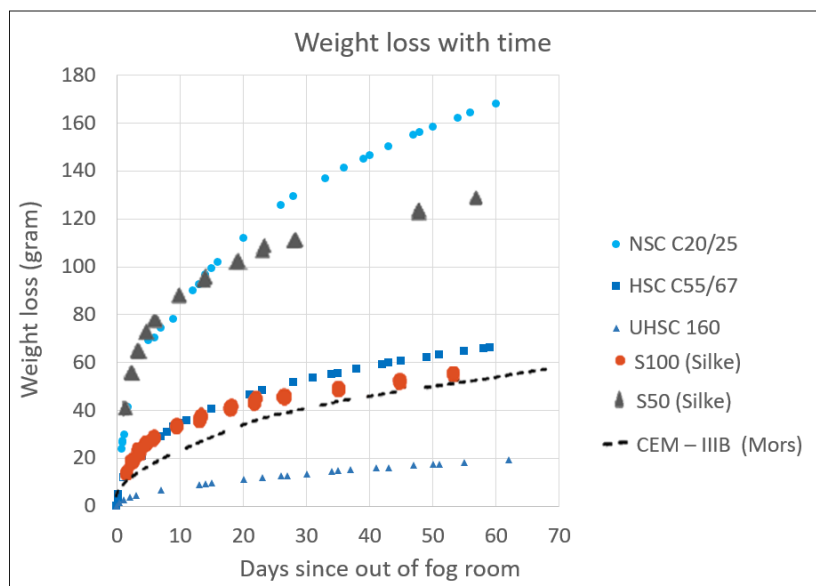


Figure 5.2: Comparison of the weight loss with increasing concrete ages of different concrete mixes

5.2. Effect of the parameters on the trend of mechanical properties

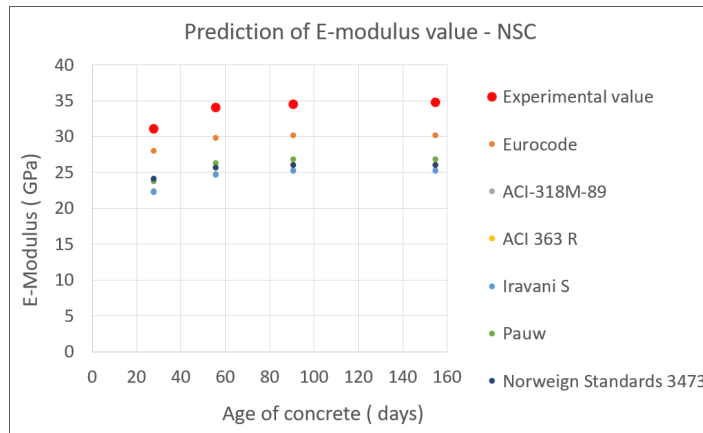
From the literature study, it is concluded that there is no consensus on the understanding of the trend of mechanical properties with time which is aggravated due to the complex inter dependency of the various parameters like the type of curing conditions, varying specimen sizes and the type of concrete. Based on the experimental results obtained in this study, it is aimed to give more clarity on the trend obtained for the ordinary concrete mixes in time.

The results shown in the previous chapter does indicate that in general, for the chosen curing conditions, there are no such major reduction in the trend of the studied mechanical properties in time. The table 5.1 shows the development of mechanical properties in time relative to the 28 day value, for the different concrete mixes exposed to the 28DM curing regime.

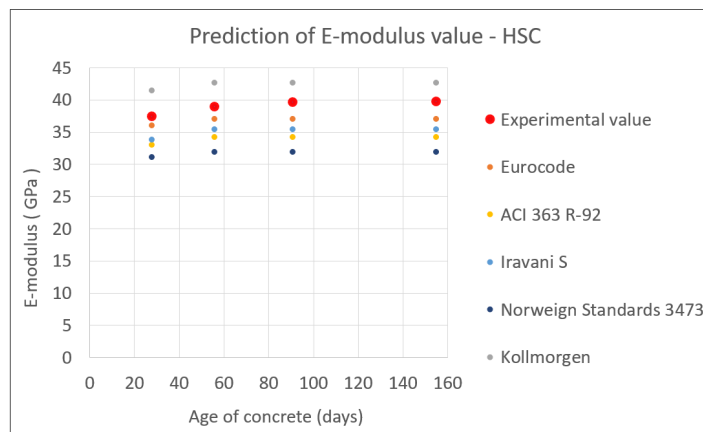
Table 5.1: Mechanical properties for the three types of concrete mixes relative to 28 days

Mechanical Properties relative to 28 days									
Age (days)	NSC			HSC			UHSC		
	CS	E-mod	STS	CS	E-mod	STS	CS	E-mod	STS
28	1	1	1	1	1	1	1	1	1
56	1.23	1.1	1.21	1.1	1.04	1.01	1.15	1.03	1.07
91	1.28	1.11	1.22	1.09	1.06	1.05	1.17	1.04	0.99
155	1.18	1.12	1.24	1.03	1.06	1	1.24	1.06	0.91

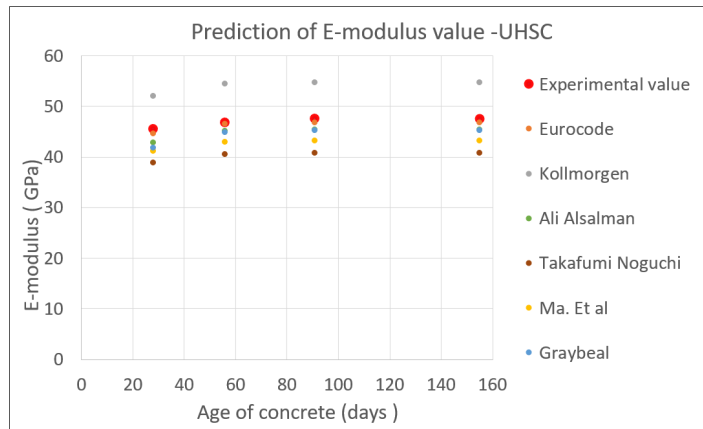
It is observed that for the NSC and HSC mixes, there is an increasing trend of the compressive and splitting strength within the period of 28 to 91 days. However, the trend stabilizes over the period of 155 days. This trend of temporary increase followed by stabilization is possibly due to the development of eigen stresses which was highlighted in the study by Popovics [34]. It is expected that due to non uniform drying, there are tensile eigen stresses at the surface and compressive ones at the centre. From the inspection of cubes using an optical microscope, it is confirmed that there are no surface cracks observed which indicates that the tensile eigen stresses generated at the surface do not exceed the tensile strength. As a result, the compressive eigen stresses which is generated at the centre delays the ultimate load and increases the splitting tensile strength. In case of the UHSC mix, over a period of 155 days, the compressive strength shows an increasing trend whereas the splitting strength shows a decreasing trend. One of the probable cause of increase of compressive strength could be the higher degree of hydration as a result of the high cement content. However, the drop in the splitting tensile strength is bewildering. Thus, in case of UHSC mixes, no clear conclusion can be made and the specimens need to be tested further in time in order to arrive at a conclusion. With regard to the elastic modulus, it is observed that it increases at a lesser rate compared to the compressive strength, for all the three mixes. This different rate of increase makes it questionable to use the empirical relations as discussed in the literature study for the the determination of elastic modulus from the compressive strength. Indeed, it is observed that the accuracy of these equations for the determination of elastic modulus seems questionable throughout the age (as shown in figure 5.3) implying that these equations are invalid for the curing condition chosen in this study (28 day moist curing).



(a)



(b)



(c)

Figure 5.3: Comparison of mechanical properties of cement based concrete mixes with Geopolymer ones
 (a) Compressive Strength (b) Elastic Modulus (c) Splitting Tensile Strength

With regard to the curing regimes, two variations are employed in the study- the 28 day Moist curing (28DM) and Continuous Moist (CM) curing regime. In figure 5.2, the ratio (R) of the compressive strength using 28DM curing regime and that using CM regime is reported for the current experimental regime and the results are compared with the literature. It is observed that, for the HSC mix, at a period of 91 days, the strength is the same for the samples cured under both 28DM and CM regimes. This is more or less comparable to the similar water cement ratio mixes used by Carrasquillo et al. [9] and Hameed [16] in which they expect a minimal decrease of the 28DM cured samples relative to the CM ones at the same age. However, the results of the mix by Iravani [19] report 25% higher value for the 28DM samples compared to the CM ones. In case of the

NSC mixes, the results in the literature by Carrasquillo et al. [9] and Ozer and Ozkul [31] report almost similar values for both the regimes, however for the current NSC mix, there is a 7% reduction for the 28DM samples compared to the CM ones. Since the curing regime employed and the water cement ratio are more or less similar, the variability in the values could be as a result of the varied moisture state of the specimen at the time of testing. This leads to the development of eigen stresses which influences the trend as highlighted earlier. The positive influence of drying due to the compressive eigen stresses is evident from the result of Iravani [19]. However, drying does not always leads to increase of compressive strength due to the complexity in evaluating the positive and negative effects of combined air and water curing as highlighted by the study of Conroy-Jones and Barr [11]. The similar reasons also hold for understanding the influence of varied curing regime on the splitting tensile strength. As seen in figure 5.4, there is a slightly higher value measured at 91 days for CM samples with respect to the 28DM ones, in case of the NSC mix. In comparison, for a similar water cement ratio mix, Hanson [17] obtained higher value for the 28DM samples. Therefore, in case of the combination of air and water curing, the final value of the compressive and splitting tensile strength actually depends on multiple parameters like current state of ongoing hydration and the magnitude of the eigen stresses across the cross section.

Table 5.2: Comparison of the compressive strength of 28DM regime to the CM regime from various literature

Moist curing period (days)	Drying period (days)	$R = \frac{(\text{Strength}_{28\text{DM}})_{\text{test age}}}{(\text{Strength}_{\text{CM}})_{\text{test age}}}$						
		HSC				NSC		
		Carrasquillo (C70) w/c : 0.32	Hameed (C60) w/c : 0.32	Iravani (C65) w/c: 0.4	Current Experiment (C55/67) w/c : 0.45	Carrasquillo (C30) w/c : 0.7	Baris (C25) w/c : 0.7	Current Experiment (C20/25) w/c : 0.6
0-28	28-56			1.12				
0-28	28-91	0.96	0.98	1.25	1.00	0.99	1.05	0.93
0-28	28-147			1.21				
0-28	28-180						0.975	

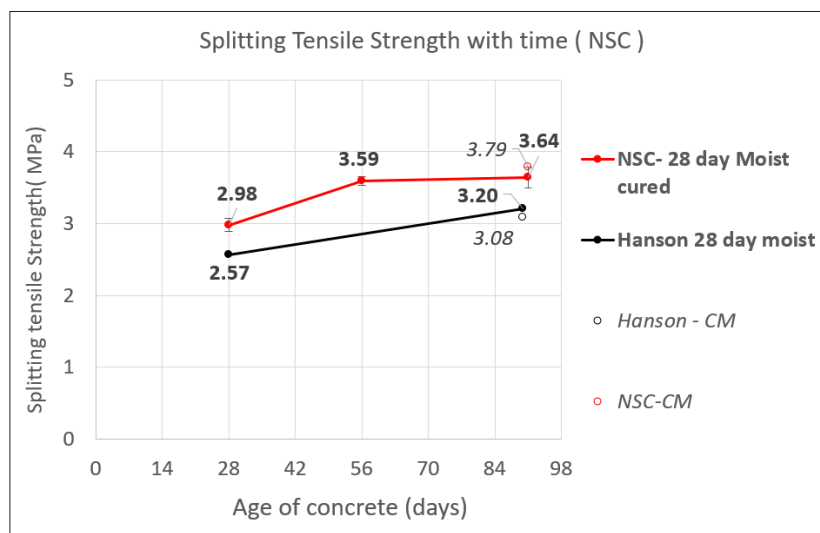


Figure 5.4: Comparison of the splitting tensile strength of 28DM regime to the CM regime for NSC mix with the data from Hanson [17]

In the case of Elastic modulus, it is evident from table 5.3 that the prolonged moist curing for a period of 91 days (CM regime) is more or less comparable to the 28 day moist cured samples (28DM) for all the three

concrete mixes. As a comparison, the HSC mix of similar water cement ratio is compared to the mix prepared by Asselanis et al. [5], indicated by blue box in figure 5.5 in which a mere 3% increase is found for the CM based samples as compared to the 28DM ones.

Table 5.3: Comparison of CM/28DM regime for Elastic Modulus of different mixes at 91 days

E-modulus at 91 days (in MPa)					
Concrete type	Continuously Moist cured (CM)		28 day Moist cured (28DM)		CM/28DM
	Mean	SD	Mean	SD	
NSC	35	2.6	34.4	1.2	1.07
HSC	40.2	1.1	39.6	0.8	1.01
UHSC	46.5	1.3	47.5	0.4	0.98

GROUP No	CURING CONDITIONS	Weight Changes (g)	Compressive strength	Elastic modulus
			MPa (psi)	GPa (10^6 psi)
1	1 d	—	38.4 (5570)	—
2	7 d	- 36.9	62.8 (9100)	30.3 (4.4)
3		+ 12.9	77.5 (11240)	37.2 (5.4)
4	28 d	- 11.6	99.2 (14390)	40.7 (5.9)
5		+ 16.1	98.8 (14330)	41.4 (6.0)
6		- 53.4	81.2 (11780)	35.2 (5.1)
7	56 d	+ 0.9	105.2 (15260)	42.1 (6.1)
8		+ 17.9	97.6 (14160)	43.4 (6.3)
9		- 57.2	82.3 (11930)	35.2 (5.1)



Figure 5.5: Comparison of the elastic modulus of various regimes as reported in Asselanis et al. [5]

It is reported from the literature study that the effect of drying on the strength properties could vary for the different specimen sizes of the samples considered. From the results shown in the previous chapter, it is evident that with increasing age, there is a clear traditional size effect observed i.e increase of strength with decreasing specimen sizes for both the compressive strength (see figure 4.2) and the splitting tensile strength (see figure 4.6) when the continuously moist cured (CM) regime is considered. However, in case of the 28 day moist curing (28DM) regime, there is no clear trend observed for the compressive strength as shown in the figure 4.3. Until the period of 56 days, traditional size effect is seen with the 50mm specimens having the largest strength. However, at the period of 155 days, the 150mm samples have the highest strength followed by the 50mm samples and the 100 mm ones, which have the lowest strength. This unclear trend is possibly due to the opposing battle between the drying effect (reduction of strength for smaller size specimens) and traditional size effect as explained by Soroka and Baum [37].

In this regard, the results of the current experimental regime are compared with the results obtained by Soroka and Baum [37] for the compressive strength of different specimen sizes measured at 28 and 90 days (as shown in the figure 5.6). It is observed that at 28 days, for regime E, a somewhat traditional size effect is seen with lower strength for 100 and 150mm samples as compared to the 50mm ones. This is comparable to regime C which also follows the traditional size effect. However, at 90 days, there is a combination of both

drying effect and traditional size effect which is evident from the regime C which shows almost stable value for all specimen sizes. In comparison, the regime E does not show a clear trend as 100mm specimen size has the lowest strength compared to the 50mm and 150mm samples. However, in case of regime F, it is comparable to regime D as both are under continuously moist cured regime. In a nutshell, it is clear that whenever there is a combination of air and water curing regime, analyzing the trend becomes complicated as the final value of the strength would depend on the dominant behaviour of either drying or traditional size effect.

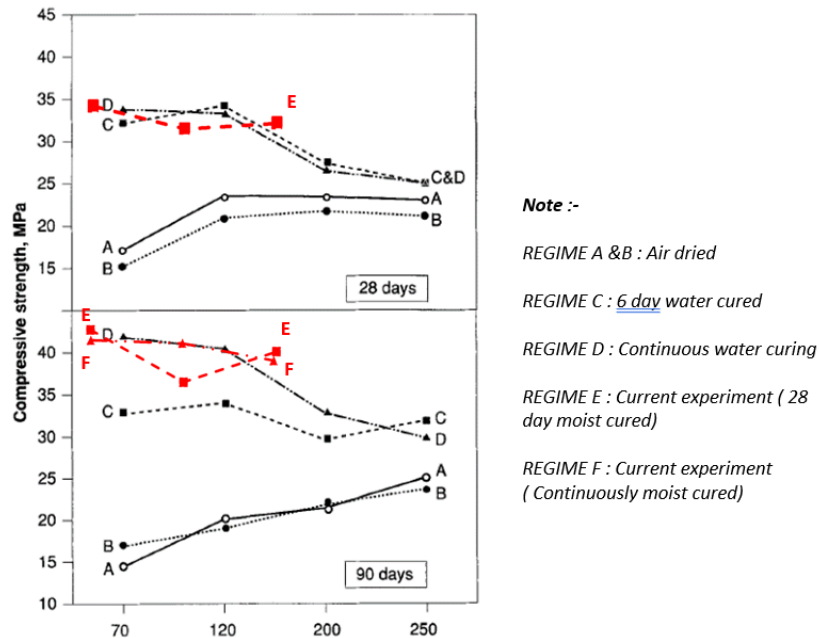


Figure 5.6: Comparison of the compressive strength of various regimes based on different specimen sizes with the results of Soroka and Baum [37]

Interestingly, the drying effect as mentioned in Soroka and Baum [37] is based on the assumption that there is a greater negative effect of drying (appearance of cracks) for smaller specimens as they have a larger volume of outer affected zones with respect to the entire volume. However, as already mentioned before, drying can also benefit the compressive strength as long as the tensile eigen stresses at the surface do not exceed the tensile strength of concrete. For the current experimental regime, this seems to be the case as there are no surface cracks observed for the specimens exposed to the similar drying conditions. Accordingly, the trend shown in the figure 4.3 is also expected to be influenced by eigen stresses, wherein a general tendency of increasing period followed by a stabilizing period is observed especially for 50mm and 100mm specimens. Although, in case of the 150mm specimens, only the increasing trend is captured and the specimens need to be tested in future to confirm the trend.

In case of the splitting tensile strength for different sized specimens, there is a clear traditional size effect seen when continuously moist cured regime is considered (see figure 4.6). However, even when 28 day moist cured regime is considered, it still follows the traditional size effect trend throughout the observed period (see figure 4.7). Interestingly, it is observed that similar to the case of compressive strength, there is a particular trend of increase and stabilization behaviour, which is expected to be due to the development of eigen stresses. Moreover, this trend seems to differ for the varying specimen sizes with a rapid increase and stabilization trend seen for the 50mm specimens followed by the 100mm specimens. In case of 150mm specimens, as similar to the trend of the compressive strength, an increasing trend is seen even at 155 days and the specimens need to be tested in future to check if there is a stabilizing trend.

It is understood that the inter-dependency between the various parameters is indeed a complex one with no clear trend observed especially in the case of the compressive and splitting tensile strength. The uncertainty is mostly caused due to the resulting effect of the combined curing (air and water) conditions coupled with the interaction of the traditional and drying size effect phenomenon. Further, it is observed that the trend is also influenced by the development of eigen stresses across the specimen which are temporary in nature and not

usually captured in the experiments. Thus, it is clear that the complex interaction between the parameters cannot be solely understood based on the experimental results.

5.3. Analysis of Modelling results

From the previous section, it is clear that the complexity in understanding the trend of the mechanical properties with time solely on the basis of experimental results is quite challenging. In this regard, the modelling approach is used which can allow to single out the influence of the corresponding parameters and help understand the experimental results at a greater depth. Moreover, as already mentioned previously in chapter 3, the focus is limited to understanding the tensile behaviour by simulating the direct, splitting tensile and flexural strength tests. The results of these tests are reported in the previous chapter and now it is aimed to analyze these results and give more clarity on the trend.

With regard to the trend of splitting tensile strength, in case of the NSC specimens, it is observed that drying after the 28 day moist curing period (28DM) leads to increase in the strength with time as compared to the continuously moist cured (CM) samples. Although, the magnitude and timing of increase seems to be dependent on the size of the specimen. On comparison with the experimental trend until 155 days (see figure 5.7), it is noted that FEMMASSE replicates the experimental trend accurately throughout the observed period in case of the 150mm specimens. For the 100mm specimens, FEMMASSE is able to replicate the experimental trend until 56 days, after which it follows a continuously increasing trend contrary to the experimental trend which seems to stabilize from 56 day onward. With regard to the 50mm specimens, FEMMASSE is able to predict the rapid increase at the 56 days as shown by the experimental results too. However at later stages, FEMMASSE predicts a gradual decrease of the splitting strength contrary to the experimental trend which shows a massive drop at 91 days followed by stabilizing period until 155 days. The differences in the results might be either due to the assumptions taken in the model or due to errors in reporting the experimental results.

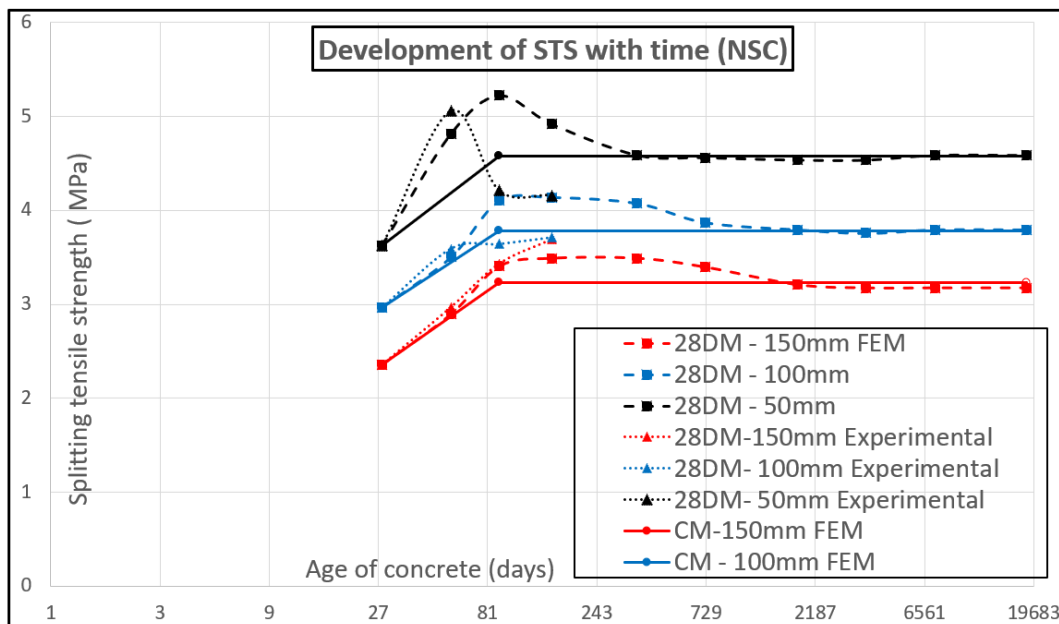


Figure 5.7: Development of Splitting tensile strength (STS) with time for Normal Strength concrete (NSC) of different sizes

Even though there are slight differences in the experimental and modelling results, it is observed from the comparison that the model actually predicts the general trend for NSC mixes in which drying after 28DM regime increases the splitting strength in the initial period followed by the stabilizing effect at the later stages. Initially, it is important to understand why there is trend of general increase followed by a stabilizing period. It was mentioned earlier that due to the non uniform drying, there are tensile stresses developed at the surface

and compressive stresses at the core. Moreover, according to the mechanical scheme of the splitting test (as shown in the figure 5.8), there is a compressive zone just underneath the point load and support, and tensile zone in almost entire middle part of the specimen. Generally, the splitting failure occurs with an initial crack in the tensile region which projects outwardly towards the surface causing ultimate failure. However, now due to the effect of drying especially in the initial period, there are tensile stresses at the surface and compressive stresses in the centre. If these tensile stresses do not exceed the tensile strength of concrete, the compressive stresses at the core delays the failure load and leads to higher splitting strength. However, in the later period, the effect of drying slows down due to which there are lesser magnitude of compressive stresses at the core compared to the initial period which results in the stabilizing of the trend.

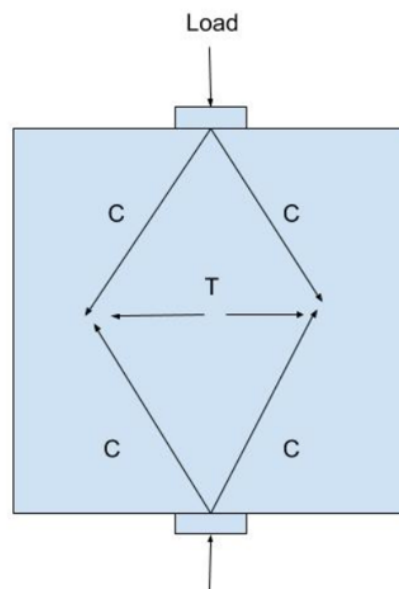


Figure 5.8: Mechanical scheme of the splitting test on a cube

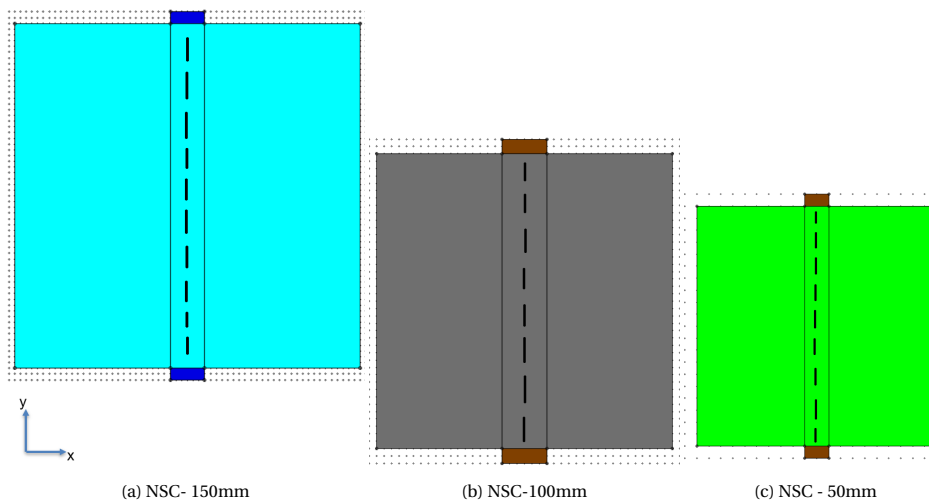


Figure 5.9: Cross section cut as indicated by the dotted black line for the NSC specimens

The successive increasing and stabilizing trend of splitting tensile strength on drying is noted to vary for the different specimen sizes. It is believed that further introspection on the obtained trend might help in understanding the phenomenon at a greater depth. For that purpose, the stress contours and stress profile (across the cross section as shown in the figure 5.9) are plotted corresponding to the different ages as highlighted by yellow in the figure 5.10. This will help to understand the stress state of the specimen before testing. It is to

be noted that the stresses across the cross section for all the specimen sizes are plotted in the same graph for better synthesis of the results.

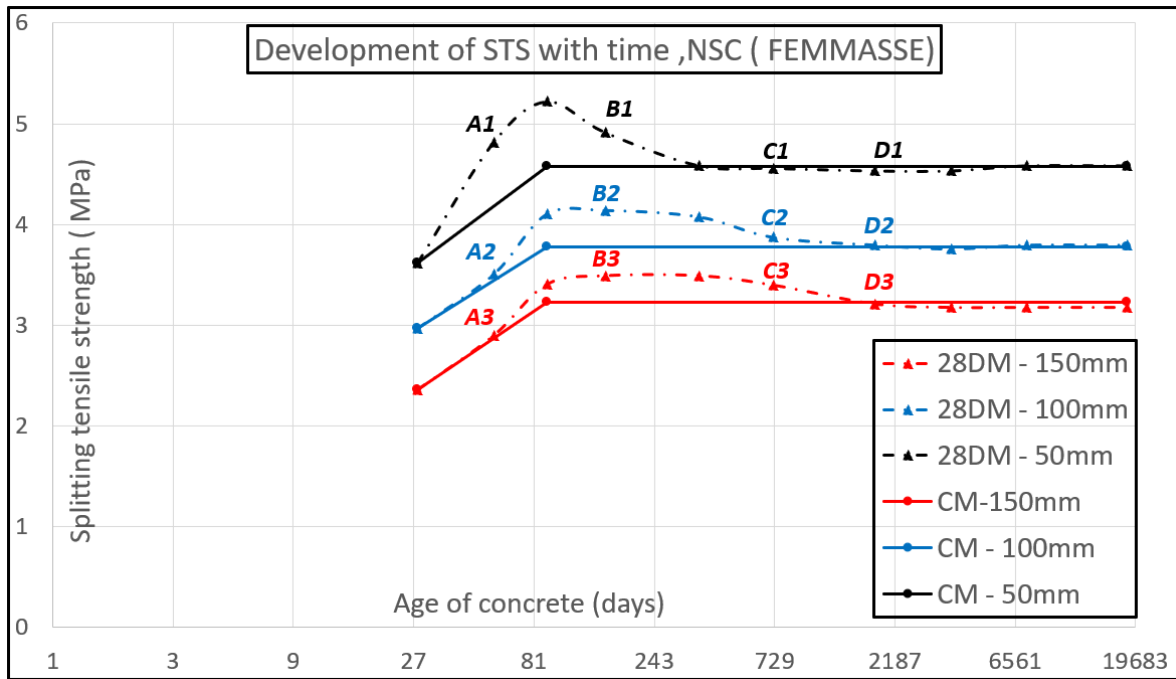


Figure 5.10: Development of Splitting tensile strength (STS) with time for Normal Strength concrete(NSC) specimens. In the figure A,B,C,D corresponds to concrete age of 56 days,155 days, 2 years and 5 years respectively and 1,2,3 indicate the specimen size of 50mm,100, and 150mm respectively

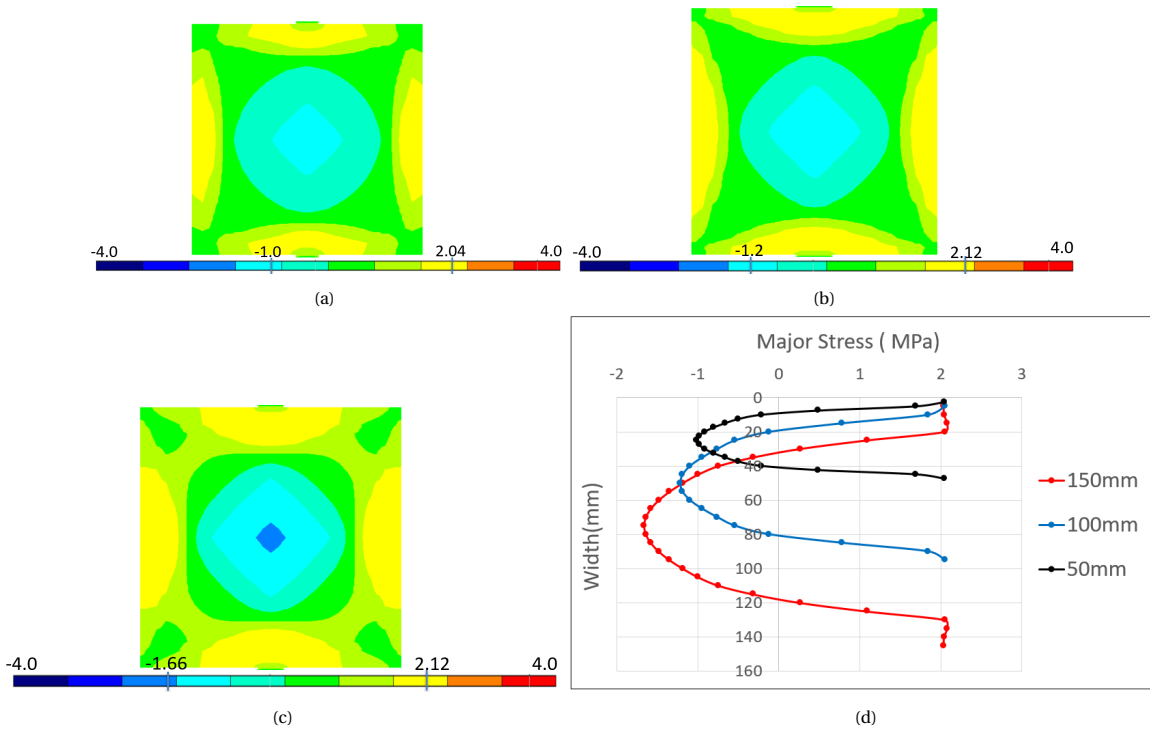


Figure 5.11: Major stress contours for (a) Point A1 - 50mm specimen (b) Point A2- 100mm specimen and (c) Point A3 - 150mm specimen (d)Combined Stress Profile at location A across the cross section as indicated in 5.9

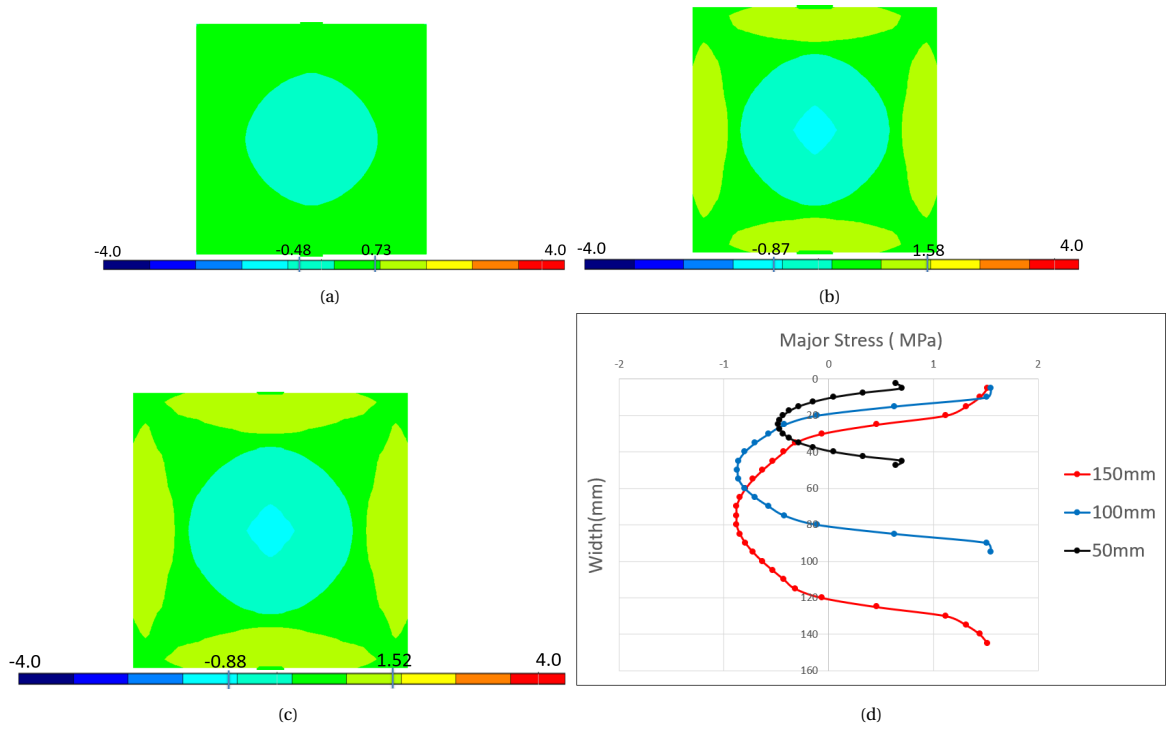


Figure 5.12: Major stress contours for (a) Point B1 - 50mm specimen (b) Point B2- 100mm specimen and (c) Point B3 - 150mm specimen (d) Combined Stress Profile at location B across the cross section as indicated in 5.9

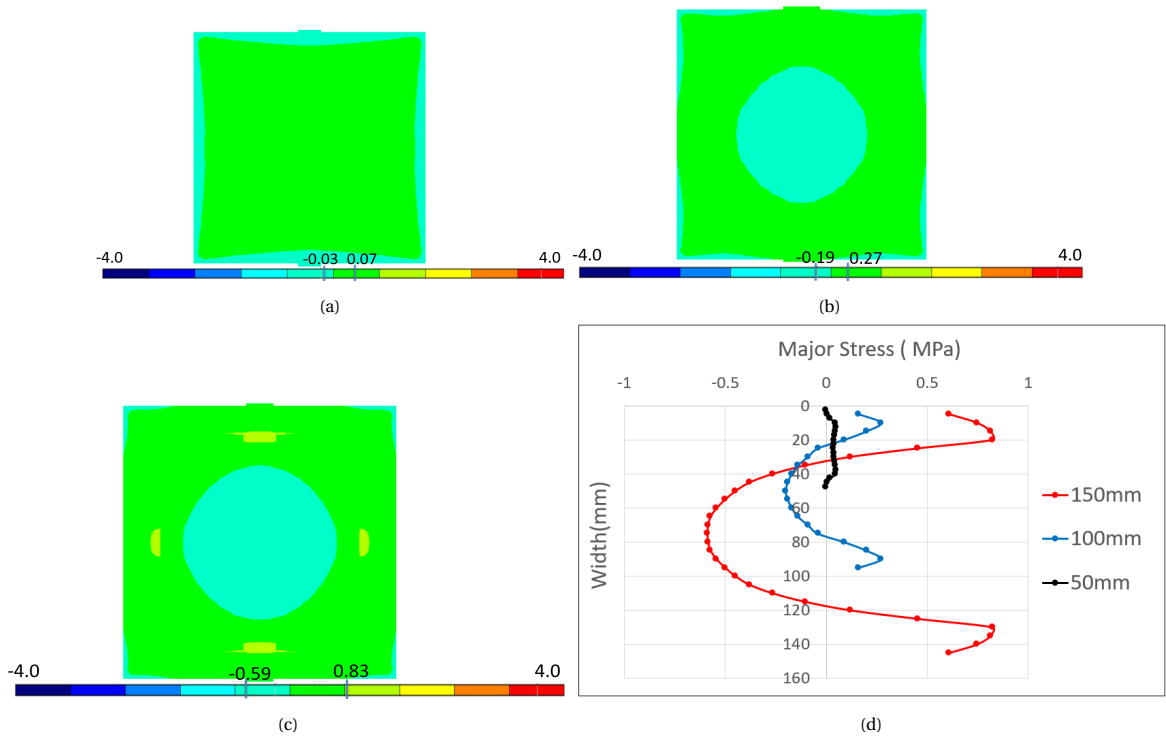


Figure 5.13: Major stress contours for (a) Point C1 - 50mm specimen (b) Point C2- 100mm specimen and (c) Point C3 - 150mm specimen (d) Combined Stress Profile at location C across the cross section as indicated in 5.9

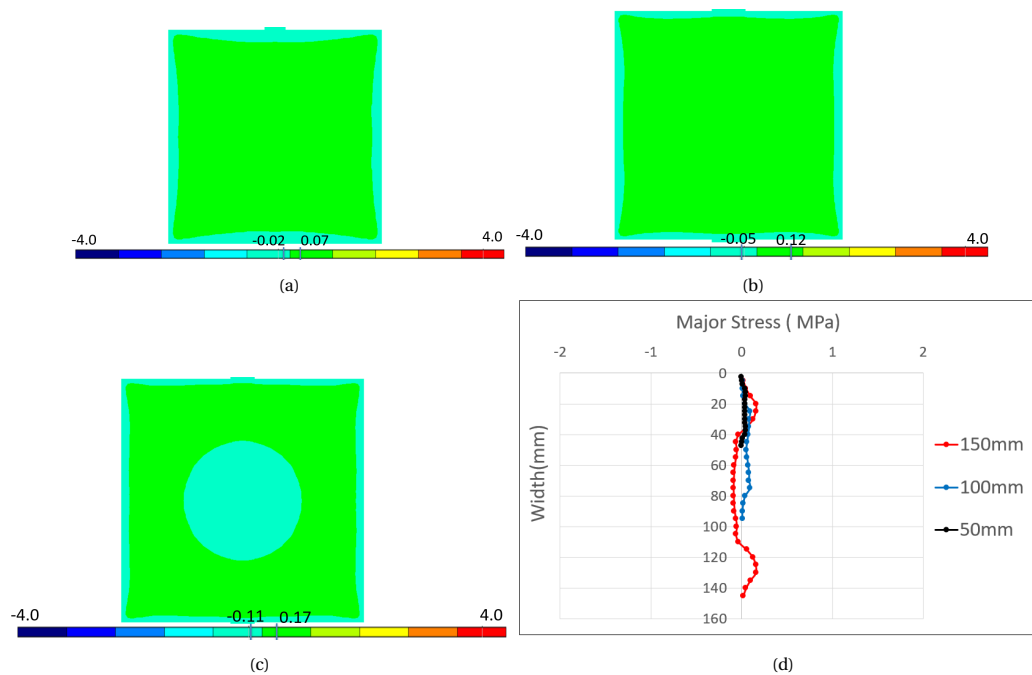


Figure 5.14: Major stress contours for (a) Point D1 - 50mm specimen (b) Point D2- 100mm specimen and (c) Point D3 - 150mm specimen (d) Combined Stress Profile at location D across the cross section as indicated in 5.9

Based on these stress contours and stress profile plots, the trend obtained in the figure 5.10 can be understood. In case of the 50mm specimens, it can be observed there are high compressive stresses at point A1, but these stresses start to reduce then onwards and almost die out at points C1 and D1. This explains the trend of the 50mm specimens where the maximum value corresponds to the location when there are maximum compressive stresses. In case of the 100mm and 150mm specimen too, the trend is explained similarly based on the stress profile and the stress plots. It is observed that at 2 years (location C), the 150mm specimens(C3) still have considerable compressive stresses as compared to the 100mm ones(C2). This explains the negligible increase due to drying for 100mm specimen and still considerable increasing trend for 150mm ones. However, at 5 years time (location D), even the 150mm ones(D3) have negligible compressive stresses which explains the final stabilization of the trend.

In case of the HSC mixes, it is seen that FEMMASSE results in a completely different trend with a sequence of increasing and decreasing behaviour contrary to the experimental trend, which shows more or less a stable value until the observed period of 155 days. The inaccuracy in replicating the experimental trend by FEMMASSE suggest that the assumed hygral parameters of HSC mixes based on the logical assumptions from the NSC ones might be incorrect. However, the trend of HSC specimens using FEMMASSE matches more or less with the obtained trend by Eva O. L. Lantsoght [13] for a similar HSC strength mix (C55/67). Although, the exact period of the drop and successive increase differs for both the cases. This may be due to the fact that the testing frequency in the tests conducted by Eva O. L. Lantsoght [13] is larger, and the drop in strength might have occurred at an earlier age, as is the case in the FEMMASSE simulations of the HSC specimens of the current experimental regime.

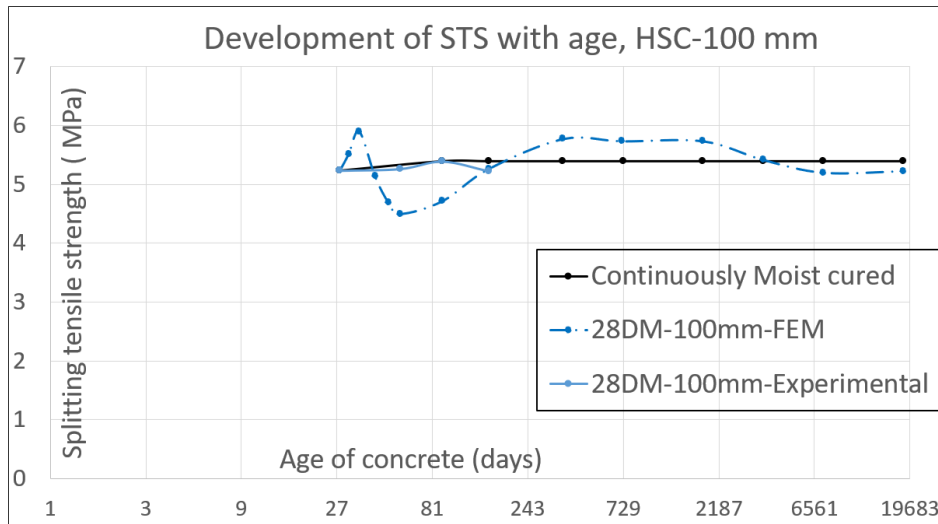


Figure 5.15: Development of Splitting tensile strength (STS) for high strength concrete (HSC) specimen - 100mm cube

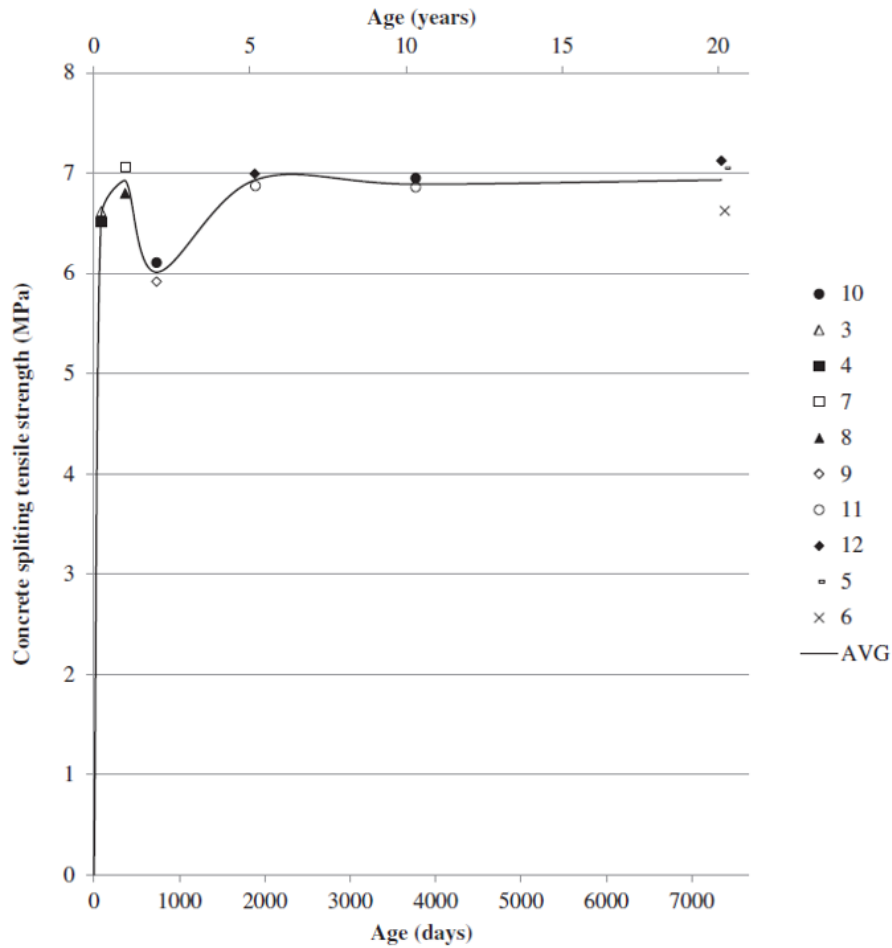


Figure 5.16: Development of the splitting tensile strength with age for a High Strength concrete mixture (C55/67) [13]

In any case, it is clear now that the effect of drying on the HSC specimens is different as compared to the NSC ones. In this regard, it is further aimed to understand the obtained trend using FEMMASSE by also additionally incorporating the different sized specimens as shown in the figure 5.15. It is evident that the general pattern for all the three specimen sizes are quite similar but the timing and the magnitude of increase/decrease seems to differ. Thus, it is clear that drying has a different effect on the trend of splitting tensile strength of the HSC specimens contrary to the NSC ones. In order to understand the reasoning behind it, the major stress profiles (at the same cross section as NSC specimen) and stress contours are made corresponding to the points as indicated in the figure 5.17.

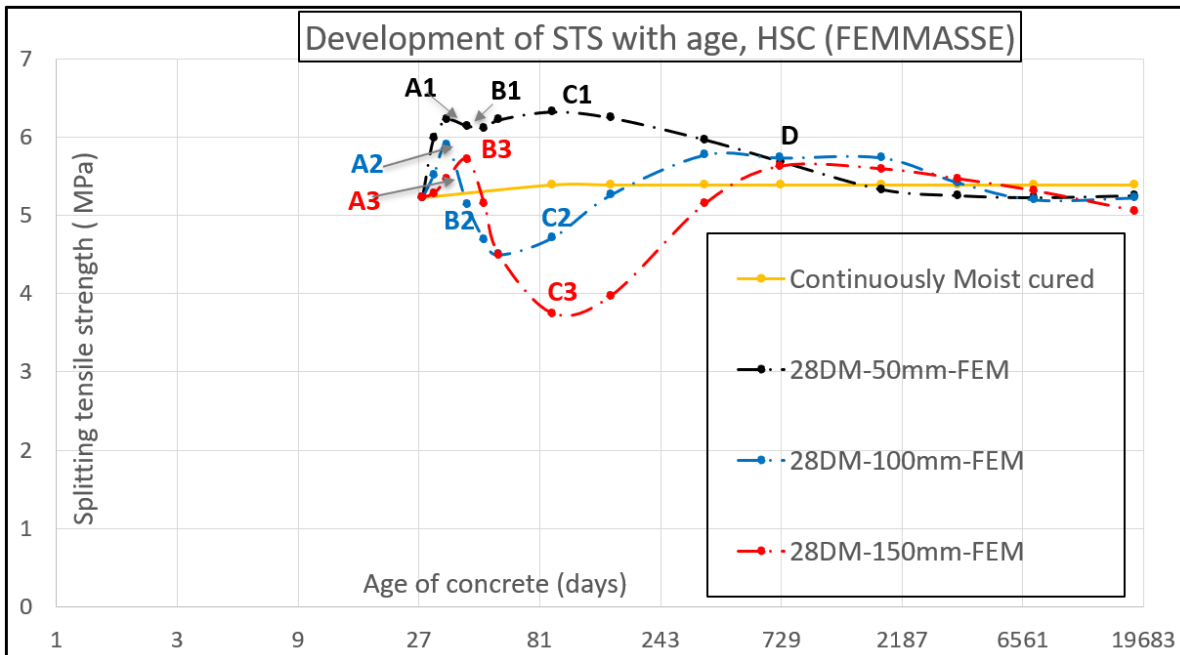


Figure 5.17: Development of Splitting tensile strength (STS) with time for High Strength concrete (HSC) specimens. In the figure A,B,C,D correspond to the concrete age of 35 days, 49 days, 91 days and 2 years respectively. Index 1,2,3 indicate the point corresponding to the 50mm, 100mm and 150mm specimens respectively

It is observed from these figures that at location A, there are high compressive stresses at the centre especially for the 50mm specimen (Point A1) resulting in an increasing trend. However, at location B, in spite of having sufficient compressive stresses at the centre, the value drops particularly for the 100mm (B2) and 150mm (B3) specimens due to the high tensile stresses at the surface which is almost equal to the tensile strength of the concrete. At location C, the tensile stresses at the surface are reduced for 50mm (C1) and 100mm (C2) specimen sizes, resulting in the gradual increase of trend due to the compressive stresses at the centre. However, in case of 150mm specimen (C3), there are still tensile stresses at the surface with the magnitude close to the tensile strength, resulting in a downward trend. Although, at location D, the 150mm (D3) specimens regain its strength owing to the reduction of the tensile stresses and delaying effect of ultimate load due to compressive stresses at the centre. From location C to D and onwards, the downward trend of 50mm specimen is due to its faster attainment of hygral equilibrium due to which the compressive stresses are reduced at the centre and the trend starts to stabilize. It is observed that the delaying of ultimate load due to the compressive stresses at the centre is only valid if the tensile stresses at the surface are below the tensile strength.

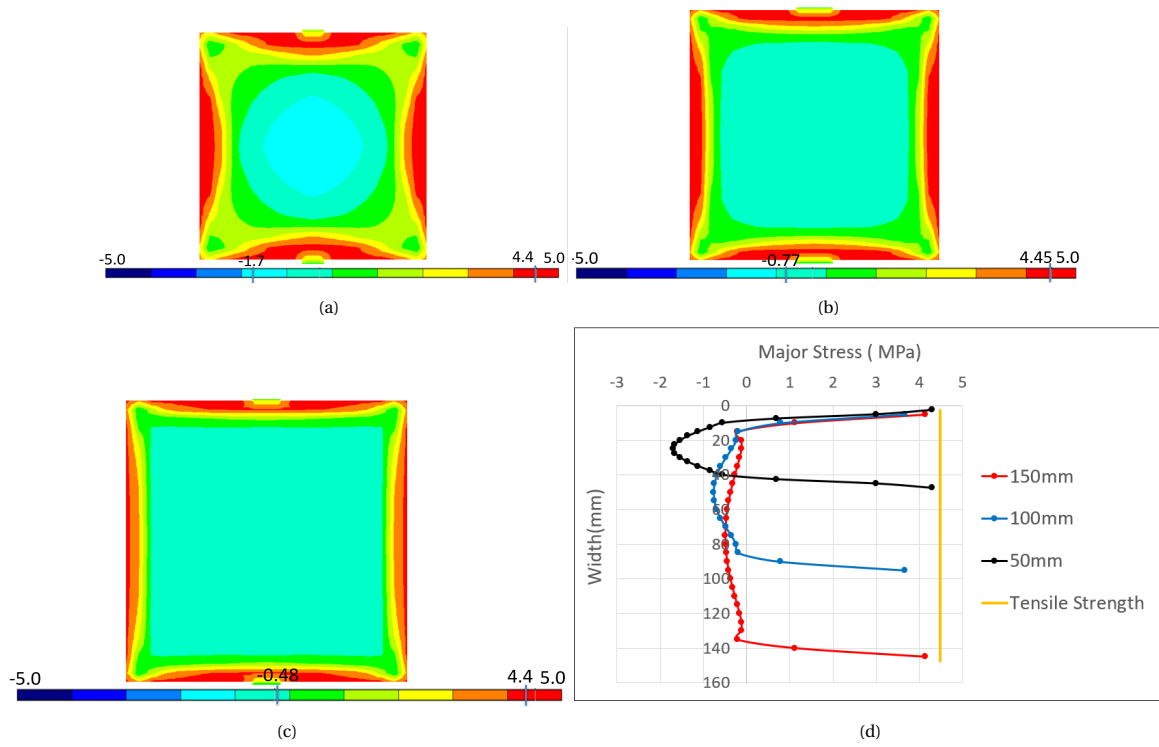


Figure 5.18: Major stress contours at location A - 35 days (a) A1-50mm specimen (b) A2-100mm specimen and (c) A3- 150mm specimen ; (d)Combined Stress Profile at location A - 35 days across the cross section as indicated in 5.9

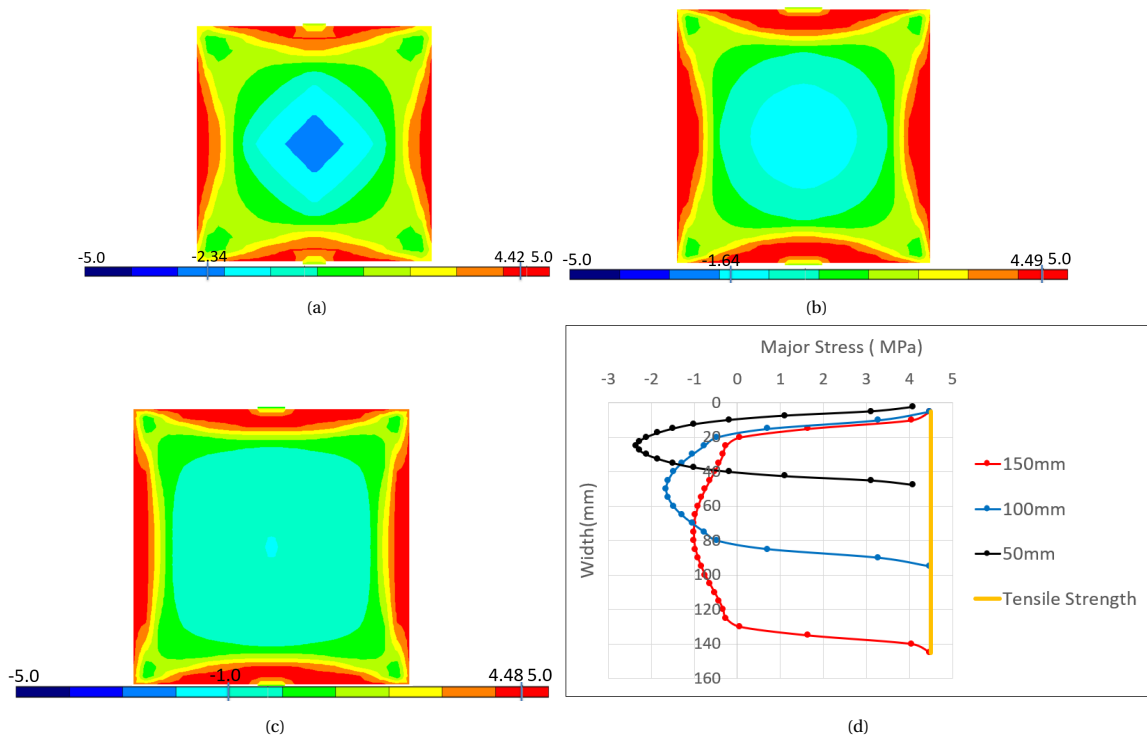


Figure 5.19: Major stress contours at Location B - 49 days (a) B1- 50mm specimen (b) B2- 100mm specimen and (c) B3-150mm specimen ; (d)Combined Stress Profile at point B -49 days across the cross section as indicated in 5.9

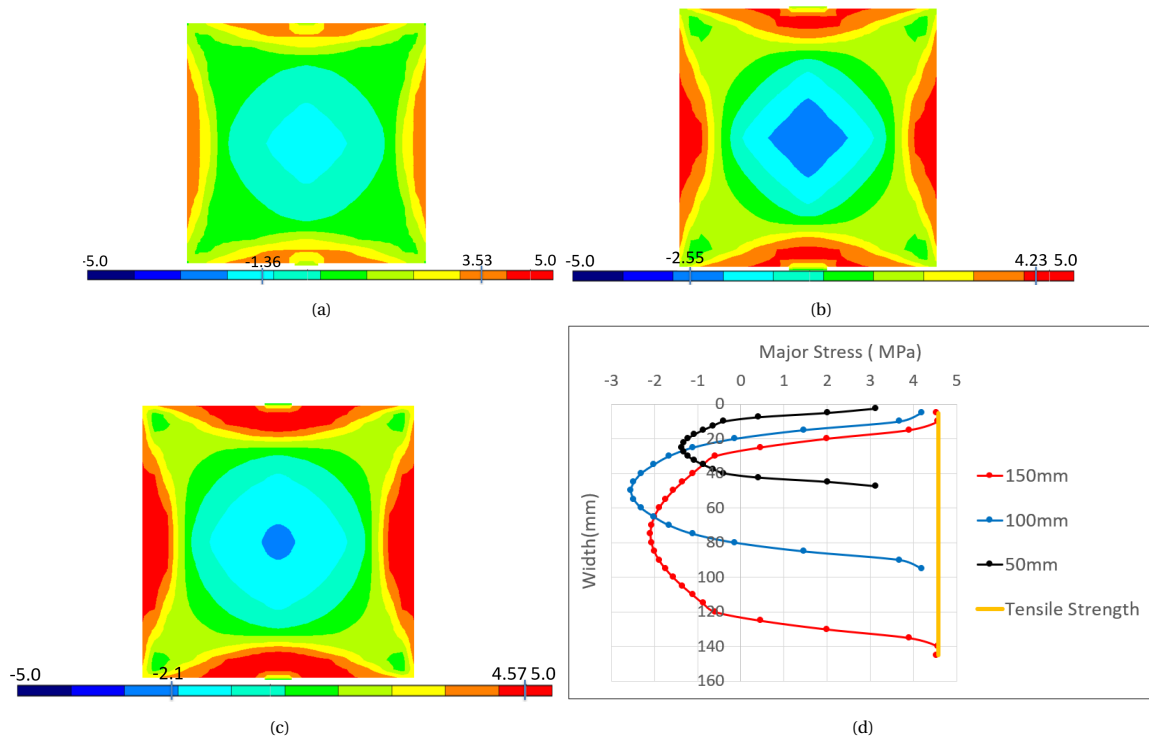


Figure 5.20: Major stress contours at Location C - 91 days (a) C1- 50mm specimen (b) C2- 100mm specimen and (c) C3-150mm specimen. (d) Combined Stress Profile at point C - 91 days across the cross section as indicated in 5.9

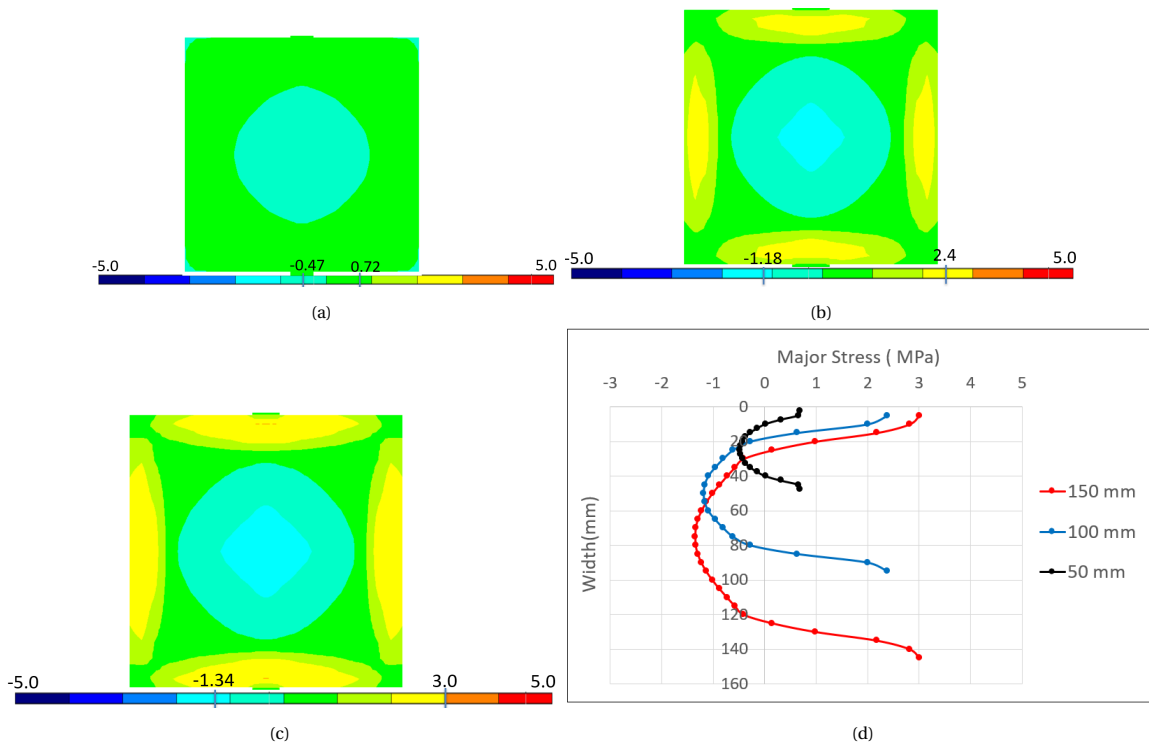
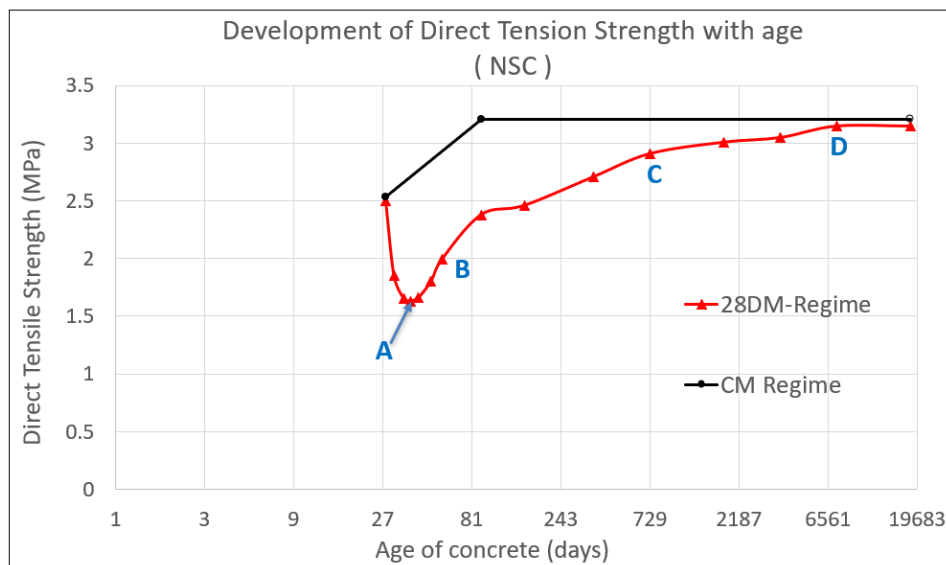


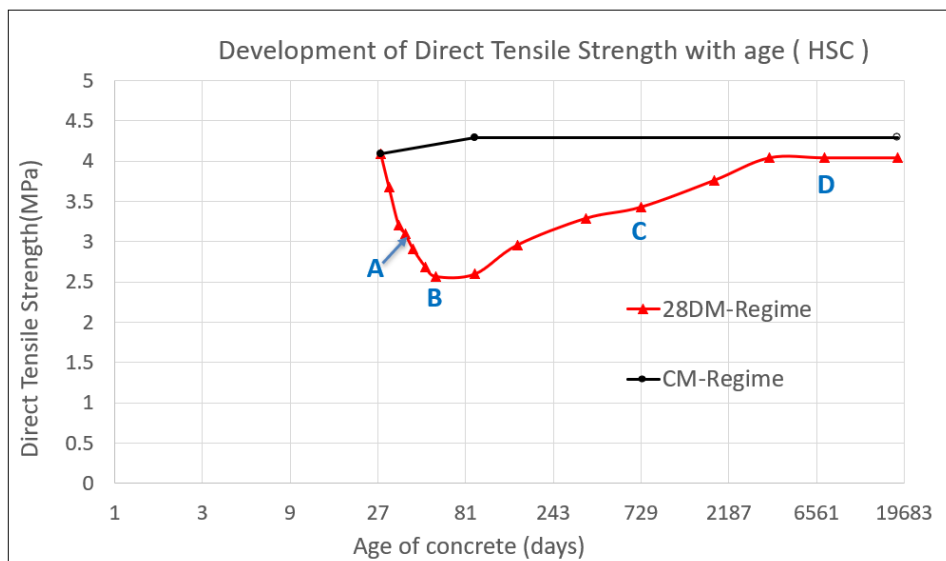
Figure 5.21: Major stress contours at Location D - 2 years (a) 50mm specimen (b) 100mm specimen and (c) 150mm specimen ; (d) Combined Stress Profile at point D - 2 years across the cross section as indicated in 5.9

Apart from the splitting strength, FEMMASSE has also been used to simulate the direct tensile and the flexural

strength tests in order to get more idea on the effect of drying on the tensile behaviour. In case of the direct tension strength, it is observed that drying after moist curing of 28 days leads to temporary reduction for both the NSC and HSC specimens (see figure 5.22). However, at later ages, the trend starts to increase again ultimately reaching to almost the same value as of the continuously moist cured specimens. In order to understand the reason for the temporary reduction followed by an increasing trend, the mechanical scheme of the test and resulting stress profile due to drying have to be taken into account. Due to the application of line load at the top surface, uniform tensile stresses are developed across the whole cross section. With regard to understanding the influence of stresses due to drying, stress profiles across the cross section are made at the indicated points as shown in the figure 5.22. Additionally, at these indicated points, stress contours are also displayed. This would help to understand the trend of direct tensile strength in general and also the differences in the trends for NSC and HSC specimens.



(a)



(b)

Figure 5.22: Development of direct tensile strength with age for (a) NSC specimens (b) HSC specimens

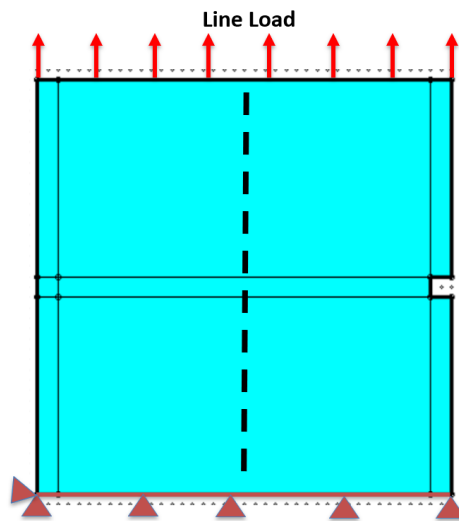
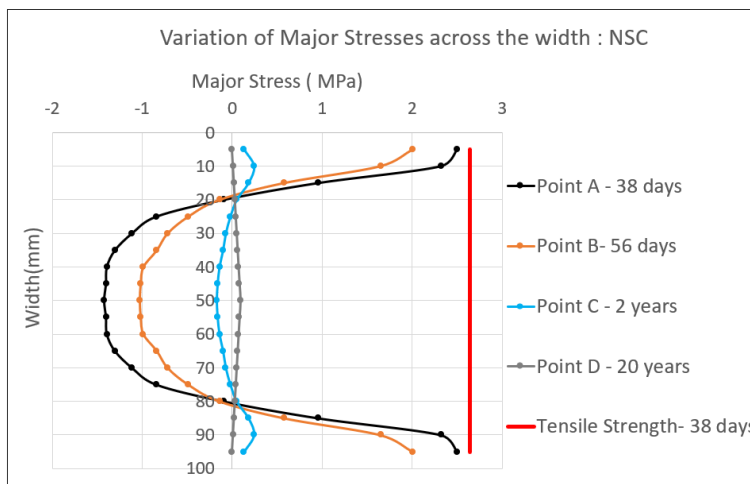
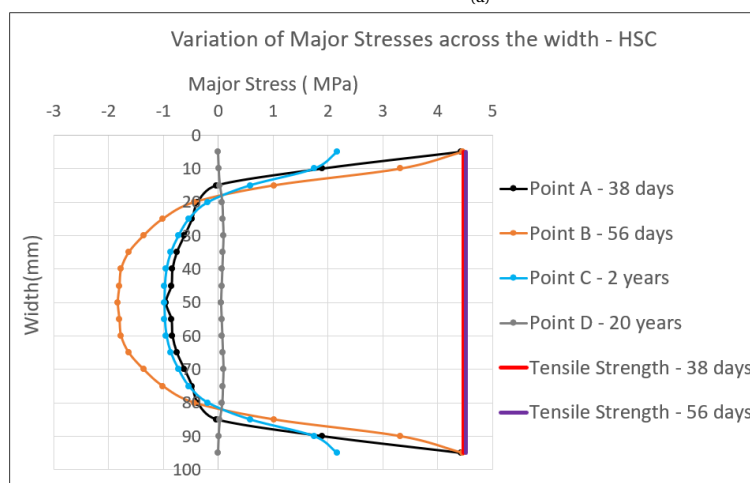


Figure 5.23: Mechanical scheme of the direct tensile model used in FEMMASSE



(a)



(b)

Figure 5.24: Major stress profile across the cross section for the various locations as indicated in 5.22 for (a) NSC specimens (b) HSC specimens

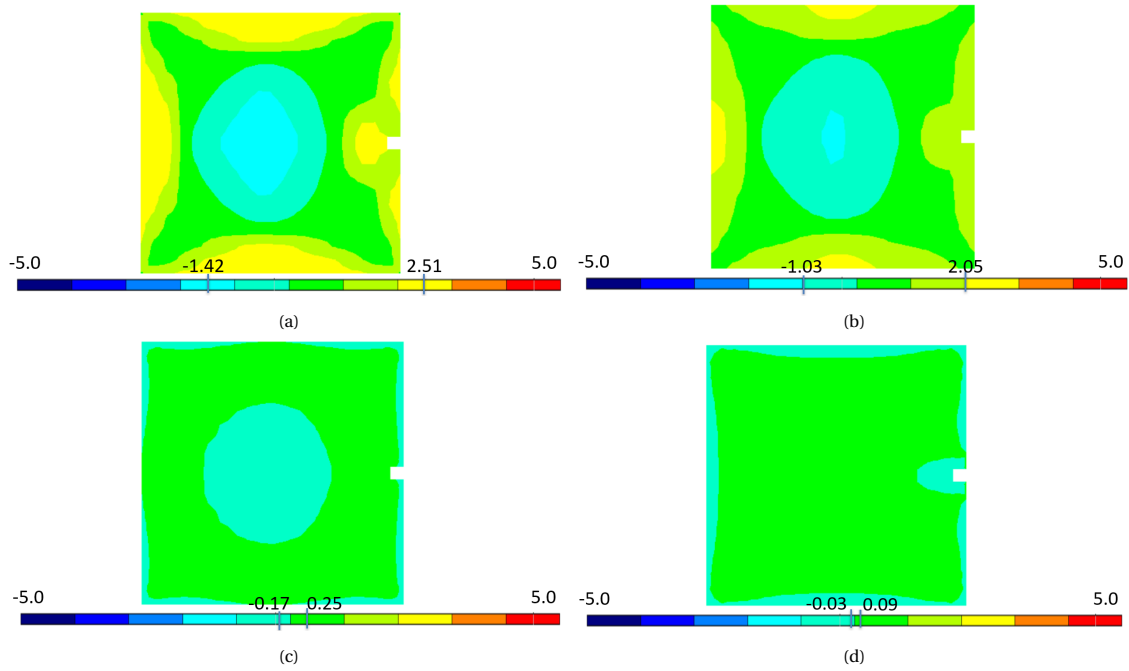


Figure 5.25: Major stress contours for NSC specimens at (a) Point A - 38 days (b)Point B- 56 days (c) Point C - 2 years and (d) Point D- 20 years

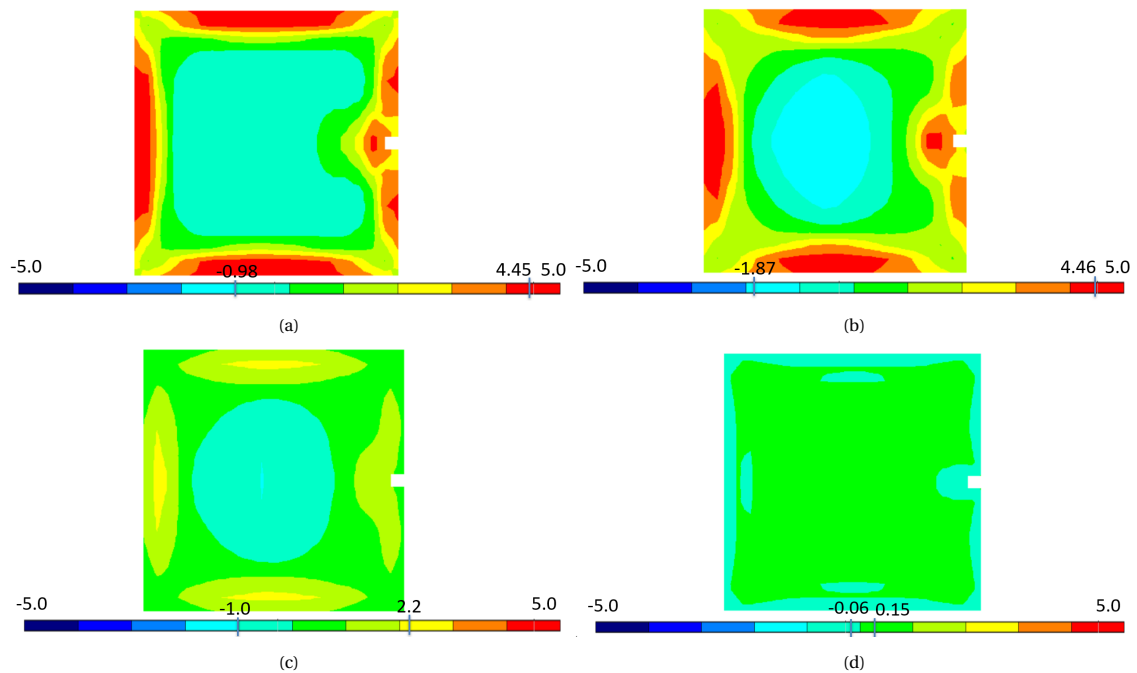


Figure 5.26: Major stress contours for HSC specimens at (a) Point A - 38 days (b)Point B- 56 days (c) Point C - 2 years and (d) Point D- 20 years

From the stress profiles and stress contours, it can be observed that in general due to non uniform drying, there are tensile stresses at the surface and compressive stresses at the core. Thus, as a result of the tensile stresses at the surface, the tensile capacity is already reduced, which results in a lower measured value of the direct tensile strength. However, as the drying progresses, the specimen attains moisture equilibrium leading to lesser tensile stresses at the surface relatively. This results in the gradual increase of the trend of direct tensile strength. However, it is also observed that the period of increasing and decreasing trend differs

for the NSC and HSC specimens. At 38 days (point A), there are high tensile stresses at the surface for both NSC and HSC specimens, which leads to a reduction in the tensile capacity for both these specimens. At 56 days (point B), the tensile stresses reduce considerably in case of NSC specimen resulting in the increase of trend. However, in case of HSC specimen, the tensile stresses are still close to the tensile strength resulting in lower tensile capacity. This is due to the relatively slow drying of the HSC specimen owing to its lower film and diffusion coefficient, implying that the tensile stresses are retained for a longer duration of time. Although at 2 years (point C), the HSC specimens show an increasing trend owing to the lesser tensile stresses at the surfaces due to the reduction in moisture gradient. Finally, at 20 years (point D), it is observed that both the specimens show a stabilized trend as the magnitude of the stresses are negligible as a result of the specimens attaining hygral equilibrium.

Until now, the simulations of the direct tensile test is based on the model wherein a small notch is considered at the side. The fact that the notch is exposed to drying can affect the actual value of the measured direct tensile strength. In order to check this, a new model is used wherein an imperfection is made at the centre of the specimen, such that it is not affected by drying (stated in chapter 3). Initially, the tensile strength is compared for both the specimens with a notch and an imperfection under continuously moist cured conditions. The tensile strength is calculated taking into account the reduced area and the results are found to be similar for both the cases. However, the trend is found to differ on the incorporation of drying conditions. Upon drying, it is observed that the general trend obtained is similar for both the model with a notch (henceforth referred as N-S) and an imperfection (referred as I-S). However, the model with the notch seems to be more negatively affected at the onset of drying.

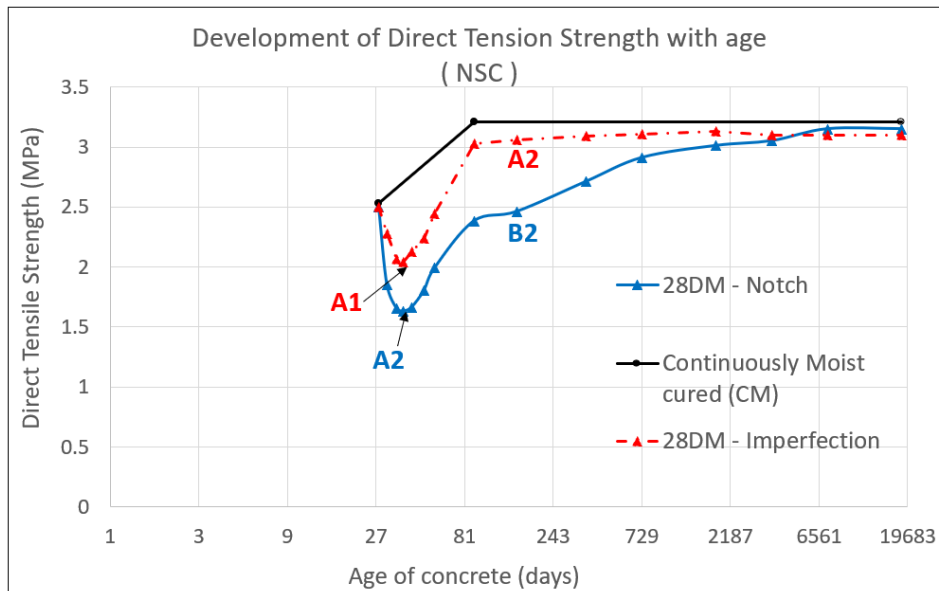


Figure 5.27: Development of the direct tensile strength for the model with a notch and an imperfection. Note : A1 and A2 indicates the value of the imperfection and notch model respectively at 38 days. B1 and B2 indicates the value of the imperfection and notch model respectively at 91 days

From the stress contours, it is evident that in case of the Y direction, the magnitude of the stresses are similar for both the N-S and I-S specimens. However, on looking at the X direction, the N-S specimens have varied distribution of stresses particularly at the location of the notch, where the tensile stresses due to drying are reduced. However, from the crack width plots, it is evident that the N-S specimen fails at a lower load as compared to the I-S ones at both 38 days (location A) and 91 days (location B). The probable reason might be due to the presence of notch at a region where the tensile capacity is already reduced due to drying. This leads to faster propagation of the tensile crack in the X-direction. In case of the I-S specimens, the reduced tensile capacity at the edges leads to generation of tensile cracks upon loading. But, the initiation of crack at the imperfection is delayed due to the high compressive stresses at the region. Thus, it is clear although the effect of drying on the direct tensile strength is the same, but the magnitude of the drop and regain of trend is determined whether a notch or an imperfection is modelled.

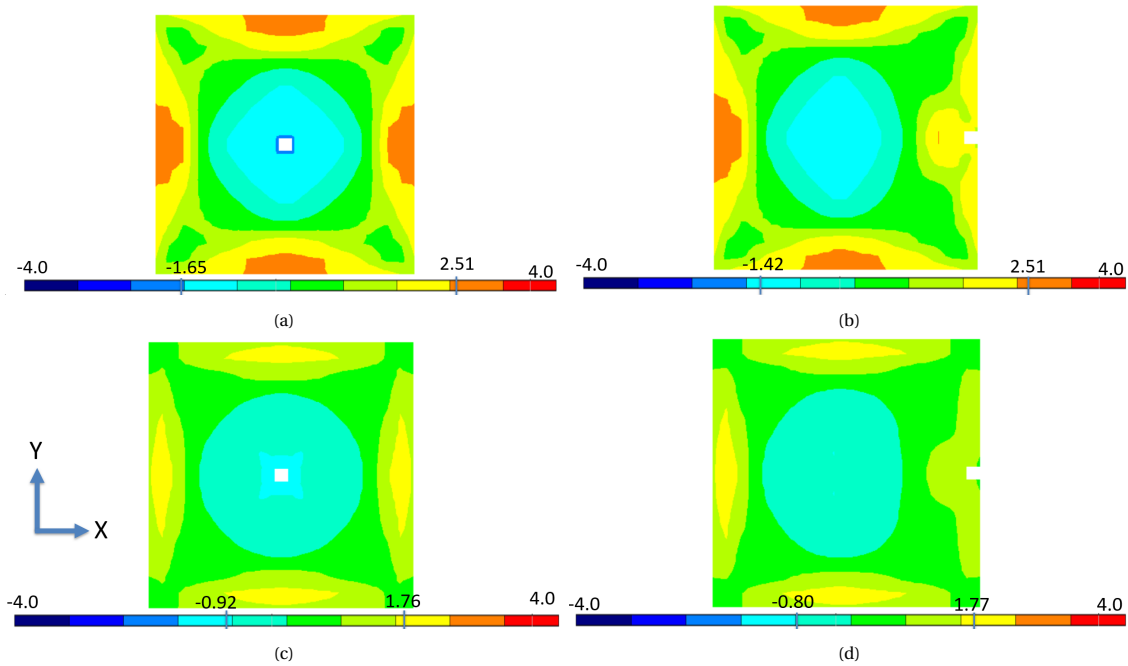


Figure 5.28: Major stress contour plots at the location (a) A1 - 38 days (b) B1 - 38 days (c) A2 - 91 days (d) B2 - 91 days

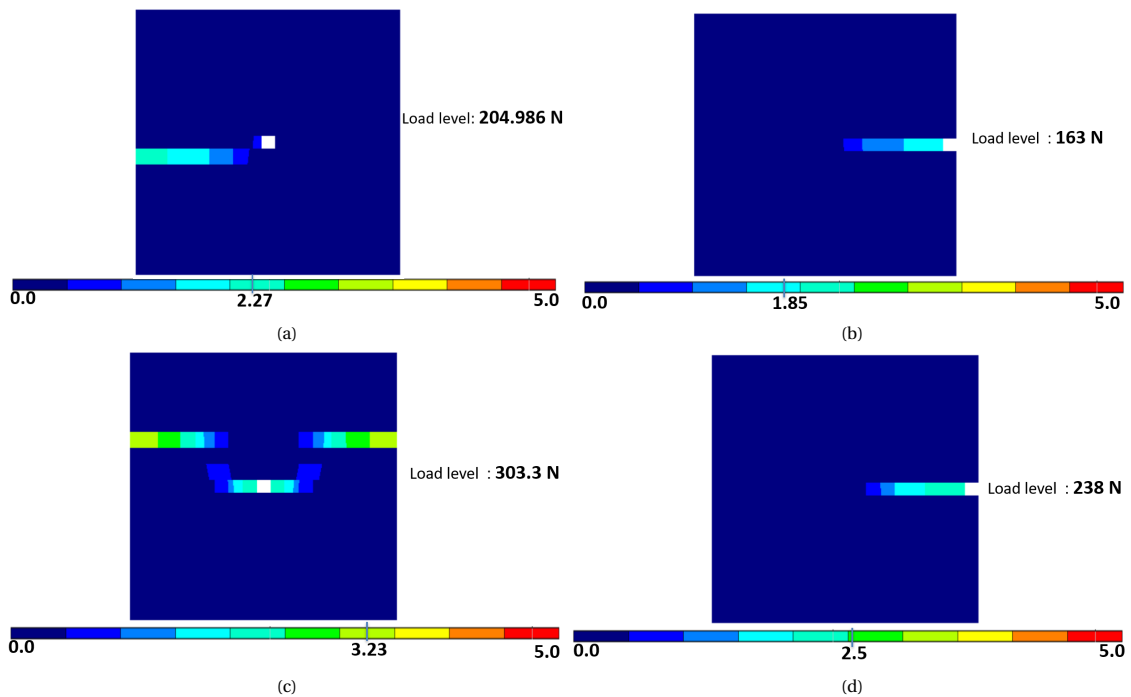


Figure 5.29: Crack width contours at the location (a) A1 - 38 days (b) B1 - 38 days (c) A2 - 91 days (d) B2 - 91 days

It is interesting to note that the trend obtained for the direct tensile strength using FEMMASSE is comparable to the results obtained by Bonzel as cited in Hordijk and Reinhardt [18], mentioned earlier in chapter 2. Although, in the study, cylindrical specimen of height 300mm and diameter 150mm is used. As mentioned earlier in chapter 4, due to the difficulty in simulating cylinders for tensile tests, cubes are used after verifying that they have almost similar humidity profile across the width as the cylinders. Thus, in order to make a still fairer comparison with the results of Bonzel, direct tensile test is simulated using a 150mm cube instead of the previously used 100mm ones. The comparison is done using a model with an imperfection in the centre.

From the comparison, as shown in the figure 5.30, it can be observed that in both the cases, the general trend is the same with a drop until 42 days followed by an increasing trend. However, the difference lies in the trend of the continuously moist cured specimens. As the testing conditions of these moist cured specimens are not mentioned, it is difficult to make any direct comparisons.

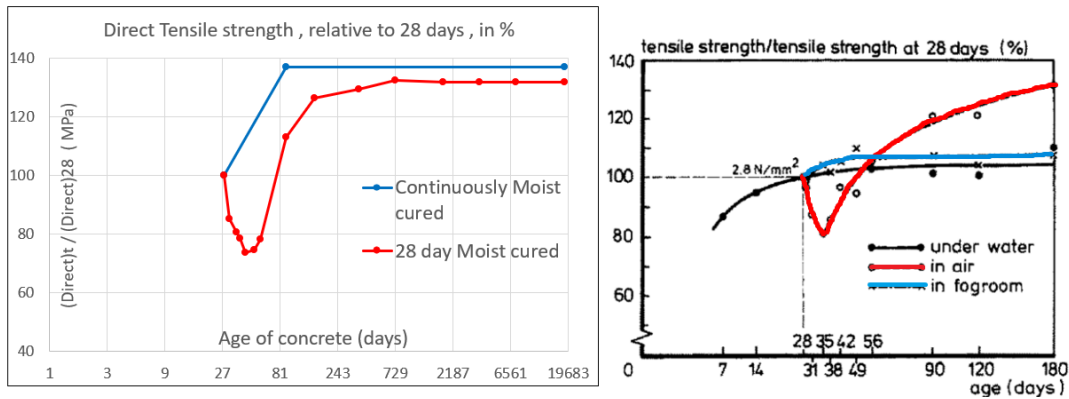


Figure 5.30: Comparison of the direct tensile trend of (left) current simulation using FEMMASSE and (right) trend from the study of Bonzel

With regard to the trend of flexural strength, the general trend obtained is the same as direct tensile strength wherein there is an initial drop followed by gradual increase. In order to understand the corresponding trend of flexural strength, the mechanical scheme of the test and resulting stress profile due to drying have to be taken into account. Although, in the flexural test set up, the specimen loaded in compression, but the deformed shape is such that there are tensile stresses at the bottom surface. Once these tensile stresses at the bottom reaches the tensile strength of concrete, the crack is initiated and on successive increase of loading, the crack is propagated ultimately leading to failure. With regard to understanding the influence of stresses due to drying, stress profiles are made at the cross section as shown in the figure 5.31 for the different ages of concrete as indicated by the different points in the figure 5.32. Additionally, at these locations, stress contours are also displayed. This would help to understand the trend of flexural strength in general and also the differences in the trends for NSC and HSC specimens.

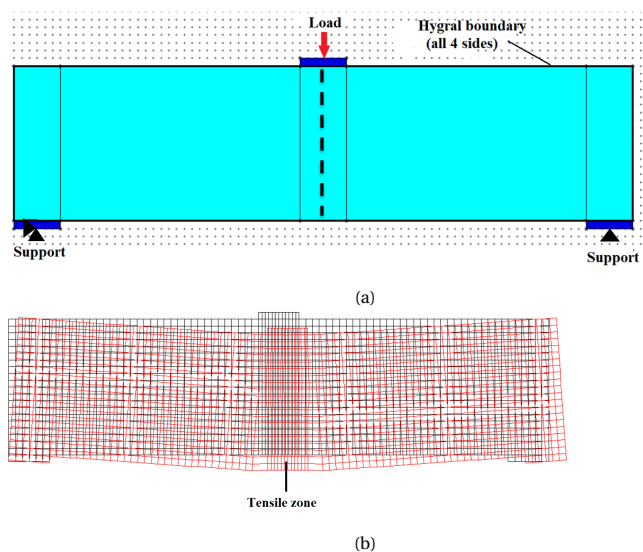
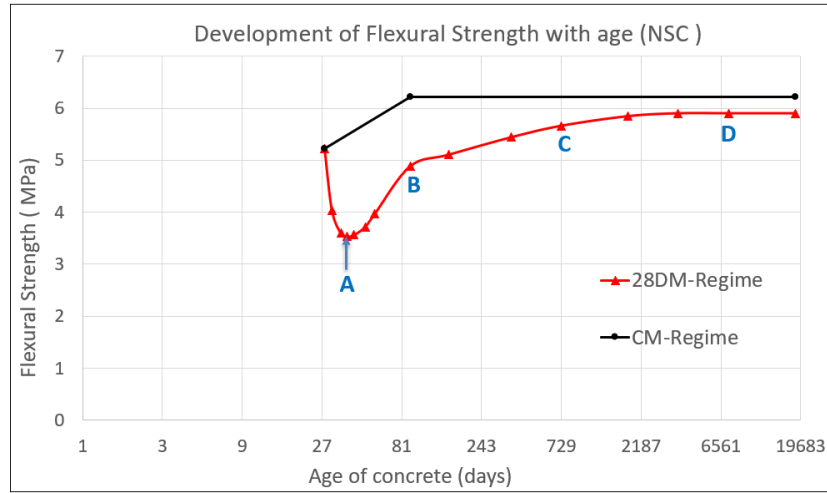
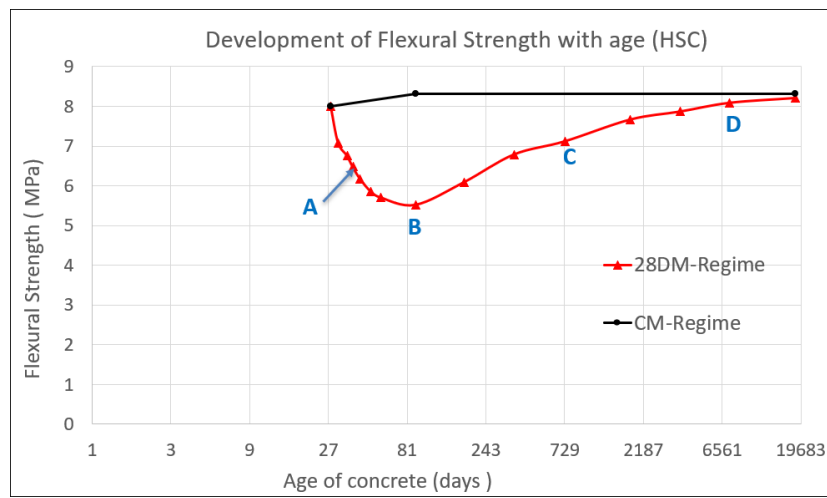


Figure 5.31: (a) Cross section cut as indicated by dotted black line for the flexural test specimen (b) General deformed shape of the specimen loaded under flexural test set up



(a)



(b)

Figure 5.32: Development of flexural strength with age for (a) NSC specimens (b) HSC specimens

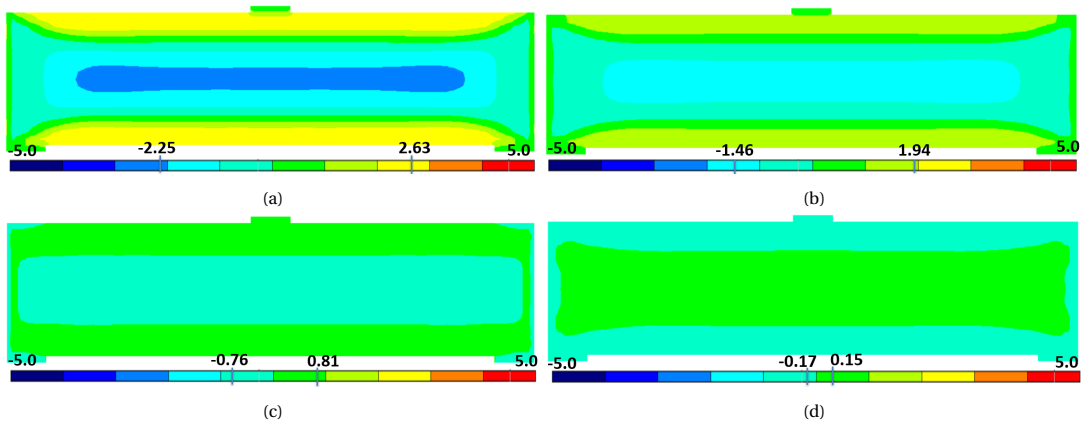


Figure 5.33: Horizontal stress contours for NSC specimens at (a) Point A - 38 days (b) Point B - 91 days (c) Point C - 2 years and (d) Point D - 20 years

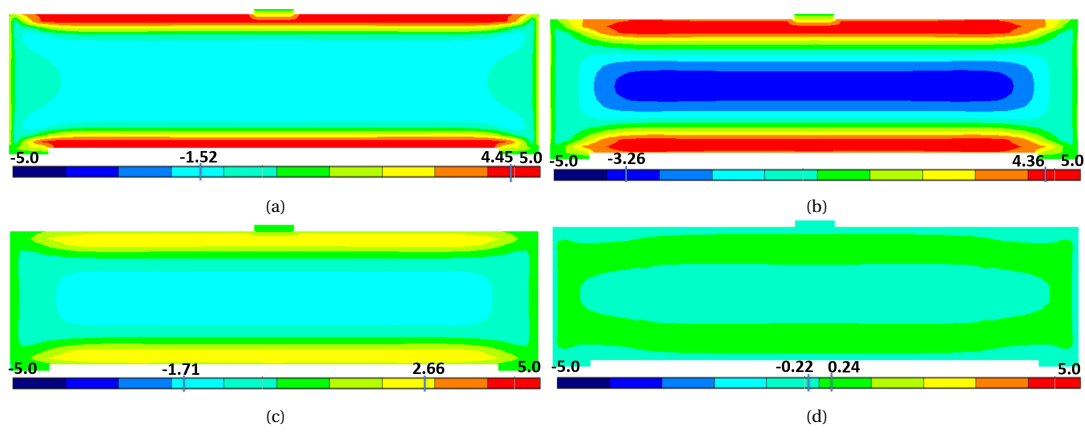
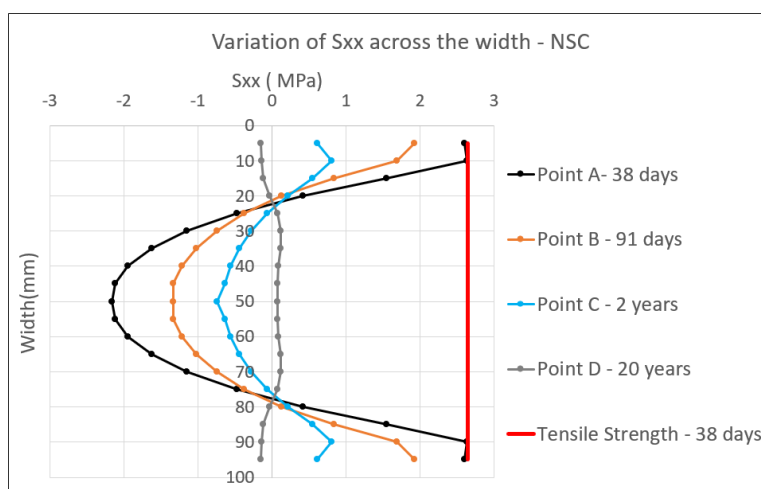
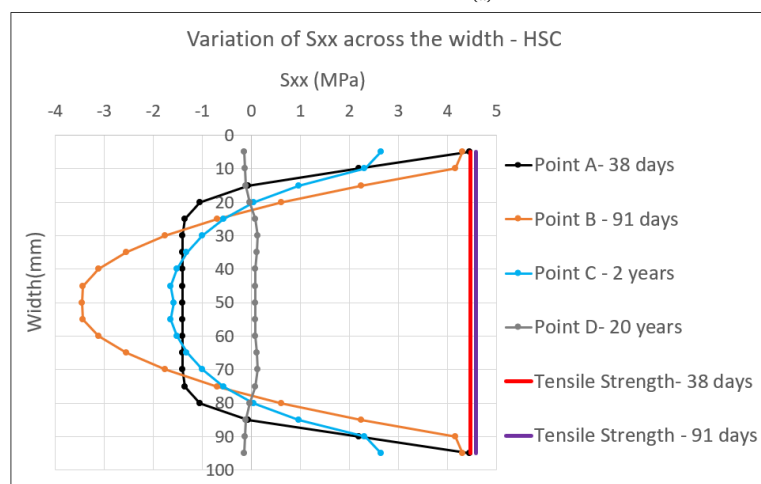


Figure 5.34: Horizontal stress contours for HSC specimens at (a) Point A - 38 days (b) Point B - 91 days (c) Point C - 2 years and (d) Point D - 20 years



(a)



(b)

Figure 5.35: Horizontal stress (S_{xx}) profile across the cross section for the various locations as indicated in 5.32 for (a) NSC specimens (b) HSC specimens

From the stress profiles and stress contours, it can be observed that in general due to non uniform drying, there are tensile stresses at the surface and compressive stresses at the core. Thus, as a result of the tensile stresses particularly at the bottom surface, the tensile capacity is already reduced, which results in a lower obtained value of the flexural strength. However, as the drying progresses, the specimen attains moisture equilibrium resulting in reduced tensile stresses and consequently an increase in trend. However, it is also observed that similar to the direct tensile trend, the period of increasing and decreasing trend differs for the NSC and HSC specimens. At 38 days (point A), there are high tensile stresses at the surface for both NSC and HSC specimens, which leads to a reduction in the tensile capacity for both these specimens. At 91 days (point B), the tensile stresses reduce considerably in case of NSC specimen resulting in the increase of trend. However, in case of HSC specimen, the tensile stresses are still close to the tensile strength resulting in lower tensile capacity. At 2 years (point C), the HSC specimens show an increasing trend owing to the lesser tensile stresses at the surfaces due to the reduction in moisture gradient. Finally, at 20 years (point D), it is observed that both the specimens show a stabilized trend as the magnitude of the stresses are negligible as a result of the specimens attaining hygral equilibrium.

The influence of the specimen size on the trend of flexural strength is studied by considering a slender cross section (50x50mm). In general, it can be observed that for the slender cross section, the decreasing and the stabilizing period is quite short and quick respectively. In order to understand in more depth, the horizontal stress profiles are plotted at the various locations indicated in the figure 5.36. From the stress profiles, it can be observed that at the age of 38 days (location A), the tensile stresses at the surface are almost equal to the tensile strength for 100x100mm specimens (point A2) which leads to reduced flexural strength. However, in case of the 50x50mm specimens (point A1), the tensile stresses are considerably lower resulting in an increasing trend. At the age of 2 years (location B), the tensile stresses are considerably reduced for the 100x100mm specimens (point B1) resulting in an increasing trend. For the 50x50mm ones (point B2), there are negligible stresses in the cross section resulting in the stabilizing of the trend. In a nutshell, the slender cross sections have a reduced decreasing period due to relatively smaller moisture gradient leading to lesser magnitude of tensile stresses. Moreover, they also stabilize earlier due to quicker attainment of the hygral equilibrium resulting in negligible stresses at the cross section.

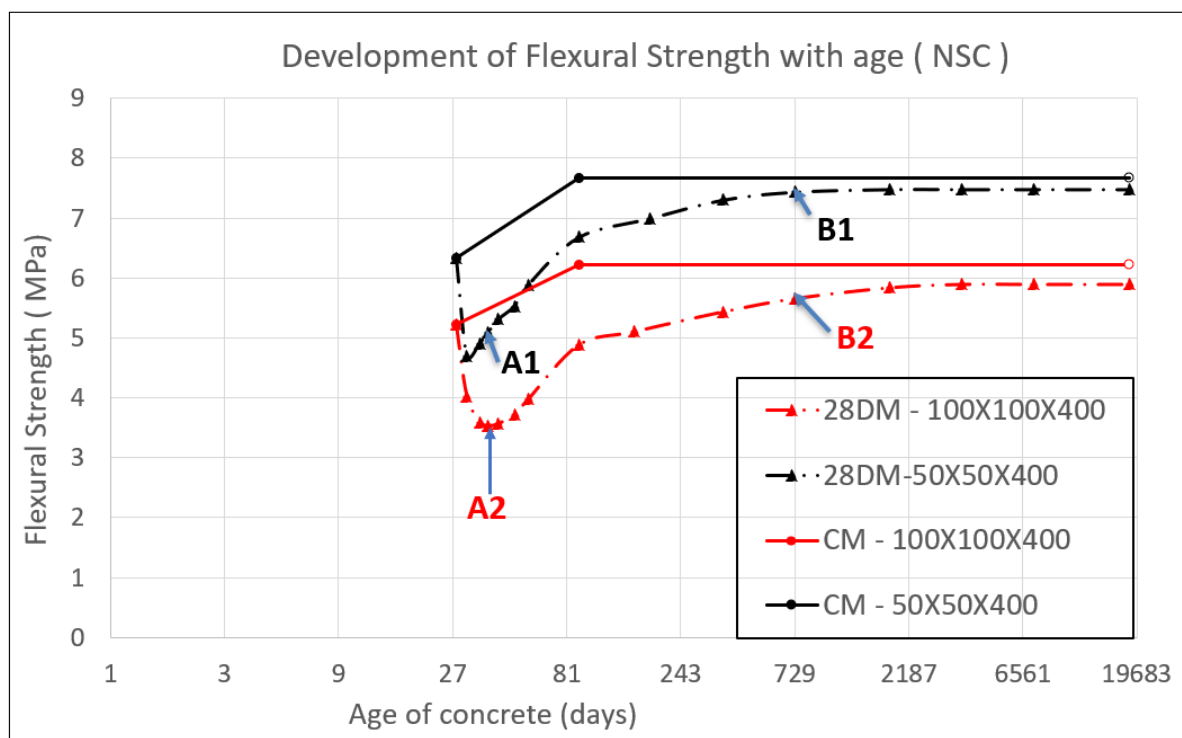


Figure 5.36: Development of Flexural strength with age for 100x100 and 50x50mm specimens

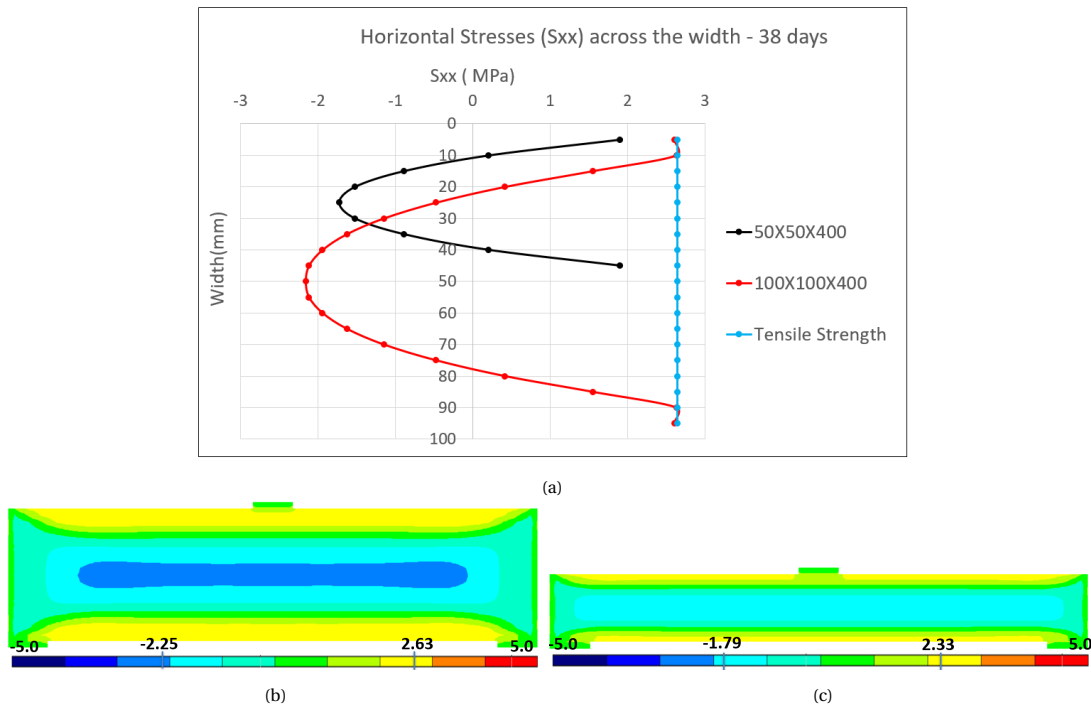


Figure 5.37: (a) Combined Horizontal stress profile across the width at 38 days (b) Horizontal stress contour plot for 100x100 specimens at 38 days and (c) Horizontal stress contour plot for 50x50 specimen at 38 days

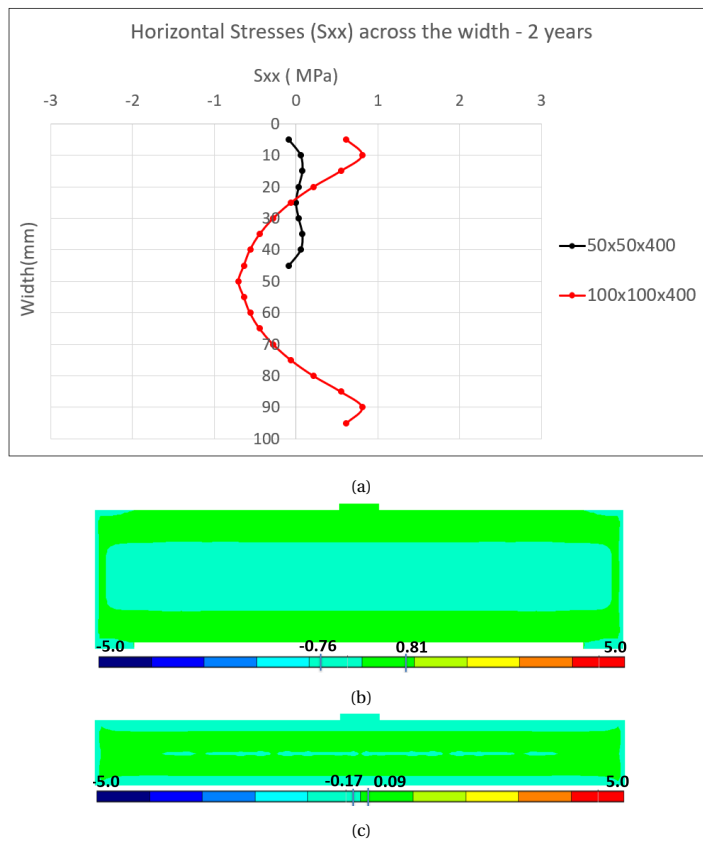


Figure 5.38: (a) Combined Horizontal stress profile across the width at 2 years (b) Horizontal stress contour plot for 100x100 specimens at 2 years and (c) Horizontal stress contour plot for 50x50 specimen at 2 years

With regard to the effect of drying on the flexural and direct tensile tests, it is observed from the results of that in general, the trend obtained is quite similar with an initial drop in strength followed by an increasing trend. However, on further comparison, it is observed that the trend of flexural strength is only comparable to the direct tension strength with a notch model and not with the imperfection model. This indicates that it is difficult to make a direct comparison of the effect of drying on the two respective strengths as the trend of direct tensile strength is dependent on whether a notch or an imperfection is modelled.

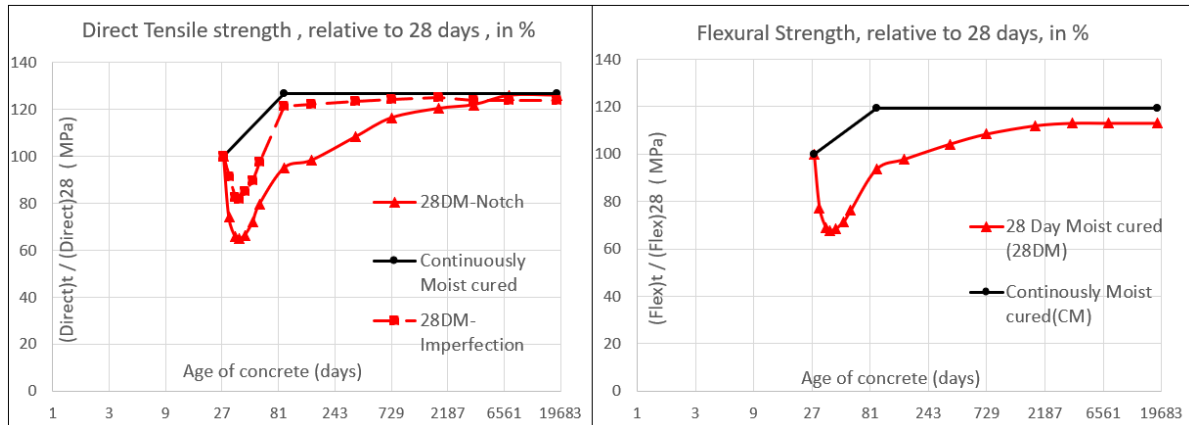


Figure 5.39: Comparison of the trend of (left) direct tensile strength using both notch and imperfection model and (right) flexural strength model

6

Conclusions and Recommendations

6.1. Conclusions

The first research objective of this study was to check if there is a reduction in the trend of mechanical properties of the ordinary concrete mixes of different strength grades with time, similar to the obtained trend for Geopolymer mixes studied by Prinsse [35], when exposed to drying at controlled lab conditions after 28 day of moist curing period. Additionally, it was also aimed to give more clarity on the complex inter-dependency of the various studied parameters (namely the curing conditions, varying specimen size and strength grade of concrete). The second research objective of this study was to see if the numerical FEM tool "FEMMASSE" could help understand the experimental results at a greater depth.

Accordingly, with the help of the experimental and numerical study, the research objectives are fulfilled and the major conclusions of the study are summarized below.

1. There is no major reduction in trend for the mechanical properties of the ordinary concrete of different grades with time, as compared to the Geopolymer concrete mixes designed by Prinsse [35]. Additionally, the comparable weight loss of S100 and S50 Geopolymer mixes to the NSC (C20/25) and HSC (C55/67) mixes respectively indicate that the effect of weight loss over time does not negatively impact the trend of the Elastic modulus of the ordinary concrete mixes (NSC and HSC) as compared to the Geopolymer ones (S50 and S100). Thus, it could be possibly concluded that the reduction of Elastic modulus with increasing moisture loss in case of Geopolymer might be due the chemistry of the Geopolymer itself.
2. For the chosen curing regimes, the empirical equations from the literature are not able to predict the elastic modulus accurately with time taking the compressive strength into account. This implies that it is preferable to conduct tests to determine the elastic modulus for greater accuracy.
3. The elastic modulus of all the three grades of ordinary concrete is not largely affected by the varying curing regimes used in the study (CM and 28DM regime), as for both the regimes, it gives almost similar value at the period of 91 days. In case of the compressive strength and splitting tensile strength, there is no specific trend observed on comparison of the experimental results with the literature. It is concluded that the final value of the strength based on the different curing regime is governed by the multiple parameters like the magnitude of the eigen stresses and the current state of ongoing hydration in the concrete specimen.
4. With regard to the specimen size effect, it is concluded that in case of the continuously moist (CM) cured regime, there is a clear traditional size effect seen in which the smaller specimen have a larger strength than the bigger ones. In case of the 28DM regime, a pattern of initial increase followed by stabilization of the trend is observed for both the compressive and splitting strength. This is assumed to be partly due to the development of varying magnitude of eigen stresses across the specimen with increasing age, which is further explained in more detail by the use of modelling.
5. With regard to the drying shrinkage, it is observed that broadly the results are in line with the literature in

which NSC mixes show the highest drying shrinkage followed by the HSC and UHSC ones for the observed period. However, the drying shrinkage models are not able to predict the experimental results accurately. The results obtained especially for the NSC samples do not follow a specific trend. On one hand there are large differences in the shrinkage strain of the three casted NSC prisms of the same mix design indicating that the differences could be due to the temperature drop which had occurred in the first three days after placing the specimen in the climate controlled room. On the other hand, the obtained weight loss pattern of all the NSC mixes are the same. This brings to the only plausible conclusion that the results of the NSC mix cannot be trusted and the variations might be due to the faulty strain measuring clocks.

6. From the FEMMASSE simulations, it is concluded that, based on the chosen hygral parameters, the attainment of the hygral equilibrium within a concrete specimen depends on the specimen size and the type of concrete mix considered. The smaller specimen sizes and the lower strength mixes are reported to attain hygral equilibrium earlier.

7. From the splitting test simulations until the period of 50 years, it is concluded that in case of the NSC specimens, drying after a moist curing period of 28 days (28DM regime) increases the strength temporarily with a gradual stabilization in the trend at later ages. This specific pattern is shown to be size dependent with the smaller specimens completing the pattern at a relatively earlier age owing to the quicker attainment of hygral equilibrium as compared to the larger sized specimens. The gradual increase and stabilization of the trend is explained on the basis of the interaction of the stresses based on the mechanical scheme of the test and the eigen stresses due to drying. Due to the mechanical scheme, compressive stresses are induced at the surface and tensile stresses at the core. However, due to drying exactly the opposite happens with tensile eigen stresses at the surface and compressive ones at the core. In the splitting test, the specimen fails from the middle as and when the tensile strength of the material is reached. However, now due to the compressive eigen stresses, the failure load is postponed and the measured splitting strength is higher than the actual strength.

8. In case of the trend of splitting strength of HSC specimens, it is concluded that drying leads to a different trend (compared to NSC specimens) wherein a successive increasing and decreasing period occurs followed by the stabilization period. This fluctuating trend is found to be similar for the different sized specimens but the magnitude of the drop/increase is concluded to be size dependent again due to the varying magnitude of the eigen stresses developed. The initial decrease in trend of HSC specimens as opposed to the increase in NSC specimens is explained on the basis of the higher magnitude of tensile stresses (close to the tensile strength) for the HSC specimens at the onset of drying. Thus, it is learnt that the effect of drying need not always have a positive (delaying) effect on the splitting strength. In case, the tensile stresses developed due to drying is almost equal to the tensile strength of concrete, there is no such delaying effect as a result of prestressing of the core. In other words, it is concluded that the delay in the failure load as a results of the compressive stresses at the core due to drying on the splitting strength is only valid if the tensile stresses at the surface is well below the tensile strength of the concrete specimen.

9. In case of the flexural strength simulations using FEMMASSE, it is concluded that drying after 28 day moist curing period leads to a temporary reduction followed by an increasing trend in case of both NSC and HSC specimens. The trend is again explained on the basis of the interaction of the stresses due to the mechanical scheme of the test and (eigen) stresses due to drying. The mechanical scheme of flexural tests leads to tensile stresses at the bottom surface. Since, there are already (eigen) stresses at the surface due to drying, the tensile capacity is reduced and thus the measured flexural strength is lower than the actual strength. Moreover, the trend of flexural strength is also observed to depend on strength grade of concrete and specimen size. With regard to the strength grade, the HSC specimens have a higher reduction period due to the relatively longer retainment of the tensile stresses at the surface as compared to the NSC ones. With regard to the size dependency, it is concluded that the slender specimens have a short reduction and a quicker stabilizing period owing to the faster attainment of the hygral equilibrium.

10. In case of the direct tensile strength, the general trend of initial reduction followed by gradual stabilization is the same as the trend of flexural strength. The already existing tensile stresses at the surface due to drying reduces the tensile capacity and on the application of tensile load, the measured tensile strength is lower than the actual strength. Moreover, in case of the direct tensile strength, it is observed that upon drying, although the general trend of initial reduction followed by gradual stabilization is the same for both notched and im-

perfection specimens, the magnitude of the reduction and time of stabilization in trend does differ with the notched specimens having a relatively higher reduction and a delayed stabilization period as compared to the specimen with an imperfection. The reduced measured value of the notched specimen is explained based on the location of the notch (at the surface) where the tensile capacity is already reduced due to drying. In case of the imperfection model, the imperfection is located at the centre i.e in a region of high compressive stresses (due to drying). Thus, although the tensile capacity is reduced at the surface due to drying, the ultimate failure only occurs when the crack in the imperfection conjoins the crack from the surface. This leads to a slightly higher measured tensile strength upon drying as compared to the notched specimens.

11. In a nutshell, from the simulation of the tensile tests, it is concluded that for the surface failure tests like the flexural and direct tensile tests, drying (28DM regime) initially reduces the tensile capacity at the surface leading to the temporary decrease of tensile strength. However, as the moisture gradient reduces, the trend starts to stabilize provided that there is no microcracking. However in case of the internal failure tests like the splitting tensile test, drying increases the splitting strength due to the presence of the compressive stresses at the core leading to a prestressing effect. Thus, it is understood that eigen stresses play a huge role in the final value of the measured material strength and unless there is hygral equilibrium, it can lead to an overestimation (in case of splitting) and underestimation (in case of flexural and direct tensile) of the measured material strength as compared to its actual strength. It can be inferred from the study that in practice, especially for mass concrete structures, the experimentally obtained material strength used for the design of structure could be incorrect due to the influence of eigen stresses, which might be present almost throughout the service period.

6.2. Recommendations

Based on the obtained results and the conclusions of the current research, few recommendations are made :-

1. For the experimental part, an interesting area of research would be to try out different types of cement (other than CEM-1 type) and check if similar trend in the development of mechanical properties with time is observed. Moreover, in this study, a relatively longer moist curing period of 28 days is opted in order to compare the results with the Geopolymer mix of Prinsse [35]. In the future, the curing period can be reduced to 7 or 14 days (as a closer depiction of practice) and then study the trend of the properties with time.
2. For the modelling part, an interesting research area would be to work on the extension of the model by incorporating the thermal model taking the effect of self desiccation into account. Moreover, the effect of relaxation of concrete could also be considered. It is believed that incorporating these additional effects along with the hygral and hydration effects already considered could give a more realistic depiction of the humidity and stress profile of the concrete specimen. Consequently, a more accurate prediction of the trend can be attained.

Appendices

A

Drying Shrinkage Models

This appendix shows the drying shrinkage models found in the literature reported in the study of Nassif et al. [29].

Eurocode 2 (CEB-FIP Model)

This model is applicable for concrete with strength class C20/25 until C90/105. The trend of drying shrinkage in time is given by the following equation :-

$$\epsilon_{cd}(t) = \beta_{ds}(t, t_s) \cdot k_h \cdot \epsilon_{cd,0} \quad (\text{A.1})$$

where,

$\epsilon_{cd,0}$ = Nominal unrestrained drying shrinkage value , k_h = coefficient depending on notional size h_o

$$\beta_{ds}(t, t_s) = \frac{t - t_s}{t - t_s + 0.04 \cdot (h_o)^{1/3}} \quad (\text{A.2})$$

where,

t = age of concrete at present time (days) and t_s = age of concrete at the end of curing period (days)

$$h_o = \frac{2A_c}{u}$$

where,

A_c is the cross sectional area and u is the perimeter of cross section exposed to drying.

ACI Comiittee 209 Model

This model is valid for all the concrete strength class range. The only important criteria is that the concrete must be moist cured for at least 7 days. The unrestrained shrinkage strain at any time t is given as,

$$\epsilon_{sh}(t) = \frac{t}{\eta + t} \cdot \epsilon_{sh}(u) \quad (\text{A.3})$$

where,

$$\epsilon_{sh}(u) = 780\gamma_{sh}X10^{-6}[inm/m]$$

$\eta = 35$ for 7 day or greater moist period

t = time after shrinkage considered

γ_{sh} = product of correction factors

Bazant B3 Model

This model takes into account the RH, size and shape of the specimen, curing conditions and cement type. The shrinkage strain is given by,

$$\epsilon_{sh} = -S(t).k_h.\epsilon_{sh,\infty} \quad (A.4)$$

where,

$$k_h = 1 - h^3, h < 0.98$$

$$\epsilon_{sh}(\infty) = -\alpha_1\alpha_2[0.019w^{2.1}f_{cm}^{-0.28} + 270]X10^{-6}$$

w = water content in kg/m^3

α_1 and α_2 = constants related to cement type and curing conditions respectively

$S(t)$ = time curve

where,

$$S(t) = \tanh\left\{\left(\frac{t-t_c}{\tau_{sh}}\right)^{0.5}\right\}$$

where.

$$\tau_{sh} = 0.085t_c^{-0.08}f_{cm28}^{-0.25}[2k_s(v/s)]^2$$

k_s = shape correction factor

v/s = volume to surface ratio

t_c = age of curing days

t = end of moist curing period

GL2000 Model

This model is the modified version of Eurocode model. The shrinkage strain is given by

$$\epsilon_{sh}(t) = \epsilon_{sh,\infty}.\beta(h).\beta(t) \quad (A.5)$$

where,

$$\epsilon_{sh,\infty} = 1000 \times 10^{-6} \cdot K \frac{30}{f_{cm28}}$$

$$\beta(h) = 1 - 1.18h^4$$

$$\beta(t) = \left\{ \frac{t-t_c}{t-t_c+0.15(v/s)^2} \right\}^{0.5}$$

where,

$\epsilon_{sh,\infty}$ = ultimate drying shrinkage strain

$\beta(h)$ = correction term for effect of humidity

$\beta(t)$ = correction term for effect of time

K = Shrinkage coefficient depending on cement type

f_{cm28} = compressive strength at 28 days

h = humidity

t_c = age of concrete curing

t = end of moist curing

v/s = volume to surface ratio

Miyazawa and Tazawa Model

This is an improved model and can be applied to both normal and higher strength concrete until w/c till 0.2. The drying shrinkage strain is given by the following equation :-

$$\epsilon_d(t, t_d) = \beta_d(t) \cdot \epsilon_{d,0}(RH) \quad (A.6)$$

where,

$$\epsilon_{d,0}(RH) = e \left\{ 1 - \exp \left\{ \frac{RH - RH_0}{t_1} \right\} \right\}$$

$$\beta_d(t) = \left\{ \frac{\frac{t-t_d}{t_1}}{350 \left(\frac{h}{h_0} \right)^2 + \frac{t-t_d}{t_1}} \right\}$$

where,

$\epsilon_d(t, t_d)$ = drying shrinkage from t_d to t (10^{-6})

$\beta_d(t)$ = coefficient for showing trend of drying with age

$\epsilon_{d,0}(RH)$ = ultimate drying shrinkage

RH = ambient relative humidity, 40% < RH < 100%

RH_0 = Specific relative humidity

$$h_0 = \frac{2A_c}{u}$$

$t_1 = 1$ day

B

Mesh Analysis

This appendix shows the results of the mesh analysis performed to see if there are any dependency of the obtained humidity and stress profile on the size of the mesh element.

For the study, three variations of square mesh element sizes are opted : 2.5mm, 5mm and 10mm (see figure B.1).

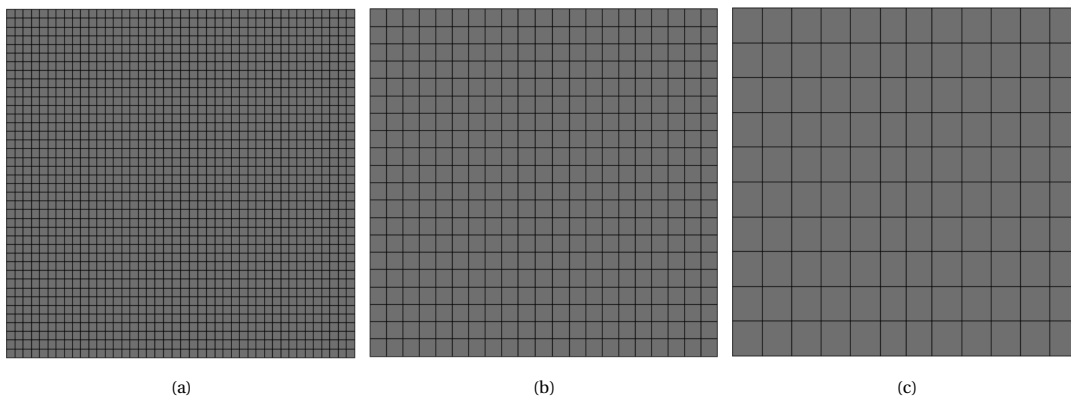
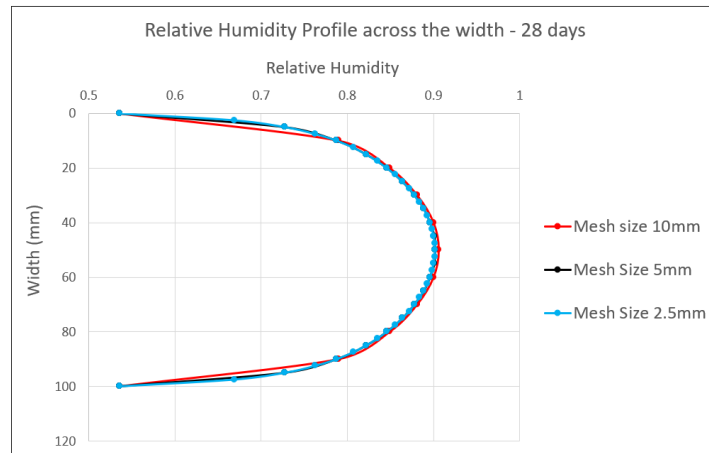
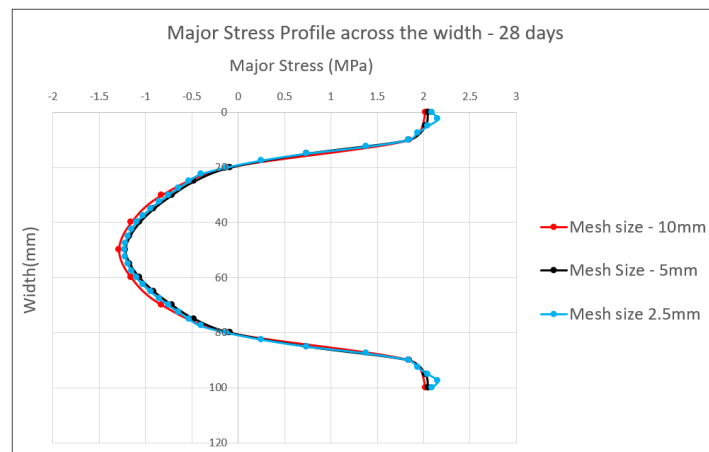


Figure B.1: NSC concrete specimen of mesh element size (a) 2.5mm (b) 5mm (c) 10mm

It is observed from the humidity and stress profile at 28 days shown in the figure B.2 that there is no such mesh dependency.



(a)



(b)

Figure B.2: (a) Variation of relative humidity profile across the width of the specimen - 28 days (b) Variation of major stress across the width at 28 days

Bibliography

- [1] Aci 318m-89.
- [2] En 1992-1-1.
- [3] Pierre-Claude Aitcin, Buquan Miao, William D Cook, and Denis Mitchell. Effects of size and curing on cylinder compressive strength of normal and high-strength concrete. *Materials Journal*, 91(4):349–355, 1994.
- [4] Ali Alsalman, Canh N Dang, Gary S Prinz, and W Micah Hale. Evaluation of modulus of elasticity of ultra-high performance concrete. *Construction and Building Materials*, 153:918–928, 2017.
- [5] Jon G Asselanis, Pierre-Claude Aitcin, and Povindar K Mehta. Effect of curing conditions on the compressive strength and elastic modulus of very high-strength concrete. *Cement, concrete and aggregates*, 11(1):80–83, 1989.
- [6] F Michael Bartlett and James G MacGregor. Effect of moisture condition on concrete core strengths. *Materials Journal*, 91(3):227–236, 1994.
- [7] Z. P. Bazant and L. J. Najjar. Drying of concrete as a nonlinear diffusion problem.
- [8] S Carmona. Effect of specimen size and loading conditions on indirect tensile test results. *Materiales de Construcción*, 59(294):7–18, 2009.
- [9] Ramon L Carrasquillo, Arthur H Nilson, and Floyd O Slate. Properties of high strength concrete subject to short-term loads. In *Journal Proceedings*, volume 78, pages 171–178, 1981.
- [10] Peng Chen, Changyong Liu, and Yuyin Wang. Size effect on peak axial strain and stress-strain behavior of concrete subjected to axial compression. *Construction and Building Materials*, 188:645–655, 2018.
- [11] GA Conroy-Jones and BIG Barr. Effect of curing on the tensile strength of medium to high strength concrete. *Magazine of Concrete Research*, 56(3):151–158, 2004.
- [12] Ir. R.T. Koekkoek Dr. ir. Y. Yang. Measurement report on the transition between flexural and shear failure of rc beams without shear reinforcement.
- [13] Ane de Boer Herbert van der Ham Eva O. L. Lantsoght, Cor van der Veen. Long-term material and structural behavior of high-strength concrete cantilever bridge: Results of 20 years monitoring.
- [14] fib, editor. *International Federation for Structural Concrete-Codetype models for structural behaviour of concrete*.
- [15] Benjamin A Graybeal. Compressive behavior of ultra-high-performance fiber-reinforced concrete. *ACI materials journal*, 104(2):146, 2007.
- [16] Ali H Hameed. The effect of curing condition on compressive strength in high strength concrete. *Diyala journal of engineering sciences*, 2(1):35–48, 2009.
- [17] JA Hanson. Effects of curing and drying environments on splitting tensile strength of concrete. In *Journal Proceedings*, volume 65, pages 535–543, 1968.
- [18] DA Hordijk and HW Reinhardt. Fracture of concrete in uniaxial tensile experiments as influenced by curing conditions. *Engineering Fracture Mechanics*, 35(4-5):819–826, 1990.
- [19] Said Iravani. Mechanical properties of high-performance concrete. *Materials Journal*, 93(5):416–426, 1996.

- [20] Paul Klieger. Effect of mixing and curing temperature on concrete strength. In *Journal Proceedings*, volume 54, pages 1063–1081, 1958.
- [21] Dalibor Kocab, Barbara Kucharczykova, Petr Misak, Petr Zitt, and Monika Kralikova. Development of the elastic modulus of concrete under different curing conditions. *Procedia engineering*, 195:96–101, 2017.
- [22] Byung Jae Lee, Seong-Hoon Kee, Taekeun Oh, and Yun-Yong Kim. Effect of cylinder size on the modulus of elasticity and compressive strength of concrete from static and dynamic tests. *Advances in Materials Science and Engineering*, 2015, 2015.
- [23] Mao Lin, Mitsuki Itoh, and Ippei Maruyama. Mechanism of change in splitting tensile strength of concrete during heating or drying up to 90. *Journal of Advanced Concrete Technology*, 13(2):94–102, 2015.
- [24] Andrew Logan, Wonchang Choi, Amir Mirmiran, Sami Rizkalla, and Paul Zia. Short-term mechanical properties of high-strength concrete. *ACI materials journal*, 106(5):413, 2009.
- [25] Mladena Lukovic. Influence of interface and strain hardening cementitious composite (shcc) properties on the performance of concrete repairs.
- [26] VM Malhotra. Effect of specimen size on tensile strength of concrete. In *Journal Proceedings*, volume 67, pages 467–480, 1970.
- [27] Ippei Maruyama, Hiroshi Sasano, Yukiko Nishioka, and Go Igarashi. Strength and young's modulus change in concrete due to long-term drying and heating up to 90 deg. *Cement and Concrete Research*, 66:48–63, 2014.
- [28] P.K. Mehta and P.J.M. Monteiro. *Concrete: Microstructure, Properties, and Materials*. McGraw-Hill's AccessEngineering. McGraw-Hill Education, 2013. ISBN 9780071797870. URL <https://books.google.nl/books?id=X84TAgAAQBAJ>.
- [29] Hani Nassif, Nakin Suksawang, and Maqbool Mohammed. Effect of curing methods on early-age and drying shrinkage of high-performance concrete. *Transportation research record*, 1834(1):48–58, 2003.
- [30] Adam M Neville and Jeffrey John Brooks. *Concrete technology*. Longman Scientific & Technical England, 1987.
- [31] Baris Ozer and M Hulusi Ozkul. The influence of initial water curing on the strength development of ordinary portland and pozzolanic cement concretes. *Cement and Concrete Research*, 34(1):13–18, 2004.
- [32] Jong-Sup Park, Young Kim, Jeong-Rae Cho, and Se-Jin Jeon. Early-age strength of ultra-high performance concrete in various curing conditions. *Materials*, 8(8):5537–5553, 2015.
- [33] L. J. Parrott. *Simplified Methods of Predicting Deformation of Structural Concrete (Englisch)*.
- [34] Sandor Popovics. Effect of curing method and final moisture condition on compressive strength of concrete. In *Journal Proceedings*, volume 83, pages 650–657, 1986.
- [35] Silke Prinsse. Alkali activated concrete : Development of material properties and flexural behaviour of reinforced beams over time.
- [36] H Abdul Razak and HS Wong. Re-evaluation of strength and stiffness relationships for high-strength concrete. *Asian Journal of Civil Engineering (building and housing)*, 5(1-2):85–99, 2004.
- [37] I Soroka and H Baum. Influence of specimen size on effect of curing regime on concrete compressive strength. *Journal of materials in civil engineering*, 6(1):15–22, 1994.
- [38] Ed. K. van Breugel. *Concrete Structures under Imposed Thermal and Shrinkage deformations*.
- [39] Van Vliet. Size effect in tensile fracture of concrete and rock.
- [40] Jaap Weerheijm. *Understanding the tensile properties of concrete*. Elsevier, 2013.
- [41] F.H. Wittmann. Fracture mechanics and durability of high performance concrete.

-
- [42] Zhang Yunsheng, Sun Wei, Liu Sifeng, Jiao Chujie, and Lai Jianzhong. Preparation of c200 green reactive powder concrete and its static–dynamic behaviors. *Cement and Concrete Composites*, 30(9):831–838, 2008.
- [43] Yong Zhou, Jie Gao, Zhihui Sun, and Wenjun Qu. A fundamental study on compressive strength, static and dynamic elastic moduli of young concrete. *Construction and Building Materials*, 98:137–145, 2015.